Ásta Björk Jónsdóttir

The function of the BRCA2 protein and centriole mobility during cytokinesis studied with live-cell microscopy

PhD THESIS

UNIVERSITY OF ICELAND

FACULTY OF MEDICINE

November 2010

Ásta Björk Jónsdóttir

The function of the BRCA2 protein and centriole mobility during cytokinesis studied with live-cell microscopy

Supervisor

Prof. Jórunn E. Eyfjörð, D.Phil.

Advisors

Prof. Hans J. Tanke, Ph.D. and Dr. Károly Szuhai, Ph.D., M.D.

Doctoral Committee

Prof. Hans J. Tanke, Ph.D., Prof. Helga M. Ögmundsdóttir Cand. Med., Ph.D.,
Prof. Jóhannes Björnsson M.D., Dr. Károly Szuhai, M.D., Ph.D.,
Prof. Peter Devilee Ph.D. and Prof. Jórunn E. Eyfjörð, D.Phil.

UNIVERSITY OF ICELAND, FACULTY OF MEDICINE

CANCER RESEARCH LABORATORY

&

LEIDEN UNIVERSITY MEDICAL CENTER

DEPARTMENT OF MOLECULAR CELL BIOLOGY

Ásta Björk Jónsdóttir

Hlutverk BRCA2 próteinsins og hreyfanleiki deilikorna í frymisskiptingu könnuð með rauntímamyndgreiningu á lifandi frumum

Leiðbeinandi

Prof. Jórunn E. Eyfjörð, D.Phil.

Meðleiðbeinendur

Prof. Hans J. Tanke, Ph.D. and Dr. Károly Szuhai, Ph.D., M.D.

Doktorsnefnd

Próf. Hans J. Tanke, Ph.D., Próf. Helga M. Ögmundsdóttir Cand. Med., Ph.D.,
Próf. Jóhannes Björnsson M.D., Dr. Károly Szuhai, M.D., Ph.D.,
Próf. Peter Devilee Ph.D. and Próf. Jórunn E. Eyfjörð, D.Phil.

HÁSKÓLI ÍSLANDS, LÆKNADEILD

RANNSÓKNASTOFA Í KRABBAMEINSFRÆÐUM

&

LEIDEN UNIVERSITY MEDICAL CENTER

DEPARTMENT OF MOLECULAR CELL BIOLOGY

ISBN 978-9979-9918-8-5

Prentun: Háskólaprent ehf.

Reykjavík, Ísland, 2010

Fyrir mömmu og pabba

ÁGRIP Á ÍSLENSKU

Kímlínustökkbreytingar í *BRCA1* og *BRCA2* geninunum auka áhættu á brjósta- krabbameini og öðrum krabbameinum. Faraldsfræðilegar og genamengisrannsóknir hafa aukið skilning á krabbameinunum sem stökkbreytingar í þessum genum valda. Rannsóknir á hlutverkum BRCA próteinanna hafa aukið þekkingu á þeim frumu- og sameindalíffræðilegu ferlum sem leitt geta til krabbameinsmyndunar og æxlisvaxtar í arfberum *BRCA* stökkbreytinga. Próteinin hafa verið tengd við mörg hlutverk innan fruma, til að mynda viðgerð á tvíþátta DNA brotum og tvöföldun geislaskauta. Í þessu doktorsverkefni hefur meðal annars verið notuð smásjártækni til að fylgjast með lifandi frumum og til að rannsaka hlutverk BRCA2 próteinsins og afleiðingar galla í því í lokaskrefi frumuskiptingahringsins, nefnt frymisskipting. Einnig voru kannaðar hreyfingar deilikorna í frymisskiptingu sem hugsanlegur stjórnunarþáttur í þessu ferli. Loks var litnun í illkynja *BRCA2* stökkbreyttum brjóstaæxlum metin út frá flæðigreiningargögnum og borin saman við stök brjóstakrabbameinsæxli.

Myndgreining á lifandi frumum er mjög gagnleg tækni til að rannsaka meðal annars frumur, frumulíffræðilega ferla, hlutverk próteina og samspil þeirra.

Hugsanlegt hlutverk BRCA2 próteinsins við frymisskiptingar var kannað með því að bera saman frumuskiptingarhraða $BRCA2^{+/+}$og $BRCA2^{+/-}$ bandvefsfruma sem voru óumbreyttar og ómeðhöndlaðar. Frumuskiptingarhraðinn var áætlaður með rauntíma myndgreiningu á lifandi frumum með því að mynda þær með sýnilegu ljósi og þannig fylgst með aðskilnaði litninga í tvær dótturfrumur og frymisskiptingu. Niðurstöður gáfu til kynna að *BRCA2* genaafurðin hefði hugsanlega hlutverki að gegna við frymisskiptingar þar sem arfblendnar *BRCA2* frumur voru marktækt lengur að skipta sér en þær sem ekki báru *BRCA2* stökkbreytingu. Þegar litað var fyrir próteininu greindist það í þyrpingu við skiptimiðjuna sem og við geislaskautin og því var kannað hvort að BRCA2 próteinið stjórni eða hafi hlutverki að gegna í lokaskrefum frumuskiptingarferlinsins með samskiptum við geislaskautin. Niðurstöðurnar staðfestu ekki þá tilgátu.

Frekari rannsóknir á lifandi frumum sem tjáðu annars vegar geislaskauts-sérhæfð og hins vegar örpíplu-sérhæfð gen tengd við flúrljómandi genaraðir í mismunadi frumulínum sýndu að hreyfingar deilikorna voru misjafnar milli fruma og frumulína og að þau ferðast aðallega eftir örpílum eða meðfram nýmynduðum kjarnahjúpnum.

Gagnstætt því sem birt hefur verið gefa niðurstöðurnar til kynna að flutningur deilikorna að skiptimiðju stjórni ekki aðskilnaði dótturfruma.

Nái frumur ekki að ljúka við frymisskiptingu getur það leitt til fjórlitnunar. Litnun illkynja *BRCA2* stökkbreyttra brjóstakrabbameinsæxla var borin saman við litnun í stökum brjóstakrabbameinsæxlum, en litnun æxlanna var áætluð út frá flæðigreiningargögnum. Fjórlitnun greindist marktækt oftar í *BRCA2* stökkbreyttum æxlum og styður þannig við þá hugmynd að BRCA2 taki þátt í frymisskiptingu. Tengsl voru milli fjórlitnunar og undirhóps *BRCA2* æxla með luminal svipgerð sem aðgreindu sig frá *BRCA2* æxlum með þrí-neikvæða svipgerð og stökum æxlum sem oftar voru mislitna.

Með myndgreiningu á lifandi frumum hefur ljósi verið varpað á frymisskiptinga ferlið. Niðurstöður gefa til kynna að BRCA2 próteinið hafi þar hlutverki að gegna og getur galli í þessu ferli leitt til fjórlitnunar og stuðlað að aukinni áhættu á krabbameinsmyndun í einstaklingum sem bera *BRCA2* stökkbreytingu. Ennfremur kom í ljós að deilikornin hreyfðust eftir örpíplum og meðfram nýmynduðum kjarnahjúp og að færsla deilikorna að skiptimiðju fyrir aðskilnað dótturfruma eru ekki jafn mikilvægur stjórnandi í þessu ferli og talið hafði verið.

Lykilorð: Frumuskipting, frymisskipting, BRCA2, geislaskaut, deilikorn, fjórlitnun, myndgreining á lifandi frumum.

ABSTRACT

Inherited mutations in the breast cancer susceptibility genes *BRCA1* and *BRCA2* increase the risk of developing breast cancer and other carcinomas. Population- and genome-wide studies have provided knowledge on cancers that are caused by mutations in these genes. Functional studies on the BRCA proteins have provided understanding on the molecular mechanisms that contribute to the development of carcinomas in *BRCA* mutation carriers and have shown that the proteins are involved in many processes within cells, such as DNA repair and centrosome duplication. The main aims of this project were to study the function of BRCA2 in the control of the last step of cell division, termed cytokinesis, using time-lapse microscopy. Also to investigate the effects of defects in the process. Furthermore, the movements of centrioles in living cells during cytokinesis were investigated as a possible controlling mechanism of the process. Finally, ploidy of malignant *BRCA2* mutated breast cancers was estimated from flow cytometry histograms and compared with sporadic breast cancers.

Live-cell imaging is a very useful technique to investigate various biological and cellular processes. The potential role of the BRCA2 protein during cytokinesis was studied by imaging living cells during cell division to estimate cell division time of *BRCA2* heterozygous and *BRCA2* wild type primary human fibroblasts. Cell division time was estimated from time-lapse images collected with bright-field light that allowed visualization of the separation of chromosomes into two daughter cells and the whole cytokinesis process. Cells that were heterozygous for a mutation in the *BRCA2* gene had delayed cytokinesis suggesting that the BRCA2 protein participates in cytokinesis. The BRCA2 protein was found to accumulate at the intercellular bridge and to concentrate at the centrosomes. This suggested that BRCA2 might regulate or play a role in cytokinesis by associating with the centrosomes. The results do not confirm that hypothesis. Further studies by imaging cells from different cell lines that expressed centriole-specific and microtubule-specific expression constructs fused with fluorescent-coding sequences, revealed variations in the positioning and mobility of the centrioles between cells and cell lines. The centrioles showed mainly microtubule dependent movements or they migrated along the nuclear envelope. These results indicate that the relocation of a

centriole to the intercellular bridge is not a general mechanism controlling abscission, contrary to some published data.

Failure of cytokinesis is known to result in tetraploidy. Ploidy was evaluated from flow cytometry histograms and ploidy aberrations in *BRCA2* mutated cancers compared with sporadic cancers. Tetraploidy was significantly more common in *BRCA2*-mutated than sporadic breast cancers, and this is consistent with the finding that the BRCA2 protein functions in cytokinesis. An association between tetraploidy and the luminal subtype was found in the *BRCA2* cancers, whereas aneuploidy was more prominent in triple-negative *BRCA2* mutated cancers and luminal sporadic breast cancers.

By investigating cell divisions with time-lapse live cell microscopy BRCA2 has been shown to play a role in cytokinesis. Tetraploidy was found to be more prominent in *BRCA2* mutated tumors than sporadic. Failure in cytokinesis can give rise to tetraploidy. Collectively, the data indicate that defects in this process may contribute to the increased cancer susceptibility in *BRCA2*-mutation carriers. Also, that centrioles migrate along microtubules and the nuclear envelope and that repositioning of centrioles towards the midbody is not a controlling mechanism for cytokinesis exit.

Key words: Cell division, cytokinesis, BRCA2, centrosome, centrioles, tetraploidy, live-cell microscopy.

ACKNOWLEDGEMENTS

"Where a cell arises
there must be a previous cell,
just as animals can only arise from animals
and plants from plants."

- Rudolf Virchow 1858 -

I was privileged to have Dr. Szuhai Károly as my supervisor during my PhD research project. Dear Károly, you taught me so much, not only those things that are useful in the laboratory as a scientist but also as a person in life. I am grateful that you shared some of your seemingly endless knowledge with me. Károly, I want to thank you for all your support.

Professor Hans J. Tanke. Dear Hans, you gave me an invaluable opportunity by allowing me to work on my project in your group; I will benefit from this forever. You were supportive and constructive at all times. I will not let you down.

Professor Jórunn Erla Eyfjörð. Dear Jórunn, it has been a long and, at times, difficult journey. When we started this research together a new phase of my life began and this helped me become who I am today. You were always open to my ideas and gave me the freedom and conviction to follow them. I am eternally grateful to you for that.

Professor Helga Margrét Ögmundsdóttir, your involvement has been extremely motivating and has helped me overcome many of the obstacles that I faced during my studies. I greatly appreciate all the time and work you dedicated to this project. We share many similar ideas, and I am thankful that we have been able to work on some of them.

Professor Jóhannes Björnsson, thank you for encouraging my enthusiasm for science throughout my studies and for your kind and positive comments during the period of writing the thesis.

My collaborators Peter Devilee and Maaike Vreeswijk, Roeland Dirks, Hans Vrolijk and Willem Sloos, thank you for your invaluable input and theoretical and technical support.

Federica Alberghini worked on a junior research project under my supervision and provided great assistance and valuable data.

Marja, Daan, Jeroen and Marije, thank you for going through this with me. I highly appreciate your friendship and support. All my very good friends and colleagues in Leiden, I miss you.

Thank you Linda for all of the special moments on the Red Chair, Sigríður Klara and Ólafur Andri for collaboration and your theoretical support.

Thank you, Marc Jongsten, my Tai Chi and Chi Kung instructor. You helped me to stay focused and to connect with myself. It is essential to find peace, both within yourself and in your surroundings, especially whilst writing.

Professor Jón Ólafur Skarphéðinsson and others at the Department of Physiology, University of Iceland, I thank you for providing me with the most ideal writing environment and facility and all the kindness.

In this world there is nothing more precious than one's family and friends. Elsku mamma, pabbi, Helga Guðný, Einar Ingi, Gunnar Sigfús, and amma Helga, I could not have done this without you. You are the best family one could wish for. My best friends, thank you for being who you are and allowing me to be part of your lives. Dear friends and family, your frequent visits and your belief in me kept me going throughout.

Finally, the financial support from Göngum Saman, Soroptimist Akranes, Iceland and International of Europe and Kvenfélag Eyrarbakka was not only financial but also very motivating and encouraging. Rannsóknasjóður Háskóla Íslands, Samtök um Krabbameinsrannsóknir á Íslandi and European Association of Cancer Research supported this research project.

CLARIFICATION OF CONTRIBUTION

Paper I – This paper describes a special phenotype, delayed cytokinesis, of primary human fibroblasts heterozygous for *BRCA2* mutation. I participated in the design of the study, performed all experiments except the interphase FISH, analyzed all the data with assistance on the statistical analysis and drafted the manuscript.

Paper II – This paper describes the variations of centriole movements during cytokinesis in three mammalian epithelial cell lines. Furthermore, it shows the usefulness of the Stacks software for the collected data. I participated in the design of the study, performed all the experiments, processed and analyzed all the data and participated in interpretation of the results. I drafted the manuscript and am the corresponding author.

Paper III – This paper describes the relationship between tetraploidy and a *BRCA2* mutation in tumors. I participated in the design of the study, collected all the flow cytometry histograms and analyzed them. I took part in interpreting the data and collaborated on the statistical analyses. I drafted the manuscript.

TABLE OF CONTENTS

LIST OF FIGURES

LIST OF TABLES

LIST OF PAPERS

This thesis is based on the following original papers:

I. Asta Björk Jonsdottir, Maaike P.G. Vreeswijk, Ron Wolterbeek, Peter Devilee, Hans J. Tanke, Jorunn E. Eyfjörd and Karoly Szuhai. *BRCA2* heterozygosity delays cytokinesis in primary human fibroblasts. Cellular Oncology 2009; 31:191-201.

II. Asta Björk Jonsdottir, Roeland W. Dirks, Johannes Vrolijk, Helga M. Ögmundsdottir, Hans J. Tanke, Jorunn E. Eyfjörd and Karoly Szuhai. Centriole movements in mammalian epithelial cells during cytokinesis. BMC Cell Biology 2010; 11(1):34.

III. Asta Björk Jonsdottir, Olafur Andri Stefansson, Johannes Björnsson, Jon G. Jonasson, Helga M. Ögmundsdottir and Jorunn E. Eyfjörd. Tetraploidy in *BRCA2* breast tumours. Submitted for publication.

LIST OF ABBREVIATIONS

APC = Adenomatous polyposis coli

APC/C = anaphase promoting complex/cyclosome

BFB = breakage-fusion-bridge

Cdc = cell division cycle

CDKs = cyclin dependent kinases

CGH = comparative genomic hybridisation

Chk = checkpoint kinase

CK = cytokeratin

CLS = centrosome localization signal

dsDNA = double stranded DNA

ER = estrogen receptor

FA = Fanconi anemia

GSCs = germline stem cells

HER = human epidermal growth factor receptor

HR = homologous recombination

MEFs = murine embryonic fibroblasts

MCC = mitotic checkpoint complex

MRN = MRE11, RAD50, NBS1

NES = nuclear export signal

NLS = nuclear localization signal

PCM = pericentriolar material

Plk-1= polo like kinase 1

PR = progesterone receptor

RPA = replication protein A

ssDNA = single stranded DNA

TNP = triple negative phenotype

INTRODUCTION

All cells arise from pre-existing cells by division as proposed by Rudolf Virchow [1821-1902] in his epigram *Omnis cellula a cellula* in 1858. After fertilization cell divisions are the major events in the development into a multicellular organism. It is essential that cells divide in a controlled manner. An equilibrium between cell divisions, proliferation and cell death is crucial. Uncontrolled growth can result in tumor formation. As early as in 1890 defects in mitosis, observed as unequal distribution of chromosomes between daughter cells and formation of non-bipolar spindles, were linked to cancer cells. For all these early and later biological observations microscopy was an essential tool.

Microscopy, a technique that was originally invented in The Netherlands and England by Antonie van Leeuwenhoek [1632-1723] and Robert Hooke [1635-1703], has been a major tool to help scientists to understand biology. *"There was in biology no one equivalent to Archimedes or Galileo; perhaps biology was just too difficult and without good microscopes cell theory was impossible."* (Wolpert, 1995). Amongst other research techniques microscopy has enabled detailed investigation of both cell divisions and the centrosomes and the consequences of their defects. Both the number and positioning of centrosomes in dividing cells can affect the cell division process, since supernumerary centrosomes can promote the formation of multi-polar spindles. Cells contain hereditary information that is passed from cell to cell during cell division. Inherited mutations in the *BRCA2* gene are known to predispose to breast cancer and other carcinomas. This research project started by combining genetics and advanced microscopy, by studying cell divisions of *BRCA2*-mutated primary cells with time-lapse imaging using bright-field light, and then continued by investigating the biology of the cell division process and centriole mobility in more detail with high resolution fluorescence microscopy and time-lapse imaging of fluorescent protein tagged target proteins. Finally, ploidy aberrations in *BRCA2* mutated malignant tumors were addressed, as a possible consequence of cell division failure.

1 MITOSIS

Walter Flemming [1843-1905] was one of the first to describe mitosis (in 1882) as the formation of paired threads (later identified as chromosomes) as reviewed by Kellogg *et al.* (Kellogg *et al.*, 1994). Mitosis is a complex and highly regulated process in eukaryotic cells where chromosomes are separated into two identical sets

and two identical daughter cells are formed. In the final stages of mitosis, cytoplasm, cellular organelles and cell membranes are in most cases equally divided between the daughter cells.

1.1 Control of mitosis – the mitotic phases and checkpoints

The mitotic phase (M phase) of the cell cycle is a relatively short period compared with interphase, which consists of G_1/G_0, S and G_2 phases. G_1 is the gap period between the end of mitosis and the start of DNA replication. During G_1 cells can enter G_0, which is a quiescent phase. S phase is the period during which DNA is synthesized and G_2 is the gap period following DNA replication and preceding mitosis (Cooper, 2000; Norbury and Nurse, 1992) (see a schematic representation in Figure 1). The whole cell cycle is controlled by cyclin dependent kinases (CDKs) that are activated by binding to cyclins that are specific for the different phases of the cell cycle and determine the targets of the kinases. Before entering mitosis the cell has to pass the G_2 checkpoint. The operation of cell-cycle checkpoints is controlled by activation and inactivation of cell division cycle (Cdc) kinases and CDKs, with post-transcriptional mechanisms such as phosphorylation, de-phosphorylation and with degradation of bound cyclins. The CDK1-Cyclin B kinase complex is decisive in the G_2 to M transition. As cells approach mitosis the Cdc25 phosphatase is activated which subsequently activates CDK1, establishing a positive feedback loop that efficiently drives the cell into mitosis (Clute and Pines, 1999; Norbury and Nurse, 1992). As a cell exits G_2 each centrosome nucleates microtubules and the mitotic spindle is formed (Doxsey *et al.*, 2005; Piehl *et al.*, 2004) (Figure 1, lower panel).The Aurora-A kinase is among proteins that regulate bipolar spindle assembly (Kufer *et al.*, 2002; Tsai *et al.*, 2003). Although the M phase is relatively short, the mitotic cell goes through several distinct phases during the division process. The G_2 to M transition starts with prophase as chromosomes condensate and the nuclear envelope starts to degrade, both controlled by the active CDK1-Cyclin B complex (Clute and Pines, 1999).

In prometaphase microtubules extend and attach to kinetochores or interact with opposing microtubules. During metaphase the chromosomes line up in an equatorial plane and the mitotic cell rounds up which is preceded by detachment from the extra-cellular matrix and neighboring cells (Thery and Bornens, 2006). The anaphase promoting complex (APC) is one of the primary controlling components in the early M phase and is activated by binding Cdc20, and this is dependent on high CDK1 activity. The spindle checkpoint inhibits Cdc20-mediated activation of the APC/cyclosome (APC/C) until all the chromosomes are correctly aligned on the microtubule spindle apparatus via their kinetochores (Peters, 2002) (Figure 1, top).

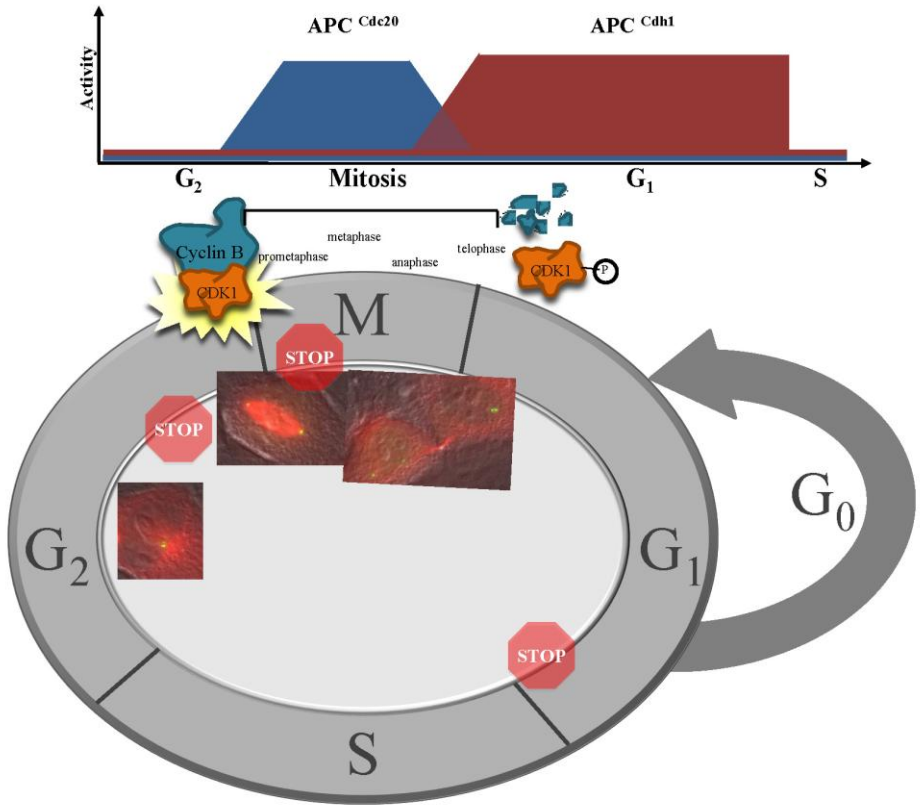

Figure 1: Schematic representation of the cell cycle with emphasis on mitosis. After cells pass the G2 checkpoint they are able to enter mitosis. Each centrosome then nucleates microtubules, the mitotic spindle is formed and centrosomes go to the opposite poles of the dividing cell. In prophase CDK1-Cyclin B translocates to the nucleus and the complex controls the initiation steps of mitosis. In metaphase, prior to anaphase the spindle checkpoint inhibits Cdc20-mediated activation of APC/C until it has ensured that all chromosomes are correctly aligned and microtubules attached to kinetochores. Cyclin B is degraded in metaphase as CDK1 is phosphorylated. APC^{Cdh1} gets activated in anaphase which mediates destruction of Cdc20 leading to inactivation of APC^{Cdc20}. During anaphase cytokinesis starts, a phase that is characterized by ingression of the cleavage furrow and formation of the intercellular bridge. The last mitotic phase is telophase and the cell division cycle is terminated with abscission, when the intercellular bridge is cut.

Binding of the mitotic checkpoint complex (MCC), which includes BubR1, Bub3, Mad2 and Cdc20, to the APC/C is dependent on an active checkpoint signal. Both Bub1 and Aurora kinase activity promote binding of the MCC to the APC/C (Meraldi and Sorger, 2005). Degradation of Cyclin B and Cdc20 begins in metaphase. Cdh1 replaces Cdc20 which keeps the APC active until the end of G_1 (Peters, 2002) (Figure 1, upper panel). Mitotic arrest ensues if the mitotic spindle cannot form or if kinetochores cannot interact normally with spindle microtubules. Daughter cells can become polyploid if the arrest is abandoned in the presence of

errors, such as replication and segregation errors (Rieder *et al.*, 1994). The normally dividing cellprogresses into anaphase, during which the sister chromatids are equally pulled towards each spindle pole. During anaphase the process of cytokinesis is started. The microtubules promote the function and ingression of the cleavage furrow as they gradually concentrate at the spindle midzone and a perpendicular ring of actomyosin contracts to form a cleavage furrow. The cleavage furrow ingresses until it reaches the midzone and creates the intercellular bridge containing a midbody (Figure 2) (Khodjakov and Rieder, 2001; Saurin *et al.*, 2008). It has been shown that microtubules and microtubule proteins in grasshopper cells are the only internal cellular components that are required to initiate cleavage furrowing (Alsop and Zhang, 2003). In mammalian cells the centrosomes have to separate for the cleavage furrow to be formed (Dechant and Glotzer, 2003) and interestingly, the cells that lack central spindle microtubules, having monopolar spindles, are both able to initiate and complete cytokinesis (Canman *et al.*, 2003). Studies on other species indicate that it is enough to have a contact between the plus end of the microtubule and the cell cortex to initiate cleavage furrowing (Inoue *et al.*, 2004).

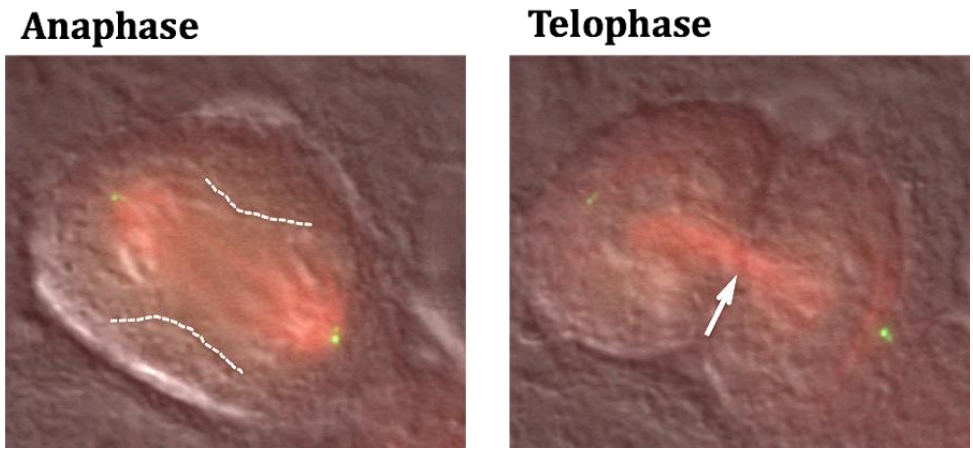

Figure 2: The process of cytokinesis starts during anaphase when the cleavage furrow ingresses (white dotted lines) and creates the intercellular bridge that contains a midbody (white arrow). The midbody consists of overlapping microtubules (in red are microtubules marked by α-Tubulin-mCherry), which nucleate from the centrosomes (green, marked by centrin1-EGFP), and additional proteins, many of which are required for cytokinesis.

Decondensing of chromosomes occurs in telophase, which follows anaphase, and the nuclear envelope is re-formed. Cytokinesis is a process necessary for completing cell divisions by cytoplasmic separation and marks the end of mitosis. During its termination step, termed abscission, the intercellular bridge is cleaved and each daughter cell then receives only one centrosome.

1.1.1 Molecular control of cytokinesis

A number of proteins and protein kinases have been implicated in the progression through cytokinesis. Of those kinases the role of the serine/threonine kinases Aurora-A and Aurora-B is best characterized. Aurora-B is a chromosome passenger protein kinase and regulates chromosome segregation and is an essential protein for cytokinesis. During anaphase and telophase several proteins assemble at the central spindle, like the MKLP1/CYK4 complex, Aurora-B kinase complex as well as the tumor suppressor BRCA2. The actomyosin ring assembly and ingression of the cleavage furrow is directed by RhoA, ECT2 and CYK4. RhoA-GTP activates downstream pathways that lead to actin polymerization and activation of non-muscle myosin II (Daniels *et al.*, 2004; Glotzer, 2005; Mishima *et al.*, 2002; Piekny *et al.*, 2005; Straight *et al.*, 2003; Yuce *et al.*, 2005). The midbody consists of overlapping microtubules and proteins, many of which are required for cytokinesis, mainly secretory and membrane-trafficking proteins, actin and microtubule associated proteins and protein kinases (Glotzer, 2005; Skop *et al.*, 2004). The Aurora-B kinase forms the catalytic core of the chromosome passenger complex together with INCENP, Survivin and Borealin. This complex remains associated with the midbody during cytokinesis (Carmena and Earnshaw, 2003; Earnshaw and Bernat, 1991).

2 THE CENTROSOMES

Centrosomes serve as scaffolds for anchoring an extensive number of regulatory proteins, and several of them are essential for cell-cycle control and cell division (Doxsey *et al.*, 2005). The centrosome in animal cells is a cytoplasmic cellular organelle, approximately 1-2 μm in diameter, usually located close to the Golgi apparatus. A mature centrosome consists of two barrel-shaped centrioles, one that is from two cell cycles before or earlier (the mother) and another inherited from the previous cell cycle (the daughter). The interconnected mother and daughter centrioles are surrounded by pericentriolar material (PCM) containing γ-Tubulin ring complex, which nucleate microtubules.

At any given time point during the cell cycle, cells have either one unduplicated or two duplicated centrosomes and therefore they, like DNA, must duplicate once, and only once, per cell cycle. CDK2-cyclin E, is a key initiator of both the centrosome and DNA duplication (Hanashiro *et al.*, 2008). In G_1, the centrosome begins to duplicate by separation of the centrioles. At early S phase procentrioles start to nucleate near the base of the pre-existing daughter and mother centrioles, that then elongate and mature (Alvey, 1985; Azimzadeh and Bornens, 2007; Doxsey *et al.*, 2005). Centrin is a small protein within the distal lumen of the centrioles. It appears in the centrioles as soon as they begin to form and remains associated with the organelles as they mature (Piel *et al.*, 2000). The two centrioles have different structures and functions. The older "mother" centriole

is associated with centriolar appendages, specific proteins such as cenexin and centrobin; it attaches microtubules and supports ciliogenesis. The younger "daughter" centriole lacks these structures (Anderson and Stearns, 2009; Gromley *et al.*, 2003; Lange and Gull, 1995; Vorobjev and Chentsov Yu, 1982). One of the first mitotic events is microtubule nucleation and formation of the mitotic spindle (Piehl *et al.*, 2004). Microtubule nucleation is partly regulated by protein phosphorylation. Plk-1 and Aurora-A are among protein kinases that promote microtubule nucleation, Aurora-A has been shown to do that through phosphorylation of the TACC proteins (Bettencourt-Dias and Glover, 2007; Gergely *et al.*, 2003).

2.1 The role of the centrosomes during cell division

Centrosomes play an important role during cell division. When cells enter mitosis they undergo considerable remodeling and repositioning of nuclear, cytoplasmic, and plasma membrane proteins. This involves the mitotic spindle, the spindle poles, kinetochores and the astral microtubules. The microtubules support transport of signaling proteins between the spindle poles and the mitotic cortex, orchestrating the spindle orientation and cell polarity. Accurate spindle orientation and polarity is necessary for efficient cell division. Notably, although cells can divide irrespective of a repositioning of the centrosomes and after depletion of one or both of the centrosomes, the presence of centrosomes ensures efficient formation of the mitotic spindle and facilitates cell division (Khodjakov *et al.*, 2000; Khodjakov and Rieder, 2001; Schaffner and Jose, 2006). In the case of absent centrosomes, their function as microtubule organizing centers can be replaced by chromatin and motor proteins (Schaffner and Jose, 2006; Vernos and Karsenti, 1995; Walczak *et al.*, 1998).

The centrosomes carry out many important and variable roles within tissues. They have been linked to the control of asymmetric division of an adult stem cell, which leads to the generation of one self-renewing stem cell and one differentiating cell. By studying spermatogenesis in *Drosophila* male germ line, it has been observed that cell cycle arrest associated with centrosome misorientation functions as a mechanism to ensure asymmetric stem cell division (Cheng *et al.*, 2008). Interestingly, studies on *Drosophila* germline stem cells (GSCs) have shown that the mother centrosome remains near the niche of the GSC, whereas the daughter centrosome migrates to the opposite side of the cell before the mitotic spindle is formed and is inherited by the cell that commits to differentiation (Yamashita *et al.*, 2007).

Many studies support the theory that centrosomes ensure cytokinesis and subsequent cell cycle progression. It has been postulated that the role of the centrosome during mitosis is to maintain and organize the astral microtubule array to facilitate cytokinesis. The centrosomes are thought to act as a scaffold or provide essential

signaling molecules required for cytokinesis progression (Doxsey *et al.*, 2005). Gromley *et al.* studied the requirement of centrosomes for completion of cytokinesis for cell cycle progression (Gromley *et al.*, 2003). Silencing of centriolin, a mother centriole component, in RPE-1 cells resulted in a dramatic increase in the percentage of late-stage mitotic cells and an increase in the percentage of binucleated cells. The cells with reduced centriolin appeared to be arrested or delayed in the final stages of cytokinesis where they remained interconnected, even though one or both of the future daughter cells had re-entered mitosis. The role of the centrioles in cytokinesis has been investigated since the 7th decade of the last century. The studies have focused on the migration of centrioles towards the midbody (Khodjakov and Rieder, 2001; Rattner and Phillips, 1973). Piel *et al.* (Piel *et al.*, 2001) observed that after the formation of the cleavage furrow a centriole migrated from the cell pole and straight to the intercellular bridge and when it repositioned back to the cell center, abscission occurred. They suggested that movement of a centriole (the mother centriole) to the intercellular bridge was essential for abscission to be executed (Piel *et al.*, 2001).

3 POLYPLOIDY AND ANEUPLOIDY

Nearly all normal mammalian cells are diploid, meaning that they have two homologous copies of every autosomal chromosome. Human diploid cells have 46 chromosomes. Polyploid cells have chromosome numbers that are a multiple of the haploid number. Polyploidy does not necessarily have to be a disadvantage. Only when growth arrest, cell death or increased genomic instability is triggered can it be catastrophic (Weaver *et al.*, 2007). Tetra- and polyploidy appears in normal hepatocytes and in megakaryocytes, where they are retained and the cells divide their nuclei successfully. Thus, so long as cells retain the cellular machinery to accurately duplicate and segregate their genome during subsequent cell divisions polyploidy can be tolerated (Guidotti *et al.*, 2003; Rubin *et al.*, 2003; Weaver *et al.*, 2007; Weglarz *et al.*, 2000). Tetraploidy is doubled diploidy and is thought to arise by one of three mechanisms: cell fusion, mitotic slippage, or a failure to undergo cytokinesis (Figure 3). During mitotic slippage the cells escape spindle-assembly checkpoint arrest and the subsequent cell cycle progression leads to endoreduplication of the genome. A failure to undergo cytokinesis may occur because of a failure or disturbance of cleavage furrow formation, giving rise to a new G_1 bi-nuclear cell with two centrosomes and two nuclei (Storchova and Pellman, 2004). Cell fusion has been shown to be proportional to malignant level of tumor cells, but cell fusion is not always catastrophic. It is for example known to take place during the formation of placenta and muscle fibers (Lu and Kang, 2009; Ogle *et al.*, 2005). Tetraploid cells can arise through failure to repair DNA damage in G_2, which combined with cell cycle progression can create chromosome bridging in anaphase resulting in tetraploid G_1 cells (Andreassen *et al.*, 2003). The cell cycle of tetraploid non-

transformed mammalian cells has been shown to be blocked in G_1 and the cell-cycle arrest to require intact p53 and pRB function (Andreassen *et al.*, 2001). This checkpoint may be critical to ensure genomic integrity (Borel *et al.*, 2002).

Tetraploid cells do not always produce tetraploid progeny (Figure 3). Abnormal mitosis of tetraploid cells can give rise to aneuploid daughter cells, but tetraploidy as an intermediate route is only one of the possible ways to aneuploidy, when the number of chromosome is not a multiple of the haploid complement. The chromosome imbalance in aneuploid cells may be more severe than tetraploidy, as the transcription and translation from the additional chromosomes may create greater stress because of the genomic unevenness (Williams and Amon, 2009). Aneuploidy can also evolve directly from diploid cells, possibly as a consequence of abnormalities of the mitotic spindle, such as mono- or multipolar spindles, or spindle checkpoint failure, which can result in missegregation of chromosome (King, 2008) (Figure 3). Elimination of regulatory mechanisms underlying centrosome duplication can lead to centrosome amplification, which increases the frequency of mitotic defects, which can result in the formation of multipolar spindle, missegregation of chromosomes and lead to aneuploidy (Figure 3). Improper attachments of chromosomes to spindle microtubules, merotelic attachment, in which one kinetochore attaches microtubules emerging from both poles, can also give rise to aneuploidy (Cimini, 2008).

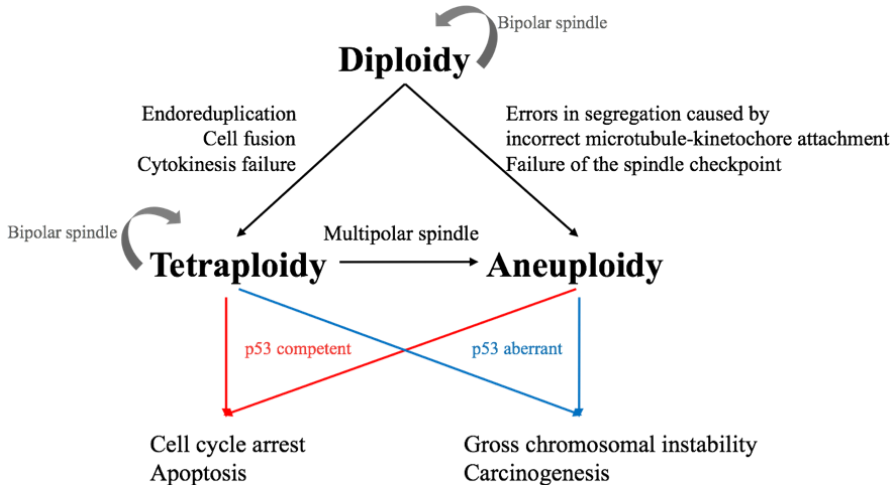

Figure 3: Summary of the potential relationships between diploidy, tetraploidy and aneuploidy. Tetraploidy can arise from diploid cells through mitotic slippage, cell fusion or a failure to undergo cytokinesis. Aneuploidy can arise directly form diploid cells or from tetraploid cells. Missegregation of chromosomes during mitosis, a consequence of a multipolar spindle, can give rise to aneuploid cells.

3.1 The centrosomes and polyploidy

Supernumerary centrosomes have been proposed to be a major source of chromosomal instability and aneuploidy. This was orignially discovered by Theodor Boveri [1862-1915] when he added a large amount of sperm to the sea urchin eggs, leading e.g. to the formation of tri- or quatri-polar spindles and subsequently to the generation of daugher cells with unequal numbers of chromosomes (Moritz and Sauer, 1996; Satzinger, 2008). Amplification of centrosomes can cause multipolar spindles and also increase the chance that three or more aneuploid daughter cells are generated during mitosis. It has been shown that newly formed tetraploid cells frequently contain two centrosomes (Nigg, 2002). The following four pathways can lead to centrosome amplification: 1) centrosome overduplication leading to increased number of centrioles around one mother centriole, which leads to multiple centrosomes in the next cell cycle, 2) reduplication, when centrosomes are duplicated more than once per cell cycle, 3) fragmentation of the PCM and 4) when two centrosomes in a G_1 tetraploid cell are duplicated in the subsequent S phase (Storchova and Kuffer, 2008). Cells that have entered G_1 with a tetraploid genome ought to be blocked to inhibit further cell cycle progression. The nature of the arrest signal is an unresolved question, but the centrosomes could possibly transmit a signal indicating their abnormal quantity (Khodjakov and Rieder, 2001). By using long-term live-cell imaging it was recently shown that cells with multiple centrosomes rarely undergo multipolar cell divisions, and the progeny of these divisions are typically nonviable (Ganem *et al.*, 2009). In the same study, it was demonstrated that the presence of extra centrosomes promoted chromosome missegregation.

3.2 Polyploidy and cancer

Aneuploidy is one of the most common characteristics of human carcinomas (Kops *et al.*, 2005). Cells which harbor chromosomal aberrations and continue cycling and dividing, or fail to complete cytokinesis by going through nuclear division without cytoplasmic separation, are potential progenitors of carcinogenesis (Storchova and Pellman, 2004).

The hypothesis that aneuploidy is the cause of cancer is over 100 years old. After studying the process of cell division Theodor Boveri hypothesized that cancer cells originated from a single progenitor cell with aberrations in chromosome numbers (Hardy and Zacharias, 2005; Satzinger, 2008). Boveri's discovery of dividing cells with multipolar spindles was contemporary with that of David Hansemann (later von Hansemann) [1858-1920]. von Hansemann found that tumors contained both dividing cells with multipolar spindles and bipolar cells with asymmetrical division of chromosomes in two daughter cells, but he remarked that this was not the cause of cancer (Bignold *et al.*, 2006; Hardy and Zacharias, 2005). The hypothesis that

cancer was caused by aneuploidy was silenced by the time that cancers where found to be clonal for somatic gene mutations (Duesberg and Rasnick, 2000). However, according to the new chromosomal theory of cancer, proposed by Duesberg *et al.* (Duesberg *et al.*, 2005) carcinogenesis is a result of chromosomal rather than genetic changes. They state that specific aneuploid karyotypes both initiate (even long before transformation) and are necessary for carcinogenesis, since this phenotype has been found prior to carcinogenesis in precancerous tissues and neoplasias of various organs (Duesberg *et al.*, 2005; Li *et al.*, 2009).

Polyploidy as an early event in tumor formation and progression has been shown for various cancers, but it seems to be tumor-specific whether this occurs as an early event, promoting carcinogenesis, or not (Margolis *et al.*, 2003). Well-differentiated infiltrating carcinomas and low-grade *in situ* carcinomas tend to be diploid. In contrast, poorly differentiated tumors display DNA aneuploidy (Yoder *et al.*, 2007). Evidence indicating that tetraploidy can trigger tumor formation comes from a study showing that overexpression of the oncogenes Eg5 and Mad2 in mice induces tetraploidization and tumorigenesis. Also, overexpression of the Aurora-A kinase has been shown to induce chromosomal instability and formation of mammary tumors as a result of failure of cytokinesis (Storchova and Kuffer, 2008). Amplification of Aurora-A kinase has been found to associate with *BRCA2* mutations in breast carcinoma (Bodvarsdottir *et al.*, 2007). HeLa cells treated with siRNA directed against the breast cancer susceptibility gene *BRCA2* and MEFs deficient for Brca2, fail to separate at the end of mitosis, and accumulate binucleated cells (Daniels *et al.*, 2004).

4 FAMILIAL BREAST CANCER

The two main breast cancer susceptibility genes, *BRCA1* and *BRCA2*, were identified through genetic linkage analysis (Miki *et al.*, 1994; Tavtigian *et al.*, 1996; Wooster *et al.*, 1995). Mutations in these genes have been shown to account for 15-40% of familial risk of breast cancer (AnglianBreastCancerStudyGroup, 2000; Peto *et al.*, 1999; Tulinius *et al.*, 2002). Over 2000 different mutations have been found in the *BRCA2* gene and thereof about half are private mutations . The *BRCA2 999del5* founder mutation is the only *BRCA2* mutation that has been found in the Icelandic population and is present in about 6-7% of all female breast cancer cases in Iceland (Thorlacius *et al.*, 1996; Thorlacius *et al.*, 1997). The estimated prevalence of the *BRCA2 999del5* mutation in the general Icelandic population is 0.4 - 0.6% (Johannesdottir *et al.*, 1996; Thorlacius *et al.*, 1997). The relative risk of breast cancer among the *BRCA1* and *BRCA2* mutation carriers is about 10- to 20- fold, which translates into 30-60% risk by age 60 (Stratton and Rahman, 2008). The risk

of developing breast cancer for *BRCA2 999del5* mutation carriers is over 70% by the age of 70, which is almost a fourfold increase from 1920 (Tryggvadottir *et al.*, 2006). Nearly 25% of women diagnosed with breast cancer by age 40 are *BRCA2* mutation carriers (Thorlacius *et al.*, 1997), indicating that it leads to early onset of the carcinoma. Inheritance of mutations in the *CHEK2, ATM, BRIP1* and *PALB2* genes is associated with increased susceptibility to breast cancer, but the relative risk is 5-10 times lower than for *BRCA1* and *BRCA2*. Other known genes associated with increased risk for breast cancer are *TP53, CDH1, PTEN* and *STK11*, each of which making a relatively small contribution to the overall familial risk of breast cancer (Johnson *et al.*, 2007; Stratton and Rahman, 2008).

4.1 Molecular classification of breast carcinomas

Breast cancers are sub-classified according to their molecular phenotype. A selection of biomarkers, including progesterone receptor (PR), estrogen receptor (ER) and human epidermal growth factor receptor 2 (HER2) (also known as v-erb-b2 erythroblastic leukemia viral oncogene homolog 2 (ERBB2) and neuro/glioblastoma derived oncogene homolog (NEU)) are commonly used for the molecular analysis (Chin *et al.*, 2006; Perou *et al.*, 2000). Expression profiling has enabled the categorization of breast cancer into five groups: luminal A and luminal B (both are clinically ER or PR positive, but luminal B tumors are not HER2 positive); HER2 positive (ER and PR negative); normal-like; and basal-like (Cheang *et al.*, 2008; Nielsen *et al.*, 2004). Basal-like tumors have a triple-negative phenotype (TNP) (ER, PR and HER2 negative). *BRCA1* tumors categorize mainly as basal-like tumors and *BRCA2* tumors are predominantly of luminal subtype.

Similarities in the genomic alteration patterns of *BRCA1*- and *BRCA2*-mutated tumors have been found with high resolution array CGH (Sorlie *et al.*, 2003; Stefansson *et al.*, 2009; Waddell *et al.*, 2010). Both types display gains and losses of chromosomes and chromosome parts, but with different regions affected (van Beers *et al.*, 2005). Structural chromosomal aberrations, such as chromatid breaks and tri- and quadri-radial chromosomes characterize *BRCA2* tumors and cell lines that are deficient for BRCA2 (Gretarsdottir *et al.*, 1998; Patel *et al.*, 1998; Tirkkonen *et al.*, 1997; Yu *et al.*, 2000). The chromosomal instability may have arisen from errors in DNA repair or replication and incomplete cell division. Other types of mitotic dysfunction such as breakage-fusion-bridge (BFB) cycles can also lead to abnormalities in chromosome number and structure and formation of bridges at anaphase (Eyfjord and Bodvarsdottir, 2005; Gisselsson, 2008; Gisselsson *et al.*, 2000; Venkitaraman, 2002).

Biallelic *BRCA2* mutations have been shown to be associated with a rare subgroup of Fanconi anemia (FA), subtype FA-D1 (Howlett *et al.*, 2002). Fanconi anemia is a recessive chromosomal instability disorder with both autosomal and X-linked inheritance. The patients show growth retardation, skeletal abnormalities, bone marrow failure, their cells are hypersensitive towards DNA cross-linking agents and these patients are predisposed to acute myeloid leukemia (AML). The average life expectancy for these patients is approximately 22 years (Levitus *et al.*, 2006; Niedernhofer *et al.*, 2005). The FA-D1 patients have a clinical feature distinct from classical FA, including an increased risk of breast cancer and childhood malignancies such as medulloblastoma and Wilms' tumor (Howlett *et al.*, 2002; Offit *et al.*, 2003). Notably, chromosomes from *BRCA2*-associated tumors show changes similar to those seen in lymphocytes from FA-D1 patients. These include end-to-end fusions, radial chromosomes and anaphase bridges (Eyfjord and Bodvarsdottir, 2005; Howlett *et al.*, 2002; Patel *et al.*, 1998). Biallelic mutations in *BRIP1* and the BRCA2 binding partner *PALB2* also cause rare subtypes of Fanconi anemia, FA-J and FA-N respectively and the FA-N patients have an identical phenotype to FA-D1 (Levitus *et al.*, 2005; Patel *et al.*, 1998; Reid *et al.*, 2007).

5 THE BRCA2 PROTEIN

The biological function of the BRCA2 gene product has been extensively studied as well as its role in cancer predisposition. It has been shown to contain several functional domains (Figure 4) and to be involved in many cellular processes.

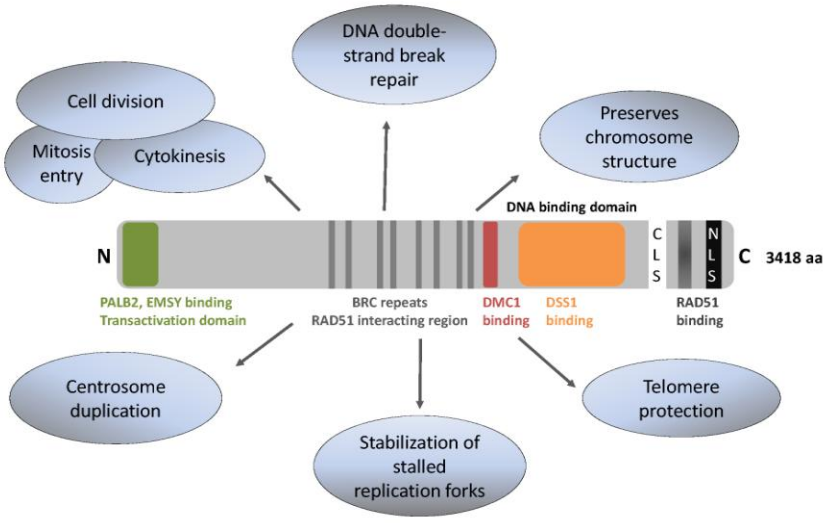

Figure 4: Schematic representation of the BRCA2 protein showing its binding domains and main functions

5.1 The functions of the BRCA2 protein

The best-known and most studied role of the BRCA2 protein is its involvement in DNA repair. The protein has been shown to be essential in error-free repair of DNA double-strand breaks. DNA double strand breaks give rise to spontaneous chromosomal translocations that promote genomic instability. These breaks seem to arise from stalled replication forks. It has been shown that when BRCA2-deficient tissue gets exposed to DNA cross-linking agents or ionizing radiation this results in chromosomal aberrations, both numerical and structural. Breakdown of replication forks has been seen in BRCA2 deficient cells, suggesting that BRCA2 preserves the stability of DNA structures at stalled replication forks (Lomonosov *et al.*, 2003). The error-free DNA double-strand break repair takes place via homologous recombination (HR) mediated by the RAD51 recombinase (Figure 5). DNA double-strand breaks are detected by MRE11, RAD50 and NBS1 composing the MRN complex, that activates the ATM kinase resulting in phosphorylation of the histone H2A coding gene H2AX at Ser139 (γH2AX). DNA repair proteins, including RAD51, 53BP1 and BRCA1 accumulate to the breakage site and form a foci (Misteli and Soutoglou, 2009; Yuan and Chen, 2010). RAD51 is directly bound to six of the eight BRC repeat motifs of BRCA2, with BRC4 having the highest affinity for RAD51 binding. BRCA2 directs RAD51 to the sites of DNA damage and loads the active form of RAD51 nucleoprotein filaments onto single stranded DNA (ssDNA) where they form extended filaments. Several RAD51 molecules are bound to each BRCA2 molecule, and these proteins are complexed independent of DNA damage, but kept inactive by the ssDNA-binding protein replication protein A (RPA). The BRC repeats block RAD51 nucleoprotein filament formation on dsDNA and thereby suppresses RAD51 assembly on double stranded DNA (dsDNA) (Ayoub *et al.*, 2009; Carreira *et al.*, 2009; Davies *et al.*, 2001; Moynahan *et al.*, 2001; Patel *et al.*, 1998; Shivji *et al.*, 2006; Xia *et al.*, 2001) (Figure 5). PALB2 interacts with BRCA2, and also binds directly to BRCA1, and serves as a molecular scaffold in formation of a BRCA2-BRCA1 complex (Sy *et al.*, 2009; Yang *et al.*, 2007). Also, DSS1 is associated with BRCA2 and functions as a co-mediator in HR (Xia *et al.*, 2006).

Ring chromosomes and chromosomes with two or more centromeres, have difficulties with segregation of sister-chromatids during mitosis which can lead to BFB cycles (Gisselsson, 2008; Williams and Amon, 2009). BFB cycles are more common in breast tumors from *BRCA2* carriers than in sporadic breast tumors (Eyfjord and Bodvarsdottir, 2005; Patel *et al.*, 1998), and have been explained by possible errors in capping of the telomeres (Eyfjord and Bodvarsdottir, 2005; Gisselsson *et al.*, 2001). To fix eroded telomeres, the highly error-prone repair mechanism non-homologous end joining is used.

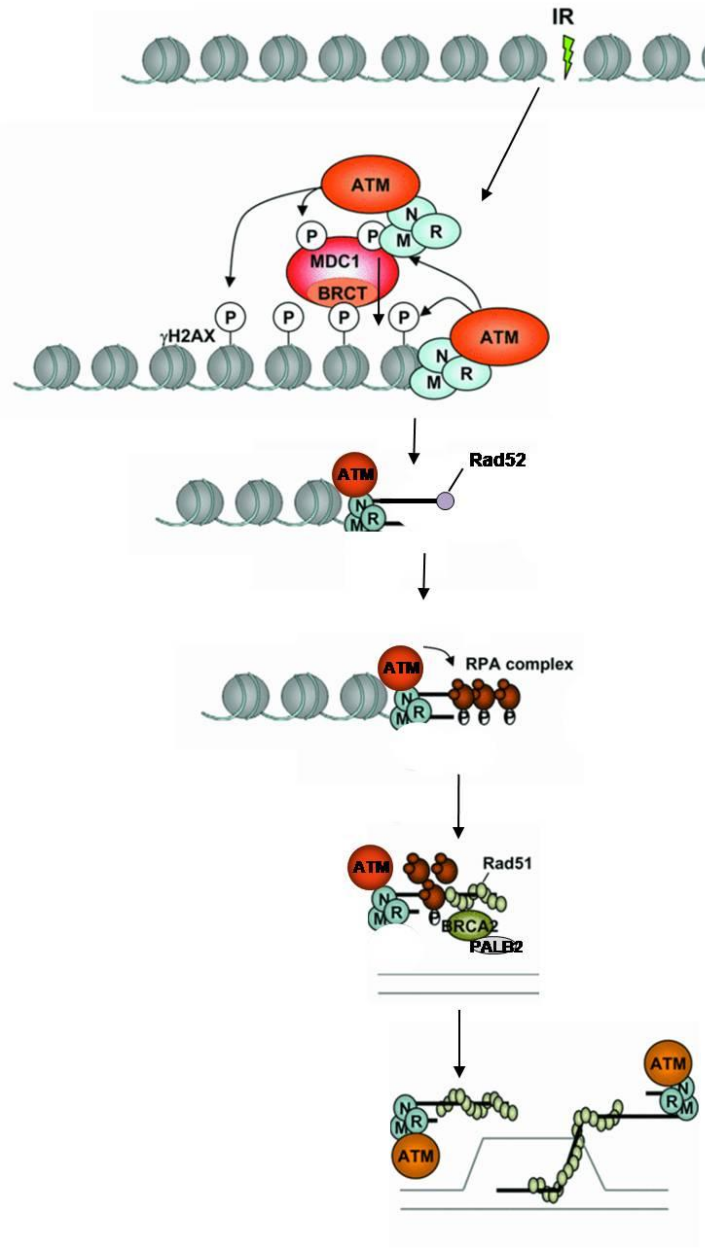

Figure 5: Repair of DNA double–strand break via homologous recombination. Following DNA double-strand breaks DNA damage response signaling is activated. MRN complex rapidly accumulate and detect the lesion and activates the ATM kinase, leading to phosphorylation of H2AX. Downstream pathways trigger RAD51 foci formation at the site of DNA double-strand breaks. Figure adjusted from (Thomson and Guerra-Rebollo, 2010).

BRCA2 has long been believed to participate in cell cycle control. The BRCA2 protein has been shown to have both a nuclear localization signal (NLS) and a centrosome

localization signal (CLS) at the C-terminal region (Figure 4). It localizes predominantly in the nucleus (Spain *et al.*, 1999; Yano *et al.*, 2000). It has been shown to have a nuclear export activity through a ^{1383}DLSDLTFLEVA^{1393} nuclear export signal (NES) motif, that is suggested to be necessary for cytoplasmic retention, and accumulation to the centrosome during S phase and early M phase (Han *et al.*, 2008; Nakanishi *et al.*, 2007).

Centrosome amplifications are well known in solid tumors, including breast tumors. A suggestion that BRCA2 participates in the regulation of centrosome duplication can be deduced from a study by Tutt *et al.* (Tutt *et al.*, 1999). They showed that absence of Brca2 in mouse cells resulted in centrosome amplifications. However this has not been followed up or studied in other cell lines and cell models. BRCA2 has been shown to bind to centrobin, a daughter centriole associated protein, which supports the hypothesis that BRCA2 participates in centrosome duplication (Zou *et al.*, 2005). BRCA2 has also been shown to interact with the cytoskeletal cross-linker protein plectin and thereby controlling the position of the centrosome (Niwa *et al.*, 2009).

5.2 Cell division and BRCA2

After cells have crossed the mitotic checkpoint, cytokinesis as well as signals essential for the completion of cytokinesis are intensely regulated. As addressed earlier, the RAD51 recombinase assembles at DNA breaks to execute DNA double-strand break repair via homologus recombination. This is mediated by BRCA2, which binds RAD51 through BRC repeats and directs it to the sites of DNA damage. BRCA2 also has a RAD51 binding motif at the C-terminus, which has been linked to the disassembly of RAD51 foci and mitotic entry since the foci do not persist in mitotic cells, not even after G_2 checkpoint suppression (Ayoub *et al.*, 2009; Shivji *et al.*, 2006). By inserting single-codon substitutions into the *BRCA2* gene it has been shown that foci disassemble more rapidly in a point mutant that has reduced binding affinity of RAD51 to the C-terminus of BRCA2 and the cells enter mitosis faster. In contrast, a point mutant with enhanced binding displayed slower disassembly of foci and delayed mitosis (Ayoub *et al.*, 2009). Inhibition of BRCA2 by antibody microinjection has been reported to delay the G_2 to M transition (Marmorstein *et al.*, 2001). The activity of the mitotic kinase polo-like 1 (Plk-1) is required for the transition from metaphase to anaphase and for cytokinesis progression. Polo-like kinase 1 hyperphosphorylates BRCA2 in M phase and the protein is then dephosphorylated during M phase exit (Lee *et al.*, 2004; Lin *et al.*, 2003). The C-terminal RAD51 interacting domain of BRCA2 is phosphorylated by cyclin-dependent kinases. The phosphorylation is low during S-phase and increases as cells proceed towards mitosis (Esashi *et al.*, 2005). Collectively, these findings link BRCA2 with progression through cell division.

A potential role for the BRCA2 protein in cytokinesis was studied in mouse embryonic fibroblasts (MEFs) and HeLa cells that were deficient for the protein (Daniels *et al.*, 2004). Cell divisions of *Brca2*$^{Tr/Tr}$ MEFs and HeLa cells treated with BRCA2 siRNA were delayed or not completed and the cells showed formation of binucleated cells. Abnormal non-muscle myosin II accumulation and furrowing was observed in HeLa cells treated with BRCA2 siRNA. BRCA2 was shown to co-localize with the Aurora-B kinase to the midbody of untreated HeLa cells (Daniels *et al.*, 2004). These results indicated that the BRCA2 protein plays a role during cytokinesis.

6 MICROSCOPY

– To see is to believe –

Since the pioneering work of Antonie van Leeuwenhoek and Robert Hooke in the seventeenth century light microscopy has undergone major improvements. Also, other types of microscopes based on different principles of imaging have been developed. Examples are electron microscopy and scanning probe microscope (scanning tunneling and atomic force microscopy), both aiming to unravel the structure of objects at higher resolution. Electron microscopy was developed by Ernst Ruska in the 1930s and has allowed investigators to characterize cellular structures in fixed cells. The centrosomes and their centrioles have been analyzed in detail with this method. For the study of biological objects, light microscopy is still the preferred method, particularly since fluorescence microscopy and adapted staining methods have become available to visualize molecules in cells and tissues with high specificity and resolution. These applications only allow investigation of fixed and stained objects with contrast agents to make structural details visible, but not the observation of dynamic interactions of molecules and other objects. If cells are to be studied in their native state (e.g. living) (ex *vivo*), standard staining procedures do not apply.

Imaging of living cells can be very informative when studying cellular processes, such as mitosis, which involves many simultaneous and visible events. Early methods of studying living cells are phase contrast microscopy (introduced by Frits Zernike in the 1930s) and Nomarski contrast, also called interference contrast microscopy (invented by Georges Nomarski in the 1950s). Vital staining procedures have been developed as a consequence of the gaining interest in the study of living cells. An example is the Hoechst 33342 nuclear stain.

A real breakthrough in microscopic observation was reached with the introduction of the fluorescent protein labeling in living cells. Osamu Shimomura, Martin Chalfie and Roger Y. Tsien received the Nobel Prize in Chemistry 2008 for the discovery and development of the green fluorescent protein, GFP. Using gene constructs (of the protein

of interest and the gene of the fluorescent protein), that are transfected into living cells, the localization and dynamics of a protein can be followed, as it has become fluorescent.

6.1 Microscopy of living cells

By adapting microscopes for phase contrast, differential interference contrast (DIC) or by using other contrast-generating optics, structures could be imaged with improved contrast. A revolutionary step forward was the use of a sensitive CCD camera on a microscope, enabling the time-lapse images of living cells. As an example, it was revealed that the fibers within the spindle were real structures that shrunk and grew and the duration of mitosis and chromosome movements were investigated in much more detail than ever before. This technique allowed identification of dynein, kinesin and kinesin-like proteins and provided explanations for how microtubules were replaced during the transition from interphase to mitosis (Paschal and Vallee, 1987; Rieder and Khodjakov, 2003; Schnapp *et al.*, 1986). This discovery was important to understand how mitosis actually takes place.

In addition, recording of the images using video cameras has been introduced to study the behavior of cells for a long time (Rieder and Khodjakov, 2003). Most cells (erythrocytes and melanocytes excepted) do not significantly absorb visible light. Bright field microscopy is therefore not optimally suited to visualize intracellular structures, although chromosomes, nucleoli and the nuclear envelope can be visualized (Frigault *et al.*, 2009; Rieder and Khodjakov, 2003). By labeling proteins of interest using the fluorescent protein labeling technology (e.g. using GFP) their localization and interaction with other proteins can be studied. Time-lapse fluorescence microscopy has additionally enabled highly informative studies on the centrosome and has led to several discoveries relating to their maturation, the nucleation of microtubules and that they ensure cytokinesis and subsequent cell cycle progression (Khodjakov and Rieder, 1999, 2001). Shortly after the introduction of centrin-labeled GFP cell lines, centrins were found to exhibit extensive movements within the cells as they proceeded through the cell cycle (Piel *et al.*, 2000).

Time-lapse imaging of living cells expressing different DNA constructs with multi-color protein labels has now become a well established research method. To obtain meaningful results, special precautions are however needed. First, the level of fluorescent protein expression must be at physiological levels. For moderate to highly expressed proteins, this is relatively easy to achieve and sensitivity of detection is generally sufficient for prolonged microscopic studies. If the expression level is low, one should avoid the tendency to artificially create higher expression levels, as studies under these conditions may not reflect real behavior. Second, recording cannot be performed endlessly, as photobleaching and phototoxicity will occur as a consequence of the

excitation process. Phototoxicity is likely the effect of oxygen radicals that are generated when excited fluorophore molecules collide with oxygen (Hoebe *et al.*, 2007; Song *et al.*, 1996). In principle, a cell can cope with this, as super oxide dismutase (SOD) will neutralize these damaging radicals. At prolonged excitation, this mechanism does not suffice, and cells will die. Also, prolonged illumination of cells in culture may interfere with cell cycle checkpoints, and thereby artificially influence cell cycle characteristics. To ensure minimal light exposure the microscope systems should be optimized to collect as much light as possible and highly sensitive detectors should be used (Hoebe *et al.*, 2007; Song *et al.*, 1996).

Finally, proper recording of the images as described above is essential, but the most important part is their interpretation. Sometimes, although being subjective, visual interpretation suffices, for instance when the observations made are very obvious. Unfortunately, that is not always the case and unbiased analytical tools and subsequent statistical validation are needed for firm conclusions. Therefore, image processing and quantitative analysis has become a crucial component of live-cell imaging. One such software was written in 1999 that allows a fully automated analysis, enabling highly sensitive object detection of fluorescent proteins from living cells, object tracking as well as visualization and measurement of quantitative parameters in time and space (Tvarusko *et al.*, 1999). This software has been used to study telomere dynamics in living cells from images obtained with time-lapse microscopy. The majority of the telomeres were observed to have low mobility while few individual telomeres showed significant degree of movement. The quantitative analysis and telomere tracking confirmed that the telomeres do not move over large distances in the cell nucleus (Molenaar *et al.*, 2003). The dynamic behavior of telomeres was recently studied with controlled light exposure microscopy. Telomeres were observed to move in distinct territories and form clusters of two or three at the interface of chromatin, which is consistent with the observations from Molenaar *et al.* who showed that telomeres have the ability to associate with each other. To estimate the dynamics of telomere movements a registration procedure for nuclear motion was applied. To track telomeres over a period of time an iterative conditional nearest neighbor algorithm was used and mobility was expressed by mean square displacement (MSD) (De Vos *et al.*, 2009). Another software enabling quantitative analysis of imaged objects in living cells is the software "Stacks" (Vrolijk *et al.*, *Manuscript in preparation*). It provides objective measurements of localization and movement and calculates numerical values for further statistical analysis.

AIMS OF THE STUDY

Genomic aberrations in breast tumors are complex and cancers from carriers of a *BRCA2* germline mutation show a high degree of chromosomal instability, which has been linked to the essential role of the BRCA2 protein in error-free DNA double strand break repair. The BRCA2 protein is a multi-motif multi-functional protein and has been suggested to function in cytokinesis, which is a highly regulated process. A number of molecules and particles are required for cell divisions, including centrioles. Incomplete cytokinesis can have severe consequences for the genomic stability of cells. The overall aim of this thesis was to investigate the function of BRCA2 in cytokinesis by estimating cell division time, consequences of failure of the process by evaluating ploidy, and to study the controlling mechanism of cytokinesis via BRCA2 and the centrioles using time-lapse microscopy.

The specific aims of the thesis were:

I. To determine whether haploinsufficiency of BRCA2 protein influences the process of cytokinesis by using live-cell imaging to monitor cell divisions of unmodified *BRCA2* heterozygous human cells.

II. To determine whether BRCA2 and repositioning of a centriole towards the intercellular bridge was involved in controlling the separation of the daughter cells. The intention was to study centriole positioning and mobility during cytokinesis in a *Brca*2 mouse cell line model. This part of the study was modified into studying the movements of centrioles in various mammalian epithelial cell lines during cytokinesis.

III. To evaluate the proportion of tetraploidy in *BRCA2* mutated breast cancer samples and compare with sporadic tumors, given that failure of cytokinesis can give rise to tetraploidy.

MATERIALS AND METHODS

MATERIALS:

Primary Human Fibroblasts

Unmodified primary human fibroblasts were cultured from skin biopsies derived from Icelandic and Dutch persons carrying a *BRCA2* mutation and non-carriers (Table 1).

Table 1: Unmodified Primary Human fibroblast Cells

Sample	Genotype	Mutation	Origin
FIS 1	*BRCA2*$^{+/-}$	999del5[*1]	Iceland
FIS 2	*BRCA2*$^{+/-}$	wild type	Iceland
FIS 3	*BRCA2*$^{+/-}$	999del5[*1]	Iceland
FNE1	*BRCA2*$^{+/-}$	1537del4[*2]	The Netherlands
FME2	*BRCA2*$^{+/-}$	wild type	The Netherlands

The Human Genetic Variation Society (HGVS) nomendature:
*1 c771_775del p.Asn257ÆYSfsx17; *2c1309_1312del p.Lys437ilefsx22

Primary fibroblasts were cultured in Dulbecco's Modified Eagle's Medium (DMEM), supplemented with 10% fetal bovine serum (FBS), penicillin (100 U/ml), streptomycin (0.1 mg/mL) and 2 mM L-glutamine. Cells were maintained at 37°C and 5% CO_2.

Epithelial cell lines

p53 deficient mouse mammary epithelial cell lines were kindly provided by Dr. Jos Jonkers, The National Cancer Institute, Amsterdam, The Netherlands. A brief description of the generation of the cell lines: By crossing transgenic mice carrying the Cre-recombinase under the K14 promoter and *p53*$^{F2\text{-}10/F2\text{-}10}$ mice expressing *Brca2* flanked by *loxP* sites, an epithelial specific inactivation of *Brca2* and *p53* was achieved in K14cre;Brca2$^{F/F}$;p53$^{F/F}$ female mice. These mice develop mammary carcinomas and skin tumors. For generation of cell lines mammary tumors were isolated from K14-Cre;*Brca2*$^{wt/wt}$;*p53*$^{F2\text{-}10/F2\text{-}10}$, K14-Cre;*Brca2*$^{wt/F11}$;*p53*$^{F2\text{-}10/F2\text{-}10}$ and K14-Cre;*Brca2*$^{F11/F11}$;*p53*$^{F2\text{-}10/F2\text{-}10}$ tumor-bearing female mice. The tumors were minced, digested and cultured until homogeneous cell morphology indicated pure epithelial cultures. The cell lines and their generation are described in more detail in the following references (Evers *et al.*, 2008; Jonkers *et al.*, 2001).

MCF 10A, normal human mammary epithelial cell line and HeLa, the cervical cancer human epithelial cell line, were obtained from the American Type Culture Collection. HeLa cell line stably expressing centrin1-EGFP was kindly provided by Dr. Fanny Gergely, Cancer Research UK Cambridge Research Institute, Cambridge, England, with permission from Dr. Matthiew Piel, who generated the stable cell line as described (Piel *et al.*, 2000).

Mouse mammary epithelial cell lines, KP-7.7 (*Brca2*$^{+/+}$), BE-KB2P-4 (*Brca2*$^{+/-}$), and KB2P-3.4 (*Brca2*$^{-/-}$), were cultured in DMEM/F12 supplemented with 10% FBS, 100 units/mL penicillin, 0.1 mg/mL streptomycin, 5 ng/mL epidermal growth factor (EGF), 50 μg/mL insulin and 5 ng/mL cholera toxin.

MCF 10A was cultured in DMEM/F12 complemented with 5% horse serum, 100 units/mL penicillin, 0.1 mg/mL streptomycin, 20 ng/mL EGF, 10 μg/mL insulin, 0.5 μg/mL hydrocortisone and 0.1 μg/mL cholera toxin.

HeLa cells were cultured in DMEM supplemented with 10% FBS, 100 units/mL penicillin and 0.1 mg/mL streptomycin. Stable centrin1-EGFP cells were cultured additionally with 0.4 mg/mL geneticin.

Breast carcinomas

Breast tumor samples from 1992-2006 that had previously been screened for the Icelandic *BRCA2 999del5* founder mutation, were selected from an Icelandic breast cancer patient cohort at the Cancer Registry and the Icelandic Cancer Society. Tumors from 101 female *BRCA2* mutation carriers were present in the cohort. Two sporadic tumor samples were selected as controls for each *BRCA2*-mutated sample, matched for year and age at diagnosis. Flow cytometry histograms were available for 71 malignant *BRCA2*-mutated breast cancers and 165 malignant sporadic breast tumors.

METHODS:

Immunofluorescence microscopy

For protein localization studies *in vitro*, cells were seeded and cultured on glass slides. After removing the culture medium the cells were washed with phosphate buffered saline (PBS) and fixed with ice-cold methanol or 3.7% formaldehyde/PBS for 12 min at room temperature (RT). Slides were washed with PBS after fixation, which was followed with washing in a blocking solution (PBS/10% serum) before blocking for 30 min at RT. Incubation with primary antibodies was performed at 37°C for 45 min. Specimens were washed with blocking solution before incubation with secondary antibodies at 37°C for 30 min. Antibody incubation was followed by washing steps with PBS and dehydration through an ethanol series (70%, 90% and 100%). Dry specimen slides were mounted in 4',6-diamino-2-phenylindole-dihydrochloride

(DAPI)/citifluor (500ng/ml) for DNA staining. Image acquisition was performed using an epi-fluorescence microscope, equipped with a Quantix CCD camera. Gray scale images were collected with 63x and 100x objectives using appropriate filters to visualize the fluorescence of the secondary antibodies and DNA stain.

Annexin V detection of apoptotic cells using live-cell microscopy

To investigate the fraction of apoptotic cells in a cell culture, staining with propidium iodine (PI) and Annexin V conjugated to the Alexa Fluor® 488 fluorophore (Alexa Fluor® 488 annexin V), was carried out using the Vybrant® Apoptosis Assay Kit #2. A novel method for utilizing Annexin V binding on adherent cells was applied, which was adjusted from a published method (van Engeland *et al.*, 1996). Cells were plated and cultured in monolayer on MatTek glass bottom culture dish. When the cells reached approximately 70% confluency they were washed with PBS. A solution composed of Alexa Fluor® 488 annexin V, 0.2 μg/mL PI and culture medium adding up to 100 μL, was added drop-by-drop onto the cells. Cells were incubated with 5% CO_2 at RT for 10 min and followed-up immediately by live-cell imaging with 5% CO_2 at 37°C.

qRT-PCR

To quantify mRNA expression levels, quantitative real-time polymerase chain reaction (qRT-PCR) was performed. Total RNA, isolated following standard procedure using TRIzol® Reagent, was treated with deoxyribonuclease 1 according to the manufacturer's instructions. First-strand cDNA was synthesized using oligo$(dT)_{20}$ and Super-script III transcriptase according to the manufacturer's instructions. The PCR was carried out in an amplification mixture containing template cDNA, iQ SYBR Green Supermix and forward and reverse primers for the mRNA sequence of interest. Reactions were run on a Bio-Rad iCycler Thermal Cycler. geNorm (Vandesompele *et al.*, 2002) was used to calculate the gene-stability for all control genes. The most stably expressed control gene was used as a reference to calculate the normalized expression level of the gene of interest, using the standard delta C_t method (Vandesompele *et al.*, 2002). The relative values for the controls were set to one.

Transfections of expression constructs

Cells were transiently transfected at approximately 30% confluency. Transfection solution containing expression constructs' DNA diluted in un-supplemented DMEM and Lipofectamine™ 2000 diluted in DMEM were incubated together at RT for 20 min. The cells were rinsed with DMEM and the transfection suspension added drop-by-drop to the culture plate and incubated for 1 hour at 37°C with 5% CO_2. Later supplemented DMEM was added and the cells cultured for 24 - 48 hrs.

For generation of α-Tubulin-mCherry expression vector, YFP from YFP-α-Tubulin expression vector (Gerlich *et al.*, 2003) (provided by Dr. Jan Ellenberg, EMBL, Heidelberg, Germany) was exchanged for mCherry by performing a polymerase chain reaction (PCR) on a mCherry expression construct (Shaner *et al.*, 2004) (kind gift of Dr. R. Tsien, Howard Hughes Medical Institute, Univeristy of California, San Diego, USA). This was followed by gel extraction and purification, digestion with restriction enzymes at 37°C for at least 2 hrs and subsequent purification steps. YFP-α-Tubulin construct was digested with the same restriction enzymes and after gel extraction and purification the mCherry sequence was ligated to the α-Tubulin expression construct.

Time-lapse live cell microscopy

It is crucial when imaging living cells that cell viability is ensured to guarantee that the biological and physiological processes being investigated are not influenced or altered.

All imaging was performed under strictly controlled conditions of temperature, CO_2 concentration and humidity, to avoid induction of stress responses, which can influence the studied processes. Timing and light exposure were kept minimal by using reduced excitation light, as the fluorescent light can cause localized heating and phototoxicity of the cell culture.

Estimation of cell division time (paper I)

We combined time-lapse microscopy and genetics when investigating the potential influence of BRCA2 haploinsufficiency on the process of cytokinesis, by using unmodified cells heterozygous for a *BRCA2* mutation and compared their cell division time with *BRCA2* wild type cells. We studied the process of cell division in primary human cells by using bright-field time-lapse imaging only, under strictly controlled conditions, since primary cells are more sensitive than cell lines.

Cells were seeded on a MatTek glass bottom culture dish and imaged when approximately 70% confluent. Cell divisions were recorded with a Leica AS MDW microscope system (Multi-Dimensional Workstation for Live Cell Imaging) consisting of an inverted phase contrast Leica DM IRE2 wide-field microscope, equipped with climate and CO_2 chambers. Transmitted light only was used when recording the dividing cells to avoid any photodamage. Time-lapse images were collected from up to 20 randomly selected positions from each culture dish, every 5 min for up to 24 hrs, with 40x objective. The images were collected from one focal plane only for every position. The Leica AS MDW software was used to generate movies from the time-lapse images collected. The condensed chromosomes are clearly visible in metaphase cells with this method. For estimation of the cell division time the beginning was set when the aligned chromosomes started to

separate (early anaphase). The division was considered to be completed when the new G_1 daughter cells were fully attached and flat on the culture surface.

In order to analyze distribution and localization of the BRCA2 protein in primary human fibroblasts with delayed cytokinesis, cells were imaged for 2 hrs prior to immunofluorescence staining, enabling identification of cells with prolonged cytokinesis.

To investigate whether daughter cells showed the same phenotypes as their progenitor cell, cells were imaged with 20x objective, in a tiled manner for up to 48 hrs.

Centriole motility and positioning (paper II)

To study the movements of the centrioles during cell division, light-microscopy and fluorescent wide-field time-lapse microscopy were combined to follow the cells through cell division and the mobility of the centrioles respectively. When studying movements of the centrioles, cell lines were transciently co-transfected with centrin1-EGFP and α-Tubulin-mCherry expression constructs and additionally a stably expressing centrin1-EGFP cell line was imaged.

Transiently transfected cells, cultured in MatTek glass-bottom culture dishes were imaged at approximately 70% confluency, (approximately 48 hrs after transfection). Cytokinesis and centriole positioning were recorded with a Leica AF6000 LX wide-field microscope system, consisting of an inverted DMI 6000B microscope equipped with a DFC350 FX monochrome digital camera and a climate chamber. 3D time-lapse image stacks were collected from up to 4 positions, each stack containing about 10 optical sections with approximately 1µm thickness, every 10 min, for up to 6 hrs. Images were collected with 63x objective, using differential interference contrast (DIC) transmitted light, a B/G/R filter with separate FITC excitation and TexasRed filter. The LAS AF software was used to project and process the collected time-lapse images and to generate movies. The time intervals and the volume imaged were kept to a minimum, to reduce illumination of cells in culture and fluorescence excitation as those factors are known to induce the formation of radicals and photo damage (Figure 6).

The tracking software Stacks (Vrolijk *et al., Manuscript in preparation*) was used to calculate and register the centriole mobility. This program allows the visualization of time-lapse 2D and 3D image data, offers movie facilities, and provides great flexibility to enhance, process and analyze image stacks.

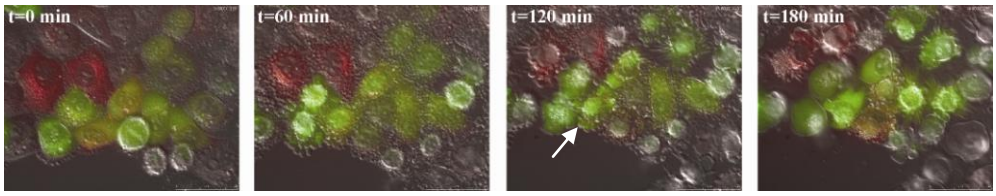

Figure 6: Phototoxicity introduces stress that can lead to apoptosis. Stable centrin1-EGFP (green) HeLa cell line transfected with mCherry-α-Tubulin (red) imaged every 10 min for 3 hrs. After 60 min the overexpressing cells show stress-induced phenotype, characterized as membrane blebbing (white arrow), and start dying after 120 min. Most cells show blebs and are dead after 180 min.

Quantification of the centriole movements

In order to track the centrioles they were segmented from the background. The software offers various methods to perform this operation. Global thresholding based on the image background was applied for the complete data set, and additionally the threshold was adjusted per individual image. Often it was easier to segment the centrioles from the background after applying 2D top-hat transformation to reduce the fluorescence fluctuations in the background. Other image transformations are also accessible within the software for enhancement, such as convolution filters, Foeriër filters, contrast enhancement and min-max filter operations. A more automatic segmentation method is a 2D and 3D watershed algorithm, which detects the centrioles as being local maxima in the 2D and 3D image sets and can find the borders of their domains as being the watershed lines between individual centrioles. Within each domain a local threshold is automatically determined to segment the centrioles from the background. The advantage of the watershed algorithm is that touching centrioles are often correctly separated.

Following segmentation the position, size and total density of every centriole was measured for all time points. Every identified centriole was assigned with a unique pseudo-color so that the centrioles could be classified as being the same when scrolling between time points. The tracks were then determined by linking the centrioles between successive time points, which have the highest probability based on previous measurements. By manual interactions tracks were split and reconnected to correct for errors made by the automatic procedure (Figure 7).

Figure 7: Tracking of centrioles during cytokinesis. Representative images of centriole tracks in living cells 30, 80 and 130 min after telophase onset. i) centiole (green), ii) overlay of centrin1-EGFP (green) and DIC and iii) an overlay of the centrin1-EGFP (green), DIC and the tracks of the centrioles for 130 min, from the onset of telophase. The table in the lower panel represents numerical values of the tracks, calculated by the software Stacks. Color of the numerical values represents the same colored track in the upper panel.

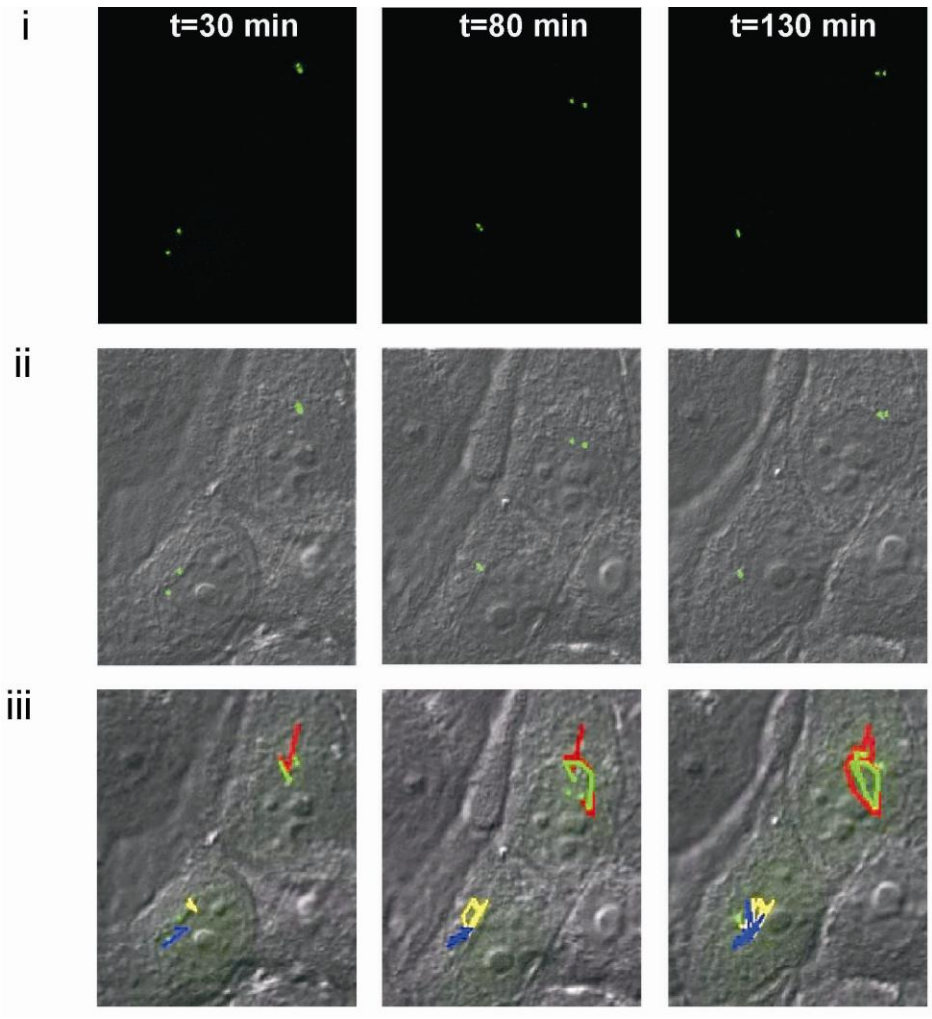

Function	Item	t=10 min	t=20 min	t=30 min	t=40 min	t=50 min	t=60 min	t=70 min	t=80 min	t=90 min	t=100 min	t=110 min	t=120 min
Distance (µm)	centriole 1	5,980	1,511	2,031	2,280	5,159	2,275	1,688	4,037	3,174	2,111	2,129	3,130
MSDp (µm²)	centriole 1	9,792	31,582	64,972	111,698	176,645	253,509	338,573	442,499	558,934	688,556	829,685	994,684
MSDt (µm2)	centriole 1	9,792	15,213	23,520	29,435	33,600	29,045	24,139	16,094	13,221	8,712	14,527	16,993
Distance (µm)	centriole 2	0,537	3,199	1,757	2,329	4,846	0,417	0,395	2,027	3,862	2,476	1,936	0,479
MSDp (µm2)	centriole 2	6,688	23,124	44,890	73,679	111,236	155,076	209,254	277,536	359,628	445,234	531,250	627,232
MSDt (µm2)	centriole 2	6,688	11,421	17,210	21,396	22,687	20,104	15,205	9,905	10,378	7,397	10,637	13,406
Distance (µm)	centriole 3	1,474	1,808	2,664	2,078	4,522	5,864	3,702	0,413	3,097	4,249	3,992	0,836
MSDp (µm2)	centriole 3	9,441	32,851	70,296	124,001	195,450	284,478	380,435	488,278	613,526	751,929	905,606	1,056,281
MSDt (µm2)	centriole 3	9,441	7,863	10,253	15,952	14,175	20,002	17,511	21,903	21,964	22,122	24,113	23,099
Distance (µm)	centriole 4	1,554	3,853	1,250	1,790	1,000	0,398	3,348	5,223	3,380	4,704	4,597	1,692
MSDp (µm2)	centriole 4	9,270	36,262	79,810	139,948	211,323	297,684	394,026	497,083	617,800	767,006	918,546	1,061,388
MSDt (µm2)	centriole 4	9,270	6,365	8,449	6,178	6,134	10,231	6,838	10,236	5,362	7,034	5,812	4,306

Finally kinetic parameters such as distance, the mean squared distance (MSDt) and the mean squared displacement (MSDp) were measured to characterize the movement of every individual centriole (Figure 7, lower panel). The distance is the Euclidian distance a centriole has moved between two adjacent time-points of a centriole. MSDt is calculated by averaging the squared distances calculated by taking the Euclidean distance between all time points = i. MSDt(1) = i+1, MSDt(2) = i+2, etc. MSDp(1) is calculated by averaging the squared distance a centriole has moved between all two successive time points, MSDp(2) by averaging the squared distance after summing the distances over all 3 successive time points, etc. Thus the MSDp function is a measure of the movement of the centriole by determining the length of the path that a centriole moves in time and was used to quantify the mobility of the centrioles during cytokinesis.

Evaluation of ploidy from flow cytometry histograms

DNA content of breast carcinomas were estimated from available flow cytometry histograms at the Department of Pathology, Landspitali University Hospital, Reykjavik, Iceland. The histograms were classified as diploid when showing a single G_0/G_1 peak. Cancer samples with at least two clear distinct peaks were classified as aneuploid. When the ratio between two distinct peaks was 1.80-2.10, and therefore the DNA content in the cells in the second peak about twice as much as in the normal peak, the cancer was classified as tetraploid. Cancers containing both aneuploid and tetraploid cells were classified as mixed aneu- and tetraploid.

RESULTS

1 CELL DIVISIONS OF PRIMARY HUMAN BRCA2 HETEROZYGOUS CELLS (PAPER I)

The aim of this study was to investigate the role of BRCA2 in cytokinesis by studying the effect of BRCA2 haploinsufficiency on the process of cytokinesis of primary human cells.

In paper I (*BRCA2 Heterozygosity Delays Cytokinesis in Primary Human Fibroblasts*) it is shown that cytokinesis was prolonged in primary human fibroblasts heterozygous for a mutation in the *BRCA2* gene. Cell divisions were monitored with bright-field time-lapse microscopy and cell division time was estimated from the images collected. Localization of the BRCA2 protein during this process was subsequently investigated.

The cell division time (Figure 8) of *BRCA2* cells ($BRCA2^{+/-}$), carrying either the Icelandic *999del5* founder mutation (FIS1) or *1537del4* mutation (FNE1), was compared to *BRCA2* wild type cells ($BRCA2^{+/+}$), FIS2 and FNE2.

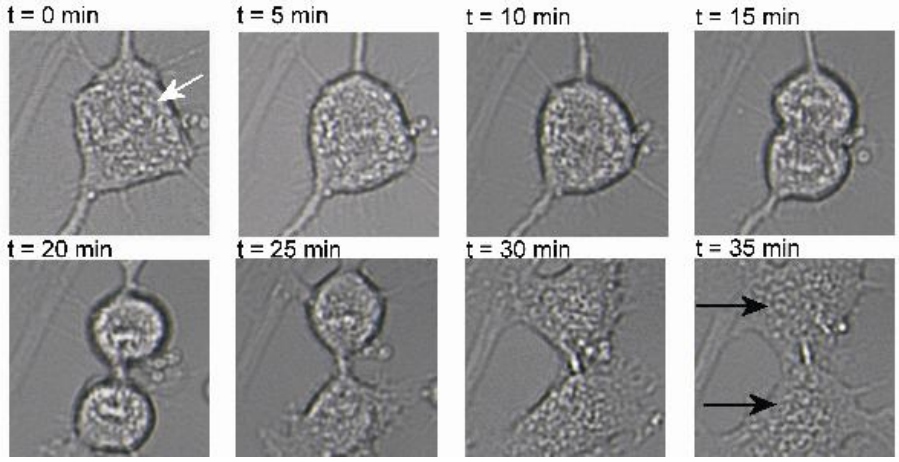

Figure 8: Cell division of primary human fibroblast cell. The cell division starts when the chromosomes that are lined up in an equatorial plane of the dividing cell (t=0 min, indicated by white arrow) start to separate (t=5 min) and continues until the two nuclei have formed (indicated by black arrow after 35 min) and the cytoplasm of the daughter cells has separated.

The mean cell division time was significantly longer in the mutated cells (*P*-value < 0.01), which showed a subset of cells with delayed cytokinesis (40 min or longer)

(Figure 9A). The average division time was 6 min longer, for *BRCA2* heterozygous (*BRCA2*$^{+/-}$) cells (33 min) than for *BRCA2*$^{+/+}$ cells (27 min) (Figure 9B).

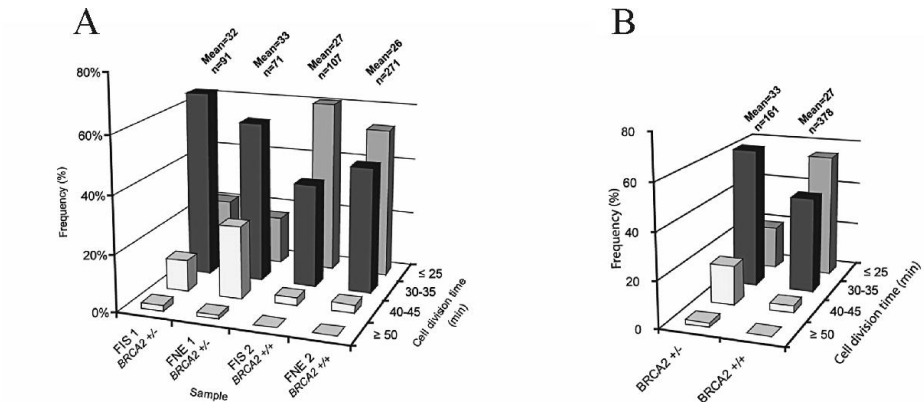

Figure 9: Frequency distribution of cell division time of primary human fibroblasts. A) The two *BRCA2*$^{+/-}$ samples, FIS1 and FNE1, show higher frequency of cells with delayed cytokinesis (> 40 min) than the two *BRCA2*$^{+/+}$ samples, FIS2 and FNE2. B) The *BRCA2* heterozygous cells have a significantly longer cell division time than the *BRCA2* wild type cells, 6 min on average.

To investigate further how the BRCA2 protein was involved in cytokinesis we studied the localization of the protein during the process by performing immunofluorescent staining using an antibody directed against the BRCA2 protein. In interphase cells, the protein showed scattered distribution, mainly nuclear. During anaphase the protein both dispersed throughout the midzone and accumulated to the intercellular bridge, adjacent to the Aurora-B kinase, as cytokinesis proceeded (Figure 10). No detectable difference was seen in the distribution pattern between *BRCA2*$^{+/+}$ and *BRCA2*$^{+/-}$ cells.

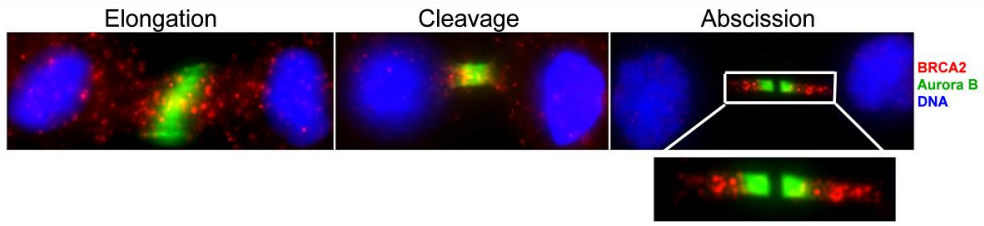

Figure 10: BRCA2 protein distribution in primary human fibroblasts during the final stages of cell division. In early steps of cytokinesis BRCA2 (red) is distributed throughout the nucleus (blue) and at the spindle midzone. As the process procedes the accumulation of the protein to the midbody increases and it concentrates adjacent to the Aurora B kinase (green) in the final stage of the process.

Quantitative real-time polymerase chain reaction (qRT-PCR) was performed on both the *BRCA2*$^{+/+}$ and *BRCA2*$^{+/-}$ samples to measure the *BRCA2* mRNA expression

levels. The *BRCA2* heterozygous mutant samples were observed to have significantly lower *BRCA2* mRNA expression (*P*-value 0.03), 0.167 and 0.254 versus 0.987 and 1.00, respectively (Figure 11).

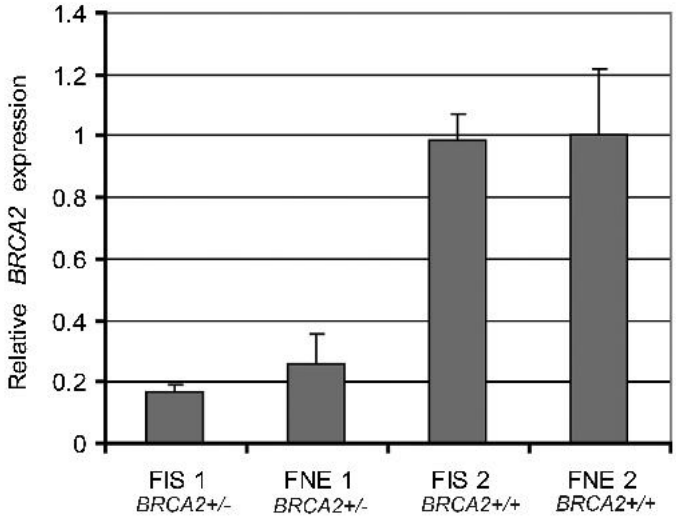

Figure 11: BRCA2 mRNA expression levels of BRCA2+/- and BRCA2+/+ primary human fibroblasts quantified with RT-PCR. The two BRCA2+/- samples, FIS1 and FNE1, show on average 5 times lower BRCA2 expression than the two BRCA2+/+ samples, FIS2 and FNE2.

Ploidy aberrations can be caused by either defect in cytokinesis or DNA replication. Polyploid cells often undergo apoptosis. We therefore estimated the frequency of aneuploid cells by propidium iodine (PI) staining and flow cytometry. This was followed-up by live-cell imaging with PI and Annexin V, to investigate the levels of aneuploid and apoptotic cells, respectively. The $BRCA2^{+/-}$ samples had a non-significant increase of cells in G_2/M, 3.8 times higher than for $BRCA2^{+/+}$ samples. Hardly any apoptotic cells were found, neither for the *BRCA2* heterozygous nor the wild type cells.

Collectively, these results indicate that the BRCA2 protein participates in and may facilitate cytokinesis in unmodified human cells.

2 CENTRIOLE MOBILITY DURING CYTOKINESIS (PAPER II AND UNPUBLISHED DATA)

BRCA2-mutated tumors and cell lines have been shown to have supernumerary centrosomes (Tutt *et al.*, 1999). BRCA2 has been shown to have a centrosomal localization signal and to localize to the centrosome during S and early M phases of

the cell cycle (Nakanishi *et al.*, 2007). Tetraploid cells frequently contain two or more centrosomes. Aneuploid cells can develop through the tetraploid route, or they evolve directly from diploid cells, possibly as a consequence of multipolar spindle or spindle checkpoint failure, resulting in missegregation of chromosomes. It is therefore of great relevance to study the centrosomes when investigating both cytokinesis and polyploidy.

2.1 BRCA2 and the centrosomes (unpublished data)

A number of centrosomal proteins exhibit cell-cycle–dependent, dynamic behavior in that they are sequentially present at more than one location in the mitotic apparatus. We found that BRCA2 undergoes a similar dynamic behavior. Previously we had seen the protein accumulate to the midbody of cells in cytokinesis. Our preliminary results from fixed material stained with antibodies directed against BRCA2 and γ-Tubulin as a centrosome marker, showed an accumulation of BRCA2 at the centrosomes, both during interphase (Figure 12A) and at the cell poles in mitotic cells (Figure 12B-D). Also, the BRCA2 protein localized at the newly formed nuclear envelope (Figure 12B&C, arrows) (Stainings performed by Federica Alberghini (Alberghini, 2008)).

Based on these data and given that a centriole had to reposition from the cell poles to the cleavage site before daughter cells separate (Piel *et al.*, 2001), we reasoned that BRCA2 modulates the dynamics of the midbody and functions in cytokinesis via the centrioles. Therefore we performed the following experiments.

To examine the effects of BRCA2 loss-of function on centriole movements and time to complete the process, p53-deficient mouse mammary tumor cell lines, which were wild type, heterozygous or homozygous for *Brca2* were used, but no such cell lines or cell models were available from human cells. Centriole movements and positioning during cytokinesis were monitored by time-lapse microscopy.

The mouse epithelial cell lines were characterized to investigate if they displayed similar phenotypes as have been described for human cell lines and tumors deficient for *BRCA2*. By monitoring the cells with bright-field time-lapse microscopy the mouse cells deficient for *Brca2* were found to have prolonged cell division time (Figure 13A). Immuno-fluorescence staining directed against γ-Tubulin to detect the centrosome, revealed that in the $Brca2^{-/-}$ mouse epithelial cells centrosome amplification was 3 times more frequent than in $Brca2^{+/+}$ cells and 2 times more frequent in $Brca2^{+/-}$ cells (Figure 13B). The nuclea-tion of the cells was investigated by fixing cultured cells and mount with nuclear stain (DAPI). Bi-nucleated cells were detected 2 times more frequently in $Brca2^{+/-}$ cells than in

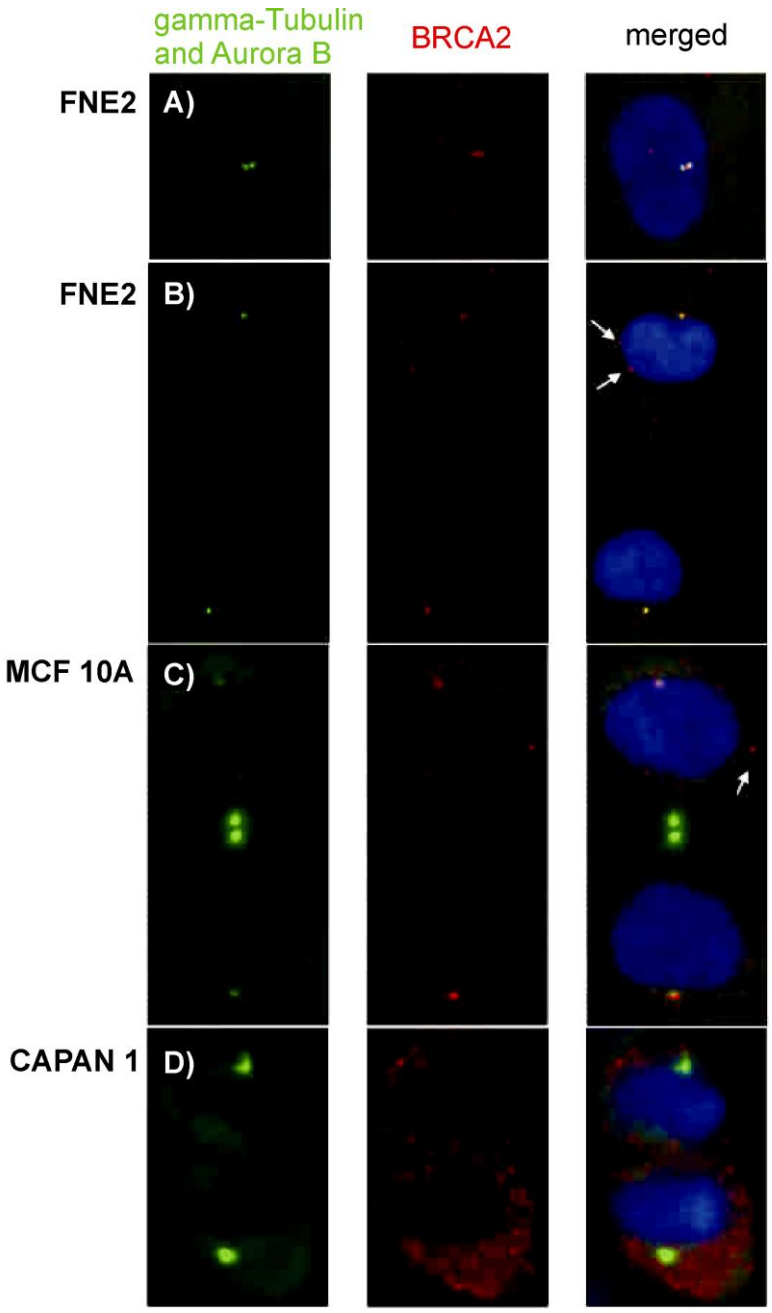

Figure 12: BRCA2 and the centrosome. A) FNE2, a primary human fibroblast, in interphase. BRCA2 (red) localizes to the centrosome (green), seen as yellow on merged image. B) FNE2 and C) MCF10A, human epithelial cell, in telophase. BRCA2 localized to the centrosome at the cell poles and also by the newly formed nuclear envelope, possibly going towards or away from the intercellular bridge (arrows). D) Capan 1, an epithelial BRCA2 deficient cell line. No staining of BRCA2 at the cell poles during telophase. Aurora B localizes to the intercellular bridge is green and is used as a marker for cytokinesis, DNA is stained blue. (Figure adjusted from Federica Alberghinis' junior research project (Alberghini, 2008)).

other cell lines studied and multi-nucleation was found to be 7 and 3.5 times more frequent in *Brca2*$^{-/-}$ than in *Brca2*$^{+/+}$ and *Brca2*$^{+/-}$ respectively (Figure 13C). Micronuclei were detected 5-6 times more frequently in *Brca2*$^{-/-}$ and *Brca2*$^{+/-}$ cells than in the *Brca2*$^{+/+}$ cells (Figure 13C). All these phenotypes can either be a cause or a consequence of polyploidy.

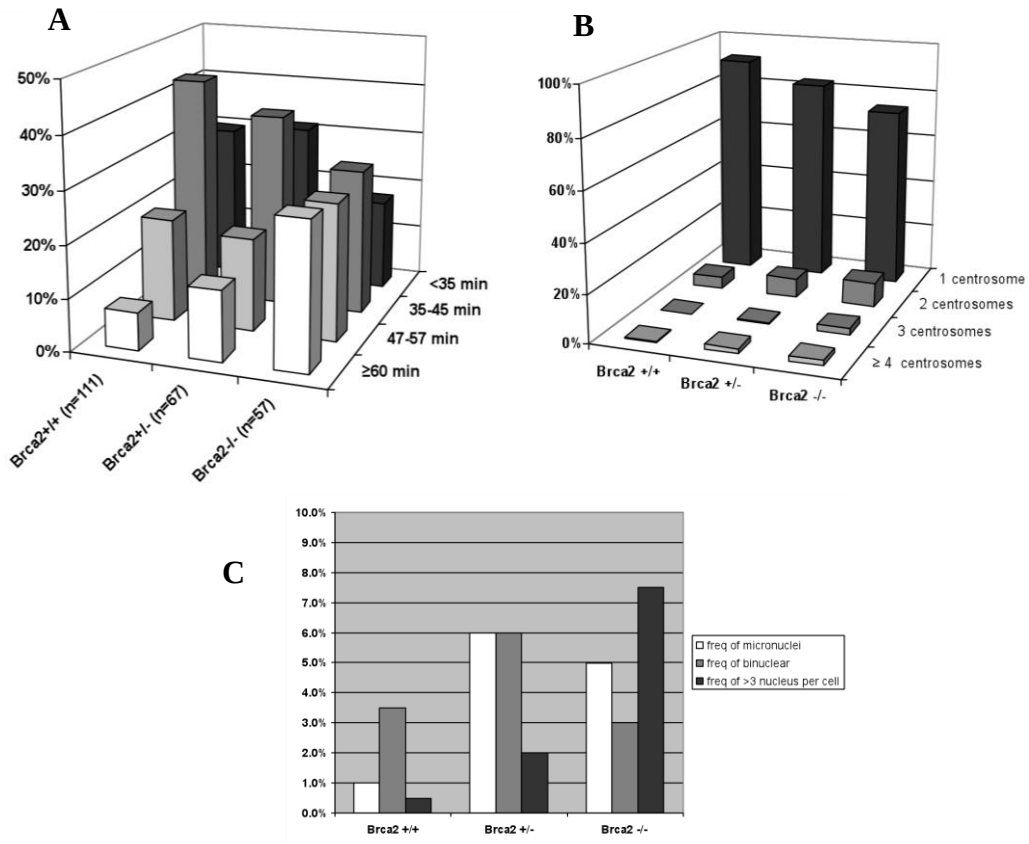

Figure 13: Characteristics of mouse p53-deficient Brca2 mouse mammary epithelial cell lines. A) Brca2 deficiency delays cytokinesis. B) The frequency of supernumerary centrosomes is highest in *Brca2*$^{-/-}$ cells. C) Bi- and multi- nuclear cells are frequent in *Brca2* heterozygous and homozygous mouse epithelial cells.

2.2 BRCA2 and the centrioles during cytokinesis (paper II and unpublished data)

In order to investigate if and then how Brca2 was involved in regulating and/or facilitating cytokinesis through the centrosome, the *Brca2*$^{+/+}$, *Brca2*$^{+/-}$, and *Brca2*$^{-/-}$ mouse epithelial cell line model was used. The cell lines were transiently co-transfected with centrin1-EGFP and α-Tubulin-mCherry expression constructs to recognize the centrioles and intercellular bridge, respectively. Centriole mobility was analyzed from 3D image stacks collected by time-lapse live-cell microscopy

every 10 min for 4 to 6 hrs, using both fluorescence excitation to detect centrioles and microtubules and DIC. DIC images allowed identification of the nuclear envelope, movements of cells and their progression through mitosis.

In agreement with previously published data (Piel *et al.*, 2001) we observed in 90% of dividing cells the separation of mother and daughter centrioles, which occurs after formation of the cleavage furrow. Despite being very mobile, migration of a centriole from the cell pole to the intercellular bridge, as observed by Piel *et al.*, was not seen in any of the *Brca2*$^{+/+}$ cells imaged that completed abscission (Figure 14).

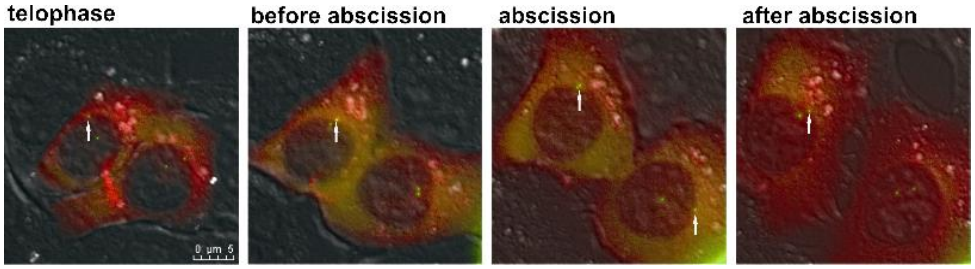

Figure 14: Centriole positioning in mammary mouse epithelial cells during cytokinesis. The centrioles are very mobile and are frequently associated with the nuclear envelope (white arrows). The images show an overlay of DIC, green, a centriole-specific centrin1-EGFP and red, an intercellular bridge marker α-Tubulin-mCherry.

The preliminary time-lapse imaging results of the *Brca2*$^{+/+}$ cell line suggested that studies of the movements of centrioles in this cell line model would not inform us about the function of the Brca2 protein in mitotic exit, as expected. Therefore, centriole movements in the *Brca2*$^{+/-}$ or *Brca2*$^{-/-}$ mouse cell lines during cytokinesis were not investigated further.

2.3 Centriole movements in mammalian epithelial cells during cytokinesis (paper II)

Subsequently, cytokinesis and centriole mobility and positioning were studied further and analyzed in various human epithelial cell lines. We asked whether the migration of a centriole to the intercellular bridge was required for cytokinesis exit.

In paper II (*Centriole movements in mammalian epithelial cells during cytokinesis*) we show that centrioles are very mobile during cytokinesis and that their movements are either along the nuclear envelope, irregular or along microtubules forming the spindle axis. Cell divisions and centriole mobility were monitored with time-lapse imaging and the centriole mobility was evaluated with the tracking software Stacks.

The human mammary epithelial MCF 10A cells and HeLa cells, both expressing centrin1-EGFP and α-Tubulin-mCherry were imaged in the same manner as the mouse epithelial cells (Result chapter 2.2). As a control for transient transfection

HeLa cells stably expressing centrin1-EGFP were used. The centrin1-EGFP HeLa cell line is the same as was used in the original study by Piel *et al.* (Piel *et al.*, 2001).

A centriole migrated to the intercellular bridge in 3 out of 11 (27%) MCF 10A cells that completed abscission, the termination step of cytokinesis. This occurred 2 times more frequently in HeLa cells and no considerable difference was found between HeLa cells transiently or stably expressing centrin1-EGFP (50 versus 55% respectively) (Table 2).

Our observations are not in accordance with published observations and we conclude that relocation of centrioles to the intercellular bridge it is not essential for completion of cytokinesis.

Table 2: Frequency of centriole(s) at the intercellular bridge of various mammalian epithelial cell lines

	Mobile centriole(s) at the intercellular bridge				
Cell line	from one daughter cell	from both daughter cells	Mobile centriole(s) not observed at the intercellular bridge	Immobile centrioles	Total
KP 7.7	0 (0%)	0 (0%)	7 (58%)	5 (42%)	12 (100%)
MCF 10A	2 (18%)	1 (9%)	7 (64%)	1 (9%)	11 (100%)
HeLa	5 (31%)	3 (19%)	3 (19%)	5 (31%)	16 (100%)
centrin1-EGFP HeLa	10 (46%)	2 (9%)	6 (27%)	4 (18%)	22 (100%)

By analyzing the movements of centrioles in both mouse and human epithelial cells, three main types of movements were detected: 1) migration along the nuclear envelope (Figure 15A), 2) migration along microtubules forming the spindle axis (Figure 15B) and 3) irregular movements, where centrioles moved in the cytoplasm or cell center with no specific direction.

Centrosomes that associated with and migrated along the nuclear envelope were detected in 58% of mouse cells, 62% of MCF10A, 75% of HeLa cells and 44% of imaged centrin1-EGFP HeLa cells. Following abscission, the centrioles and even the whole centrosome became more mobile and detached frequently from the nuclear envelope.

To circumvent subjective assessment of centriole mobility a quantitative analysis was performed using the tracking software Stacks (see Figure 7). Kinetic parameters, such as the distance a centriole moved between each time point and mean squared displacement (MSDp), were calculated to characterize the movement of every individual centriole, 4 in total for every cell. The centriolar mobility was

estimated for all cell lines and the tracking revealed that the mouse cells had the most mobile centrioles, moving 0.35 µm/min on average, which was on average 1.5-2.7 times faster than for the human epithelial cell lines.

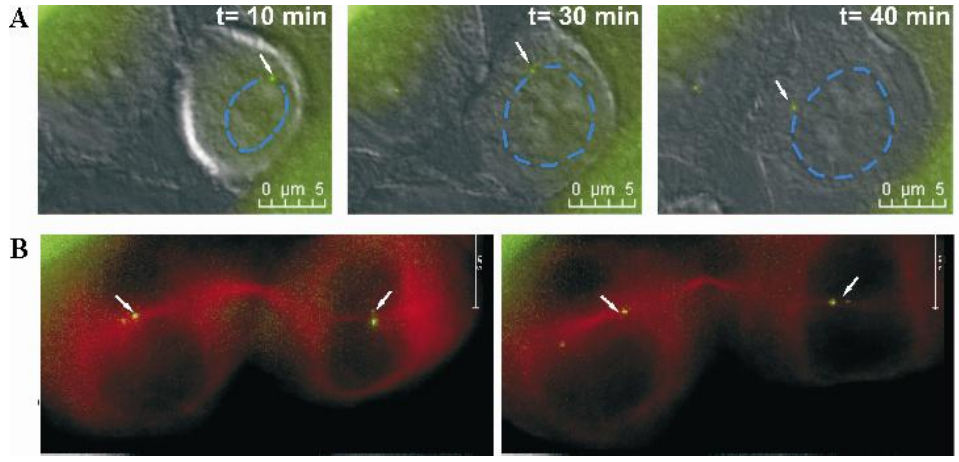

Figure 15: Centriole movements in mammary epithelial cells. A) Centrioles migrating along the nuclear envelope (emphasized by blue dotted line) (white arrow). The images show an overlay of centrin1-EGFP (green) and DIC. B) Centrioles in a dividing cell reposition from the cell pole through the cell center towards the intercellular bridge along microtubules (white arrows indicate centrioles migrating along α-Tubulin).

3 PLOIDY ABERRATIONS IN BRCA2-MUTATED BREAST CANCERS (PAPER III AND UNPUBLISHED DATA)

Impaired cytokinesis is one of the main routes to tetraploidy in cells. Carcinomas frequently have altered ploidy. To follow-up our finding that the BRCA2 tumor suppressor has a role in completion of cell division, we studied ploidy in *BRCA2*-mutated and sporadic female breast cancers.

In paper III (*Tetraploidy in BRCA2 breast tumours*) ploidy in female breast cancers from carriers of a *BRCA2* germline mutation was compared with sporadic breast cancers. Flow cytometry histograms indicating DNA content were used to estimate ploidy. Ploidy status was evaluated from 236 breast cancer patients, 71 of which were *BRCA2* mutated. Also, ploidy aberrations in association with the molecular classification of the cancers were examined for a subset of the samples.

For both *BRCA2*-mutated and sporadic cancers, less than half were diploid (42.3% (30 of 71) and 47.9% (79 of 165) respectively). There was not an overall association with *BRCA2* mutation status and ploidy aberrations (χ^2 -test 6.18, *P*-value = 0.103), but the proportion of tetraploid cancers was significantly higher in *BRCA2*-mutated breast

cancers than sporadic, where the difference was 2.9 fold, 14.1% (10 of 71) versus 4.8% (8 of 165) (χ^2 -test 4.77, *P*-value = 0.029) (Figure 16). Aneuploidy was of similar frequency in both groups, 33.8% (24 of 71) in *BRCA2*-mutated compared with 38.2% (63 of 165) in sporadic breast cancers, and so was the proportion of mixed aneu-and tetraploid cancers, 9.9% (7 of 71) versus 9.1% (15 of 165), respectively (Figure 16).

In summary, the results indicate that *BRCA2* cancers are more likely to become tetraploid compared with sporadic cancers.

Molecular classification based on ER, PR and HER-2 expression was available for 52 of the *BRCA2* mutated and 43 of the sporadic cancers. Ploidy aberrations in relation with the molecular phenotypes and the *BRCA2* status were investigated.

Thirty-seven of the 52 *BRCA2*-mutated cancers were of luminal phenotype (71.1%), the majority (54.1%) of these tumors was diploid, 13.5 % were aneuploid or mixed aneu-and tetraploid. Notably, 18.9% (7 of 37) were tetraploid (Figure 17A). Of the 15 *BRCA2*-mutated cancers that were classified as triple-negative (TNP), only 3 (20%) were diploid and 11 (73.3%) were aneuploid, which is a five times higher proportion than among luminal *BRCA2* cancers. None of the TNP cancers were tetraploid and only one was mixed aneu- and tetraploid (Figure 17A). Tetraploidy is therefore much more prominent in luminal than TNP *BRCA2* cancers.

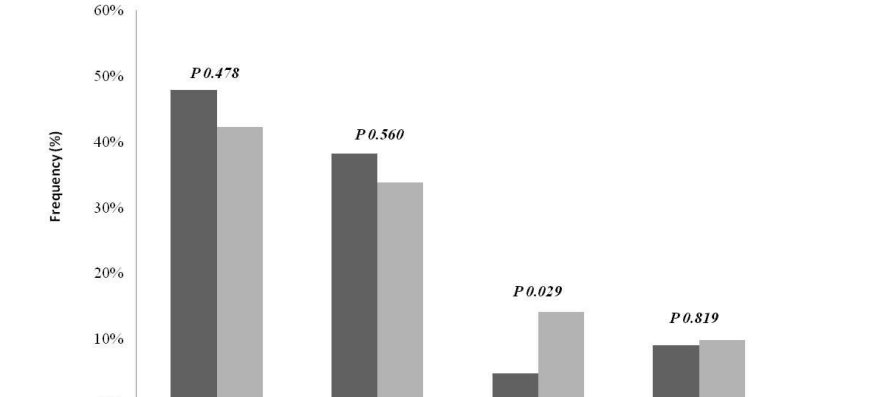

	Diploid	Aneuploid	Tetraploid	Mixed Aneu- and Tetraploid	Total
Sporadic	79 (47.9%)	63 (38.2%)	8 (4.8%)	15 (9.1%)	165 (100%)
BRCA2 mutated	30 (42.3%)	24 (33.8%)	10 (14.1%)	7 (9.9%)	71 (100%)
Total	109	87	18	22	236

χ^2test statistic 6.18, *P*-value 0.103

Figure 16: Ploidy distribution of sporadic (dark grey) and BRCA2-mutated (light grey) breast cancers. The proportion of diploidy, aneuploidy and mixed aneu- and tetraploidy was similar in sporadic and BRCA2 cancers. Tetraploidy was 2.9 fold higher in BRCA2 cancers compared with sporadic cancers (P-value 0.029), see details in table in lower panel.

For comparison we investigated whether sporadic breast cancers showed the same trend as was observed in *BRCA2* cancers. We studied ploidy in phenotypic-similar sporadic cancers, that is, those displaying either luminal or TNP phenotype. Of the 43 sporadic cancers, 29 (67.4%) were luminal and 8 (18.6%) TNP. Similar to *BRCA2* mutated cancers the majority (58.6%) of the luminal cancers were diploid. Only one sporadic cancer within the luminal subtype displayed tetraploidy. The sporadic luminal-type cancers were much more frequently aneuploid (Figure 17 B). Thus, the differences observed in sporadic cancers in terms of molecular phenotype and ploidy were contrary to those seen in *BRCA2* cancers.

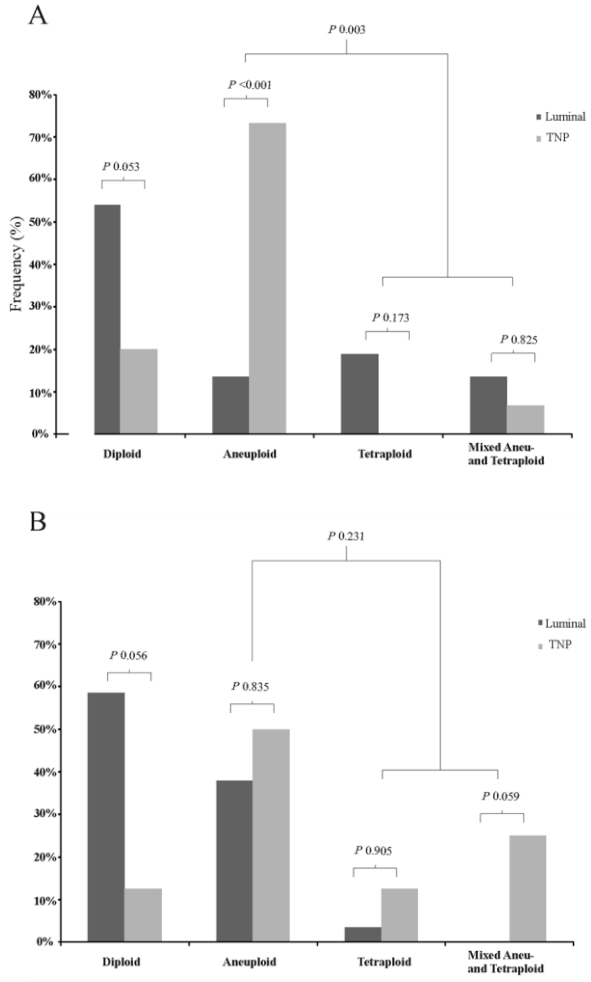

Figure 17: **Ploidy and Phenotype: Ploidy distribution of (A) *BRCA2*-mutated and (B) Sporadic breast cancers, in relation to molecular subtype. Dark grey bars represent luminal subtype and light grey triple-negative (TNP). A strong association was seen between luminal phenotype and tetraploidization. Tetraploidy or mixed aneu-and tetraploidy occurred only in *BRCA2* mutated cancers (P-value 0.003), and TNP phenotype and aneuploidy (P-value <0.001). For both study groups TNP was rarely diploid.**

Cell cycle progression of cells that carry a somatic mutation in the gene encoding the tumor suppressor p53, in addition to other genomic alterations, can lead to polyploidization (Storchova and Pellman, 2004). *TP53* mutations are highly correlated with ploidy aberrations in solid tumors. Genomic instability, including aneuploidy, in breast tumors from *BRCA2* mutation carries is highly associated with somatic *TP53* mutations (Gretarsdottir *et al.*, 1998). We investigated whether there was a correlation between polyploidy in *BRCA2*-mutated cancers with p53 aberrations. *TP53* status-information (examined with sequencing of the most frequent mutation sites) was only available for 59 breast cancer samples (25.0%), 40 sporadic and 19 *BRCA2*-mutated. Nine of the 19 (47%) *BRCA2*-mutated samples were *TP53* mutated. Of the sporadic cases, 25% were *TP53* mutated. All *BRCA2*-mutated breast tumors with additional *TP53* mutation were polyploid and all except one *TP53* mutated sporadic case were polyploid, with aneuploidy of highest frequency in both groups (Table 3).

Table 3: ***TP53* status of breast carcinoma samples, related to ploidy and the presence or absence of *BRCA2* aberrations.**

	Diploid		**Aneuploid**		**Tetraploid**		**Mixed Aneu- and Tetraploid**		
	BRCA2 wild type	*BRCA2 mut*	*BRCA2 wild type*	*BRCA2 mut*	*BRCA2 wild type*	*BRCA2 mut*	*BRCA2 wild type*	*BRCA2 mut*	Total
p53 wild type	14 (45.2%)	5 (50.0%)	1 (3.2%)	2 (20.0%)	14 (45.2%)	2 (20.0%)	2 (6.5%)	1 (10.0%)	41
p53 mut	1 (11.1%)	0 (0.0%)	6 (66.7%)	6 (66.7%)	0 (0.0%)	2 (22.2%)	2 (22.2%)	1 (11.1%)	18
Total	15	5	7	8	14	4	4	2	59

Taken together, we have studied cytokinesis and the potential consequences of cytokinesis defects by examining cell division time and ploidy aberrations respectively. We have obtained evidence for a function of the BRCA2 protein in cytokinesis. Our results suggest that the high frequency of tetraploidy in *BRCA2* associated tumors may be linked with cell division errors, particularly deficient cytokinesis.

DISCUSSION AND CONCLUSIONS

In this thesis I present that a *BRCA2* heterozygous mutation in unmodified human fibroblasts delays cytokinesis significantly. The BRCA2 protein was found to localize to the midbody and the centrosomes of dividing cells. I address whether BRCA2 functions in cytokinesis by associating with the centrosomes. BRCA2 was found to accumulate at the centrosomes, but a connection between a function of BRCA2 and the centrosomes during cytokinesis could not be confirmed. The centrioles, the central components of the centrosomes, were shown to be highly mobile during cytokinesis and were shown to migrate along microtubules and the nuclear envelope. *BRCA2*-mutated breast carcinomas of luminal subtype showed an increased frequency of tetraploidy, a phenotype that can be caused by cytokinesis defects. Collectively, the results in this thesis indicate a role for the BRCA2 protein in cytokinesis, observed as delayed cell division time and higher proportion of tetraploidy in *BRCA2* mutated material. However this is not mediated by an association with centrosomes and repositioning of a centriole to the intercellular bridge. Also that relocation of a centriole to the intercellular bridge is not essential for controlling cytokinesis exit (abscission).

1 BRCA2 AND CYTOKINESIS

Carriers of germline mutations in the *BRCA* genes are predisposed to carcinomas. The increased cancer susceptibility has been attributed to functions of the BRCA proteins in repair of DNA double strand breaks, via homologous recombination. Defects in the repair mechanisms can alter recombination pathways, giving rise to chromosomal re-arrangements, which have been stated as the main cause for chromosomal instability found in *BRCA2* tumors (Gretarsdottir *et al.*, 1998; Venkitaraman, 2002). *BRCA2* heterozygosity has been shown to account for reduced growth rate, increased cell death, heightened sensitivity to specific DNA damaging agents and reduced RAD51 foci formation after irradiation in vertebrate cells (Warren *et al.*, 2003). HeLa cells with the *BRCA2* gene silenced with small interfering RNA were found to have delayed and incomplete cytokinesis and to accumulate binucleated cells (Daniels *et al.*, 2004). The same phenotype was observed in MEFs deficient for *Brca2*. Also, $Brca2^{+/-}$ MEFs were observed to have longer cell division time than $Brca2^{+/+}$ MEFs (Daniels *et al.*, 2004). We investigated whether heterozygous cells from *BRCA2* mutation carriers displayed similar defects

regarding cytokinesis. We observed that unmodified primary human fibroblasts obtained from carriers with two different *BRCA2* mutations, the Icelandic 999del5 deletion and the 1537del4 mutation that is frequently detected in *BRCA2* mutation carriers in The Netherlands, had significantly longer cell division time than non-*BRCA2* mutated fibroblasts. Notably, only a subset of the *BRCA2* heterozygous cells had delayed cytokinesis, which made the average division time longer. The *BRCA2*$^{+/-}$ cells also had significantly lower BRCA2 mRNA expression and slightly higher number of cells in G_2/M phase of the cell cycle than *BRCA2* wild type cells. Cell lines, generated by genetic modifications or transformed in a preferred way, can be of great use when studying biological processes. However, one should always ensure that such cell lines reflect the *in vivo* situation. Our results support a previous notion that the *BRCA2* gene product plays a role in cytokinesis, which had been suggested by using genetically modified cell lines (Daniels *et al.*, 2004), by studying unmodified patient material from biopsy samples from individuals that carry a mutation in the *BRCA2* gene.

Collectively, these data suggest that BRCA2 plays a role in cytokinesis. Thus, defects in daughter cell separation, which can cause binucleation and tetraploidy or missegregation of chromosomes giving rise to aneuploidy, could contribute to the increased cancer susceptibility in *BRCA2*-mutation carriers. As only a small subset of the *BRCA2*$^{+/-}$ primary cells had prolonged division time the impact of it for the individuals carrying a mutation in the *BRCA2* gene may not be severe.

As has been introduced *BRCA2* has many functional domains. It can therefore be critical where a mutation in the *BRCA2* gene is located. The Icelandic founder mutation in the *BRCA2* gene, a 5 base pair deletion starting at nucleotide 999 in exon 9 (Thorlacius *et al.*, 1996) leads to a stop codon and the protein product of *BRCA2 999del5* has been shown to be highly unstable and rapidly degraded (Mikaelsdottir *et al.*, 2004). It can be assumed that this applies also for other early truncating mutations. It is therefore to be expected that the effect of reduction of the BRCA2 protein increases the time to complete cytokinesis, but that the level of the protein is sufficient for the process. A full-length-BRCA2 expression construct with fluorescence tagged protein would be a useful tool to study the positioning, dynamics and protein-protein interactions of BRCA2 during cell division. However, no such studies have been published, possibly due to difficulties with cloning the full-length protein (390 kDa) and its low expression levels.

2 BRCA2, THE CENTROSOMES AND CELL DIVISIONS

The centrosomes play a crucial role in ensuring the integrity of cell division. They are important both for the reproduction of cells and organisms (Rieder *et al.*, 2001).

Nuclear and cytoplasmic signaling proteins concentrate on centrosomes and other elements of the mitotic apparatus during G_2 to M transition. After the onset of anaphase, recruitment of non-muscle myosin II drives equatorial furrowing in animal cells (Straight *et al.*, 2003). Numerous proteins involved in cytokinesis, cell cycle regulation and signaling accumulate at the midbody (Glotzer, 2005). With immunofluorescence microscopy using an antibody directed against BRCA2, the protein was found to concentrate at the centrosome in all phases of the cell cycle. Also, the BRCA2 protein was detected in the intercellular bridge of mitotic cells. The accumulation of BRCA2 at the midbody increased as the cytokinesis process proceeded. Therefore, we reasoned that BRCA2 acted as a signaling mediator or scaffolding protein during cytokinesis and suggested that it could potentially be involved in centriolar positioning and movements during the process. We addressed whether the BRCA2 protein functioned in cytokinesis in association with the centrosomes. A previous publication had shown that BRCA2 accumulated at the centrosomes during S phase and the beginning of M phase, before the chromosomes align in an equatorial plane (Nakanishi *et al.*, 2007). Reports of centrosomes that localize to a region adjacent to the intercellular bridge prior to abscission date back to 1973. At that time electron microscopy was applied to study centrosomes and their centrioles and it was noticed that in fixed cells in late cytokinesis the centrioles were seen near the midbody (Rattner and Phillips, 1973), and these observations were supported by later publications (Mack and Rattner, 1993; Ou and Rattner, 2002). Studies of living cells have also shown that abscission is initiated by the repositioning of one of the four centrioles to the intercellular bridge, when the cleavage furrow has been formed, and then back to the cell center (Piel *et al.*, 2001). We investigated the process of cytokinesis, with respect of centriole movements.

Centriole movements were studied in mammary mouse epithelial cell line model, *Brca2*$^{+/+}$, *Brca2*$^{-/+}$ and *Brca2*$^{-/-}$ expressing centrin1-EGFP. Repositioning of a centriole towards the intercellular bridge was not seen in any of the centrin1-EGFP expressing *Brca2*$^{+/+}$ cells imaged. The mouse cell line model was not investigated further. Thus we were not able to demonstrate that the function of BRCA2 during cytokinesis was linked to the centrosomes, or that the centriole movements during this process were facilitated by BRCA2. The study was continued by examining centriole movements in various epithelial cell lines, to investigate whether a relocation of a centriole to the intercellular bridge was a general mechanism controlling abscission. The centrioles were monitored in HeLa, MCF 10A, and the *Brca2*$^{+/+}$ p53-deficient mouse mammary tumor cell line KP-7.7, all of epithelial origin. Relocation of a centriole to the intercellular bridge was not found to be prerequisite for completion of abscission as this was only observed in 50-55% of

HeLa cells, 27% of imaged MCF 10A cells and never for KP-7.7. Based on the observed variations in centriole mobility in different epithelial cell lines we conclude that the movements of centrioles are highly cell line dependent. It has been stated that cytokinesis rarely fails in various mammalian cell lines, in which a centriole does not migrate towards the intercellular bridge (Rieder *et al.*, 2001). Furthermore, in another study a consistent movement of centrioles to the intercellular bridge was not observed (Gromley *et al.*, 2005). These results, together with ours reveal an inconsistency regarding the controlling mechanism of abscission with respect to the centrioles. We suggest that the relocation of a centriole to the intercellular bridge is not essential for mitotic exit.

Movements of centrioles to the intercellular bridge have been shown to be associated with microtubules, suggesting that they migrate along the microtubules as they relocate to the intercellular bridge (Mack and Rattner, 1993; Ou and Rattner, 2002). In agreement with this we characterized the movements of the centrioles during cell division as being mainly along microtubules containing α-Tubulin, and also along the newly formed nuclear envelope. In line with this, emerin has been found to associate with microtubules in human cells to link the centrosome to the nuclear envelope (Salpingidou *et al.*, 2007). Whether other proteins are involved in the controlled movement of centrioles along the nuclear envelope in mammalian cells remains to be determined.

3 BRCA2 AND POLYPLOIDY

Increased frequency of tetraploidy was found in *BRCA2*-mutated cancers, when compared with ploidy aberrations in sporadic cancers. Tetraploidy has not been reported specifically for *BRCA2* cancers before. Having observed delayed cytokinesis in primary human fibroblasts from *BRCA2* mutation carriers, we suggest that the tetraploidy may be linked with cell division errors, particularly cytokinesis. Tetraploidy was almost exclusively found in *BRCA2* cancers of a luminal subtype and differed from triple-negative *BRCA2* and luminal sporadic cancers, which mainly displayed diploidy or aneuploidy. During tumor progression genome aberrations that are the most advantageous for the proliferation of the tumor cells are selected for. Why tetraploidy is maintained (rather than going into aneuploidy) in luminal *BRCA2* cancers remains to be studied.

Recent studies have shown that the second *BRCA2* allele is not consistently lost in BRCA2 tumors (King *et al.*, 2007; Stefansson *et al.*, *Manuscript submitted*). Whether the second *BRCA2* allele is lost may be tumor-specific (King *et al.*, 2007), and also whether the loss of the second allele occurs as an early or a late event during cancer progression. The second event in tumorigenesis in carriers of a *BRCA*

mutation may involve the loss of checkpoint mechanisms before inactivation of the second *BRCA* allele (if it ever happens). One of the genes most commonly mutated in cancers is the tumor suppressor *TP53*. Loss or mutational inactivation of p53 results in supernumerary centrosomes in part via allowing the activation of the CDK2-cyclin E, which is a key factor for the initiation of centrosome duplication (Borel *et al.*, 2002; Tarapore and Fukasawa, 2002). Over half of the *BRCA2 999del5* breast tumors have been shown to be non-diploid and one third to have an additional *TP53* mutation, nearly twice as many as in the sporadic group (Gretarsdottir *et al.*, 1998). Unfortunately, we could not study any associations between the p53 aberrations, polyploidy and *BRCA2* mutation status in our study, as p53 status information was only available for few of the samples included. Thus, whether p53 aberrations are associated with polyploidy, centrosome amplification, or provoke the proliferation of the luminal *BRCA2* tumors remains to be studied.

Failure of cytokinesis can lead to tetraploidy, giving rise to bi- and multinucleated cells that contain increased number of centrosomes. Binucleated cells can form mononucleated tetraploids after successful passage through the next mitosis (Storchova and Kuffer, 2008). There is limited evidence linking cancer-causing mutations with formation of tetraploid cells. Adenomatous polyposis coli (APC) mutations in mouse colorectal cancer cells have been shown to inhibit cytokinesis, by blocking initiation of furrowing, resulting in increased frequency of tetraploidy (Caldwell *et al.*, 2007). *In vitro* studies of epithelial crypt cells expressing dominant-negative APC^{1-1450} mutation showed increased numbers of bi- and multinucleation in these cells and cytokinesis failure. *In vivo* examination of epithelial cells within the intestinal crypt of $APC^{MIN/+}$ mice showed that they had misoriented mitotic spindles making them prone to cytokinetic failure and tetraploidy (Caldwell *et al.*, 2007). Based on this, it could be interesting to screen histology slides of the tetraploid *BRCA2* tumors for the frequency of bi- and multinucleated cells, which could give information whether the tetraploidy is due to defects in cytokinesis.

Cytokinesis can fail because of defects in- or deficiency of proteins mediating cytokinesis. Also, chromosome bridges formed during anaphase can cause furrow regression leading to the generation of binucleated cells. BFB cycles are more common in breast tumors from *BRCA2* carriers than in sporadic breast tumors (Eyfjord and Bodvarsdottir, 2005; Patel *et al.*, 1998; Yu *et al.*, 2000). Fused chromosomes frequently contain two or more centromeres, which makes segregation of sister-chromatids during mitosis difficult. The high degree of chromosomal re-arrangements and other genetic instability in BRCA2-deficient cell lines and tumors has been explained by repair of DNA double strand breaks via error-prone non-homologous end joining (Storchova and Pellman, 2004; Yu *et al.*, 2000). More

thorough studies on the chromosomal aberrations and the presence of anaphase-bridges in cells heterozygous for a mutation in the *BRCA2* gene might explain whether they induce a delay in cytokinesis.

Collectively, the data in this study indicate that defects in cytokinesis can contribute to the increased cancer susceptibility in carriers of a *BRCA2* mutation.

CONCLUSIONS

In this research project live-cell microscopy has been used to collect information about cytokinesis. The main findings presented in this thesis are that the BRCA2 promotes efficient cytokinesis and that abscission is presumably more dependent on other mechanisms than the positioning of centrioles.

The live-cell imaging microscopy technique allowed us to study primary human cells, with a germline mutation in the *BRCA2* gene and non-*BRCA2*-mutated cells. The separation of chromosomes between the two forming daughter cells could be investigated and the whole cytokinesis process. The results indicated that BRCA2 haploinsufficiency influenced cytokinesis, since the *BRCA2* heterozygous cells had longer cell division time. We conclude that the BRCA2 protein plays a role in cytokinesis, but the nature of its function could not be elucidated. By expressing centriole- and microtubule specific genes fused to fluorescence coding sequences in different cell lines and performing time-lapse imaging with fluorescence live-cell imaging microscopy the movements of centrioles were studied during cytokinesis. They were observed to be different between both cells and cell lines, they migrated mainly along microtubules and the nuclear envelope. The centrioles only occasionally moved to the intercellular bridge, indicating that relocation towards the intercellular bridge is not a controlling mechanism for the separation of daughter cells.

In the last part of this research project clinical data were evaluated to link the experimental data obtained at the beginning to the clinical situation. By investigating ploidy of *BRCA2*-mutated tumors and comparing with sporadic ones, we conclude that BRCA2 protects against tetraploidy, since the familial cases had a significantly higher proportion of tetraploid cells. Thus, in this thesis it is described how cancer susceptibility in *BRCA2*-mutation carriers can also be caused by cell division failure.

REFERENCES

Alberghini, F. (2008). *BRCA2 and the centrosome during cytokinesis*. Junior Research Project.

Alsop, G.B., and Zhang, D. (2003). *Microtubules are the only structural constituent of the spindle apparatus required for induction of cell cleavage*. J Cell Biol *162*, 383-390.

Alvey, P.L. (1985). *An investigation of the centriole cycle using 3T3 and CHO cells*. J Cell Sci *78*, 147-162.

Anderson, C.T., and Stearns, T. (2009). *Centriole Age Underlies Asynchronous Primary Cilium Growth in Mammalian Cells*. Current Biology *19*, 1498-1502.

Andreassen, P.R., Lohez, O.D., Lacroix, F.B., and Margolis, R.L. (2001). *Tetraploid State Induces p53-dependent Arrest of Nontransformed Mammalian Cells in G1*. Mol Biol Cell *12*, 1315-1328.

Andreassen, P.R., Lohez, O.D., and Margolis, R.L. (2003). *G2 and spindle assembly checkpoint adaptation, and tetraploidy arrest: implications for intrinsic and chemically induced genomic instability*. Mutat Res *532*, 245-253.

Anglian Breast Cancer Study Group (2000). *Prevalence and penetrance of BRCA1 and BRCA2 mutations in a population-based series of breast cancer cases*. Br J Cancer *83*, 1301-1308.

Ayoub, N., Rajendra, E., Su, X., Jeyasekharan, A.D., Mahen, R., and Venkitaraman, A.R. (2009). *The carboxyl terminus of Brca2 links the disassembly of Rad51 complexes to mitotic entry*. Current Biology *19*, 1075-1085.

Azimzadeh, J., and Bornens, M. (2007). *Structure and duplication of the centrosome*. J Cell Sci *120*, 2139-2142.

Bettencourt-Dias, M., and Glover, D.M. (2007). *Centrosome biogenesis and function: centrosomics brings new understanding*. Nat Rev Mol Cell Biol *8*, 451-463.

Bignold, L.P., Coghlan, B.L.D., and Jersmann, H.P.A. (2006). *Hansemann, Boveri, chromosomes and the gametogenesis-related theories of tumours*. Cell Biol Int *30*, 640-644.

Bodvarsdottir, S.K., Hilmarsdottir, H., Birgisdottir, V., Steinarsdottir, M., Jonasson, J.G., and Eyfjord, J.E. (2007). *Aurora-A amplification associated with BRCA2 mutation in breast tumours*. Cancer Letters *248*, 96-102.

Borel, F., Lohez, O.D., Lacroix, F.o.B., and Margolis, R.L. (2002). *Multiple centrosomes arise from tetraploidy checkpoint failure and mitotic centrosome clusters in p53 and RB pocket protein-compromised cells*. Proc Natl Acad Sci *99*, 9819-9824.

Breast Cancer Information Core. http://research.nhgri.nih.gov/bic/

Caldwell, C.M., Green, R.A., and Kaplan, K.B. (2007). *APC mutations lead to cytokinetic failures in vitro and tetraploid genotypes in Min mice*. J Cell Biol *178*, 1109-1120.

Canman, J.C., Cameron, L.A., Maddox, P.S., Straight, A., Tirnauer, J.S., Mitchison, T.J., Fang, G., Kapoor, T.M., and Salmon, E.D. (2003). *Determining the position of the cell division plane*. Nature *424*, 1074-1078.

Carmena, M., and Earnshaw, W.C. (2003). *The cellular geography of Aurora kinases*. Nat Rev Mol Cell Biol *4*, 842-854.

Carreira, A., Hilario, J., Amitani, I., Baskin, R.J., Shivji, M.K., Venkitaraman, A.R., and Kowalczykowski, S.C. (2009). *The BRC repeats of BRCA2 modulate the DNA-binding selectivity of RAD51*. Cell *136*, 1032-1043.

Cheang, M., Voduc, D., Bajdik, C., Leung, S., McKinney, S., Chia, S., Perou, C., and Nielsen, T. (2008). *Basal-like breast cancer defined by five biomarkers has superior prognostic value than triple-negative phenotype*. Clin Cancer Res *14*, 1368 - 1376.

Cheng, J., Turkel, N., Hemati, N., Fuller, M.T., Hunt, A.J., and Yamashita, Y.M. (2008). *Centrosome misorientation reduces stem cell division during ageing*. Nature *456*, 599-604.

Chin, K., DeVries, S., Fridlyand, J., Spellman, P.T., Roydasgupta, R., Kuo, W.-L., Lapuk, A., Neve, R.M., Qian, Z., Ryder, T., *et al.* (2006). *Genomic and transcriptional aberrations linked to breast cancer pathophysiologies*. Cancer Cell *10*, 529-541.

Cimini, D. (2008). *Merotelic kinetochore orientation, aneuploidy, and cancer*. Biochim Biophys Acta *1786*, 32-40.

Clute, P., and Pines, J. (1999). *Temporal and spatial control of cyclin B1 destruction in metaphase*. Nat Cell Biol *1*, 82-87.

Cooper, G.M. (2000). *The cell: A molecular approach, Second edn* (Washington, DC, AMS Press).

Daniels, M.J., Wang, Y., Lee, M., and Venkitaraman, A.R. (2004). *Abnormal Cytokinesis in Cells Deficient in the Breast Cancer Susceptibility Protein BRCA2*. Science *306*, 876-879.

Davies, A.A., Masson, J.Y., McIlwraith, M.J., Stasiak, A.Z., Stasiak, A., Venkitaraman, A.R., and West, S.C. (2001). *Role of BRCA2 in control of the RAD51 recombination and DNA repair protein*. Mol Cell *7*, 273-282.

De Vos, W., H, Hoebe, R.A., Joss, G.H., Haffmans, W., Baatout, S., Van Oostveldt, P., and Manders, E.M.M. (2009). *Controlled light exposure microscopy reveals dynamic telomere microterritories throughout the cell cycle*. Cytometry Part A *75A*, 428-439.

Dechant, R., and Glotzer, M. (2003). *Centrosome Separation and Central Spindle Assembly Act in Redundant Pathways that Regulate Microtubule Density and Trigger Cleavage Furrow Formation*. Dev Cell *4*, 333-344.

Doxsey, S., Zimmerman, W., and Mikule, K. (2005). *Centrosome control of the cell cycle*. Trends in Cell Biology *15*, 303-311.

Duesberg, P., Li, R., Fabarius, A., and Hehlmann, R. (2005). *The chromosomal basis of cancer*. Cellular Oncology *27*, 293-318.

Duesberg, P., and Rasnick, D. (2000). *Aneuploidy, the somatic mutation that makes cancer a species of its own*. Cell Motil Cytoskeleton *47*, 81-107.

Earnshaw, W.C., and Bernat, R.L. (1991). *Chromosomal passengers: Toward an integrated view of mitosis*. Chromosoma *100*, 139-146.

Esashi, F., Christ, N., Gannon, J., Liu, Y., Hunt, T., Jasin, M., and West, S.C. (2005). *CDK-dependent phosphorylation of BRCA2 as a regulatory mechanism for recombinational repair*. Nature *434*, 598-604.

Evers, B., Drost, R., Schut, E., de Bruin, M., van der Burg, E., Derksen, P.W.B., Holstege, H., Liu, X., van Drunen, E., Beverloo, H.B., *et al.* (2008). *Selective Inhibition of BRCA2-Deficient Mammary Tumor Cell Growth by AZD2281 and Cisplatin*. Clin Cancer Res *14*, 3916-3925.

Eyfjord, J., and Bodvarsdottir, S. (2005). *Genomic instability and cancer: networks involved in response to DNA damage*. Mutat Res *592*, 18 - 28.

Frigault, M.M., Lacoste, J., Swift, J.L., and Brown, C.M. (2009). *Live-cell microscopy - tips and tools*. J Cell Sci *122*, 753-767.

Ganem, N.J., Godinho, S.A., and Pellman, D. (2009). *A mechanism linking extra centrosomes to chromosomal instability*. Nature *460*, 278-282.

Gergely, F., Draviam, V.M., and Raff, J.W. (2003). *The ch-TOG/XMAP215 protein is essential for spindle pole organization in human somatic cells*. Genes Dev *17*, 336-341.

Gerlich, D., Beaudouin, J., Kalbfuss, B., Daigle, N., Eils, R., and Ellenberg, J. (2003). *Global Chromosome Positions Are Transmitted through Mitosis in Mammalian Cells*. Cell *112*, 751-764.

Gisselsson, D. (2008). *Classification of chromosome segregation errors in cancer*. Chromosoma *117*, 511-519.

Gisselsson, D., Jonson, T., Petersen, A., Strombeck, B., Dal Cin, P., Hoglund, M., Mitelman, F., Mertens, F., and Mandahl, N. (2001). *Telomere dysfunction triggers extensive DNA fragmentation and evolution of complex chromosome abnormalities in human malignant tumors*. Proc Natl Acad Sci *98*, 12683-12688.

Gisselsson, D., Pettersson, L., Hoglund, M., Heidenblad, M., Gorunova, L., Wiegant, J., Mertens, F., Dal Cin, P., Mitelman, F., and Mandahl, N. (2000). *Chromosomal breakage-fusion-bridge events cause genetic intratumor heterogeneity*. Proc Natl Acad Sci *97*, 5357-5362.

Glotzer, M. (2005). *The molecular requirements for cytokinesis*. Science *307*, 1735-1739.

Gretarsdottir, S., Thorlacius, S., Valgardsdottir, R., Gudlaugsdottir, S., Sigurdsson, S., Steinarsdottir, M., Jonasson, J.G., Anamthawat-Jonsson, K., and Eyfjord, J.E. (1998). *BRCA2 and p53 mutations in primary breast cancer in relation to genetic instability*. Cancer Res *58*, 859-862.

Gromley, A., Jurczyk, A., Sillibourne, J., Halilovic, E., Mogensen, M., Groisman, I., Blomberg, M., and Doxsey, S. (2003). *A novel human protein of the maternal centriole is required for the final stages of cytokinesis and entry into S phase*. J Cell Biol *161*, 535-545.

Gromley, A., Yeaman, C., Rosa, J., Redick, S., Chen, C.-T., Mirabelle, S., Guha, M., Sillibourne, J., and Doxsey, S.J. (2005). *Centriolin Anchoring of Exocyst and SNARE Complexes at the Midbody Is Required for Secretory-Vesicle-Mediated Abscission*. Cell *123*, 75-87.

Guidotti, J.E., Bregerie, O., Robert, A., Debey, P., Brechot, C., and Desdouets, C. (2003). *Liver cell polyploidization: a pivotal role for binuclear hepatocytes*. J Biol Chem *278*, 19095-19101.

Han, X., Saito, H., Miki, Y., and Nakanishi, A. (2008). *A CRM1-mediated nuclear export signal governs cytoplasmic localization of BRCA2 and is essential for centrosomal localization of BRCA2*. Oncogene *27*, 2969-2977.

Hanashiro, K., Kanai, M., Geng, Y., Sicinski, P., and Fukasawa, K. (2008). *Roles of cyclins A and E in induction of centrosome amplification in p53-compromised cells*. Oncogene *27*, 5288-5302.

Hardy, P.A., and Zacharias, H. (2005). *Reappraisal of the Hansemann-Boveri hypothesis on the origin of tumors*. Cell Biol Int *29*, 983-992.

Hoebe, R.A., Van Oven, C.H., Gadella, T.W., Jr., Dhonukshe, P.B., Van Noorden, C.J., and Manders, E.M. (2007). *Controlled light-exposure microscopy reduces photobleaching and phototoxicity in fluorescence live-cell imaging*. Nat Biotechnol *25*, 249-253.

Howlett, N.G., Taniguchi, T., Olson, S., Cox, B., Waisfisz, Q., De Die-Smulders, C., Persky, N., Grompe, M., Joenje, H., Pals, G., *et al.* (2002). *Biallelic inactivation of BRCA2 in Fanconi anemia*. Science *297*, 606-609.

Inoue, Y.H., Savoian, M.S., Suzuki, T., Mathe, E., Yamamoto, M.-T., and Glover, D.M. (2004). *Mutations in orbit/mast reveal that the central spindle is comprised of two microtubule populations, those that initiate cleavage and those that propagate furrow ingression*. J Cell Biol *166*, 49-60.

Johannesdottir, G., Gudmundsson, J., Bergthorsson, J.T., Arason, A., Agnarsson, B.A., Eiriksdottir, G., Johannsson, O.T., Borg, A., Ingvarsson, S., Easton, D.F., *et al.* (1996). *High Prevalence of the 999del5 Mutation in Icelandic Breast and Ovarian Cancer Patients*. Cancer Res *56*, 3663-3665.

Johnson, N., Fletcher, O., Palles, C., Rudd, M., Webb, E., Sellick, G., dos Santos Silva, I., McCormack, V., Gibson, L., Fraser, A., *et al.* (2007). *Counting potentially functional variants in BRCA1, BRCA2 and ATM predicts breast cancer susceptibility*. Hum Mol Genet *16*, 1051-1057.

Jonkers, J., Meuwissen, R., van der Gulden, H., Peters, H., van der Valk, M., and Berns, A. (2001). *Synergistic tumor suppressor activity of BRCA2 and p53 in a conditional mouse model for breast cancer*. Nat Genet *29*, 418-425.

Kellogg, D.R., Moritz, M., and Alberts, B.M. (1994). *The Centrosome and Cellular Organization*. Annual Review of Biochemistry *63*, 639-674.

Khodjakov, A., Cole, R.W., Oakley, B.R., and Rieder, C.L. (2000). *Centrosome-independent mitotic spindle formation in vertebrates*. Current Biology *10*, 59-67.

Khodjakov, A., and Rieder, C.L. (1999). *The sudden recruitment of gamma-tubulin to the centrosome at the onset of mitosis and its dynamic exchange throughout the cell cycle, do not require microtubules*. J Cell Biol *146*, 585-596.

Khodjakov, A., and Rieder, C.L. (2001). *Centrosomes enhance the fidelity of cytokinesis in vertebrates and are required for cell cycle progression*. J Cell Biol *153*, 237-242.

King, R.W. (2008). *When 2 + 2 = 5: The origins and fates of aneuploid and tetraploid cells*. Biochimica et Biophysica Acta (BBA) - Reviews on Cancer *1786*, 4-14.

King, T., Li, W., Brogi, E., Yee, C., Gemignani, M., Olvera, N., Levine, D., Norton, L., Robson, M., Offit, K., *et al.* (2007). *Heterogenic Loss of the Wild-Type BRCA Allele in Human Breast Tumorigenesis*. Annals of Surgical Oncology *14*, 2510-2518.

Kops, G.J., Weaver, B.A., and Cleveland, D.W. (2005). *On the road to cancer: aneuploidy and the mitotic checkpoint*. Nat Rev Cancer *5*, 773-785.

Kufer, T.A., Sillje, H.H., Korner, R., Gruss, O.J., Meraldi, P., and Nigg, E.A. (2002). *Human TPX2 is required for targeting Aurora-A kinase to the spindle*. J Cell Biol *158*, 617-623.

Lange, B.M., and Gull, K. (1995). *A molecular marker for centriole maturation in the mammalian cell cycle*. J Cell Biol *130*, 919-927.

Lee, M., Daniels, M.J., and Venkitaraman, A.R. (2004). *Phosphorylation of BRCA2 by the Polo-like kinase Plk1 is regulated by DNA damage and mitotic progression*. Oncogene *23*, 865-872.

Levitus, M., Joenje, H., and de Winter, J.P. (2006). *The Fanconi anemia pathway of genomic maintenance*. Cellular Oncology *28*, 3-29.

Levitus, M., Waisfisz, Q., Godthelp, B.C., de Vries, Y., Hussain, S., Wiegant, W.W., Elghalbzouri-Maghrani, E., Steltenpool, J., Rooimans, M.A., Pals, G., *et al.* (2005). *The DNA helicase BRIP1 is defective in Fanconi anemia complementation group J*. Nat Genet *37*, 934-935.

Li, L., McCormack, A.A., Nicholson, J.M., Fabarius, A., Hehlmann, R., Sachs, R.K., and Duesberg, P.H. (2009). *Cancer-causing karyotypes: chromosomal equilibria between destabilizing aneuploidy and stabilizing selection for oncogenic function*. Cancer Genet Cytogenet *188*, 1-25.

Lin, H.R., Ting, N.S., Qin, J., and Lee, W.H. (2003). *M phase-specific phosphorylation of BRCA2 by Polo-like kinase 1 correlates with the dissociation of the BRCA2-P/CAF complex*. J Biol Chem *278*, 35979-35987.

Lomonosov, M., Anand, S., Sangrithi, M., Davies, R., and Venkitaraman, A.R. (2003). *Stabilization of stalled DNA replication forks by the BRCA2 breast cancer susceptibility protein*. Genes Dev *17*, 3017-3022.

Lu, X., and Kang, Y. (2009). *Cell Fusion as a Hidden Force in Tumor Progression*. Cancer Res *69*, 8536-8539.

Mack, G., and Rattner, J.B. (1993). *Centrosome repositioning immediately following karyokinesis and prior to cytokinesis*. Cell Motil Cytoskeleton *26*, 239-247.

Margolis, R.L., Lohez, O., D. , and Andreassen, P., R. (2003). *G1 tetraploidy checkpoint and the suppression of tumorigenesis*. J Cell Biochem *88*, 673-683.

Marmorstein, L.Y., Kinev, A.V., Chan, G.K., Bochar, D.A., Beniya, H., Epstein, J.A., Yen, T.J., and Shiekhattar, R. (2001). *A human BRCA2 complex containing a structural DNA binding component influences cell cycle progression*. Cell *104*, 247-257.

Meraldi, P., and Sorger, P.K. (2005). *A dual role for Bub1 in the spindle checkpoint and chromosome congression*. EMBO J *24*, 1621-1633.

Mikaelsdottir, E., Valgeirsdottir, S., Eyfjord, J., and Rafnar, T. (2004). *The Icelandic founder mutation BRCA2 999del5: analysis of expression*. Breast Cancer Res *6*, R284 - R290.

Miki, Y., Swensen, J., Shattuck-Eidens, D., Futreal, P.A., Harshman, K., Tavtigian, S., Liu, Q., Cochran, C., Bennett, L.M., Ding, W., *et al.* (1994). *A strong candidate for the breast and ovarian cancer susceptibility gene BRCA1*. Science *266*, 66-71.

Mishima, M., Kaitna, S., and Glotzer, M. (2002). *Central Spindle Assembly and Cytokinesis Require a Kinesin-like Protein/RhoGAP Complex with Microtubule Bundling Activity*. Developmental Cell *2*, 41-54.

Misteli, T., and Soutoglou, E. (2009). *The emerging role of nuclear architecture in DNA repair and genome maintenance*. Nat Rev Mol Cell Biol *10*, 243-254.

Molenaar, C., Wiesmeijer, K., Verwoerd, N.P., Khazen, S., Eils, R., Tanke, H.J., and Dirks, R.W. (2003). *Visualizing telomere dynamics in living mammalian cells using PNA probes*. EMBO J *22*, 6631-6641.

Moritz, K.B., and Sauer, H.W. (1996). *Boveri's contributions to developmental biology--a callenge for today*. Int J Dev Biol *40*, 27-47.

Moynahan, M.E., Pierce, A.J., and Jasin, M. (2001). *BRCA2 is required for homology-directed repair of chromosomal breaks*. Mol Cell *7*, 263-272.

Nakanishi, A., Han, X.Z., Saito, H., Taguchi, K., Ohta, Y., Imajoh-Ohmi, S., and Miki, Y. (2007). *Interference with BRCA2, which localizes to the centrosome during S and early M phase, leads to abnormal nuclear division*. Biochem Biophys Res Commun *355*, 34-40.

Niedernhofer, L.J., Lalai, A.S., and Hoeijmakers, J.H.J. (2005). *Fanconi Anemia (Cross)linked to DNA Repair*. Cell *123*, 1191-1198.

Nielsen, T.O., Hsu, F.D., Jensen, K., Cheang, M., Karaca, G., Hu, Z., Hernandez-Boussard, T., Livasy, C., Cowan, D., Dressler, L., *et al.* (2004). *Immunohistochemical and clinical characterization of the basal-like subtype of invasive breast carcinoma*. Clin Cancer Res *10*, 5367-5374.

Nigg, E.A. (2002). *Centrosome aberrations: cause or consequence of cancer progression?* Nat Rev Cancer *2*, 815-825.

Niwa, T., Saito, H., Imajoh-ohmi, S., Kaminishi, M., Seto, Y., Miki, Y., and Nakanishi, A. (2009). *BRCA2 interacts with the cytoskeletal linker protein plectin to form a complex controlling centrosome localization*. Cancer Sci *100*, 2115-2125.

Norbury, C., and Nurse, P. (1992). *Animal Cell Cycles and Their Control*. Annual Review of Biochemistry *61*, 441-468.

Offit, K., Levran, O., Mullaney, B., Mah, K., Nafa, K., Batish, S.D., Diotti, R., Schneider, H., Deffenbaugh, A., Scholl, T., *et al.* (2003). *Shared Genetic Susceptibility to Breast Cancer, Brain Tumors, and Fanconi Anemia*. J Natl Cancer Inst *95*, 1548-1551.

Ogle, B.M., Cascalho, M., and Platt, J.L. (2005). *Biological implications of cell fusion*. Nat Rev Mol Cell Biol *6*, 567-575.

Ou, Y., Y. , and Rattner, J., B. (2002). *Post-karyokinesis centrosome movement leaves a trail of unanswered questions*. Cell Motil Cytoskeleton *51*, 123-132.

Paschal, B.M., and Vallee, R.B. (1987). *Retrograde transport by the microtubule-associated protein MAP 1C*. Nature *330*, 181-183.

Patel, K.J., Yu, V.P.C.C., Lee, H., Corcoran, A., Thistlethwaite, F.C., Evans, M.J., Colledge, W.H., Friedman, L.S., Ponder, B.A.J., and Venkitaraman, A.R. (1998). *Involvement of Brca2 in DNA Repair*. Mol Cell *1*, 347-357.

Perou, C.M., Sorlie, T., Eisen, M.B., van de Rijn, M., Jeffrey, S.S., Rees, C.A., Pollack, J.R., Ross, D.T., Johnsen, H., Akslen, L.A., *et al.* (2000). *Molecular portraits of human breast tumours*. Nature *406*, 747-752.

Peters, J.-M. (2002). *The Anaphase-Promoting Complex: Proteolysis in Mitosis and Beyond*. MolCell *9*, 931-943.

Peto, J., Collins, N., Barfoot, R., Seal, S., Warren, W., Rahman, N., Easton, D.F., Evans, C., Deacon, J., and Stratton, M.R. (1999). *Prevalence of BRCA1 and BRCA2 Gene Mutations in Patients With Early-Onset Breast Cancer*. J Natl Cancer Inst *91*, 943-949.

Piehl, M., Tulu, U.S., Wadsworth, P., and Cassimeris, L. (2004). *Centrosome maturation: Measurement of microtubule nucleation throughout the cell cycle by using GFP-tagged EB1*. Proc Natl Acad Sci *101*, 1584-1588.

Piekny, A., Werner, M., and Glotzer, M. (2005). *Cytokinesis: welcome to the Rho zone*. Trends in Cell Biology *15*, 651-658.

Piel, M., Meyer, P., Khodjakov, A., Rieder, C.L., and Bornens, M. (2000). *The Respective Contributions of the Mother and Daughter Centrioles to Centrosome Activity and Behavior in Vertebrate Cells*. J Cell Biol *149*, 317-330.

Piel, M., Nordberg, J., Euteneuer, U., and Bornens, M. (2001). *Centrosome-Dependent Exit of Cytokinesis in Animal Cells*. Science *291*, 1550-1553.

Rattner, J.B., and Phillips, S.G. (1973). *Independence of centriole formation and DNA synthesis*. J Cell Biol *57*, 359-372.

Reid, S., Schindler, D., Hanenberg, H., Barker, K., Hanks, S., Kalb, R., Neveling, K., Kelly, P., Seal, S., Freund, M., *et al.* (2007). *Biallelic mutations in PALB2 cause Fanconi anemia subtype FA-N and predispose to childhood cancer*. Nat Genet *39*, 162-164.

Rieder, C.L., Faruki, S., and Khodjakov, A. (2001). *The centrosome in vertebrates: more than a microtubule-organizing center*. Trends in Cell Biology *11*, 413-419.

Rieder, C.L., and Khodjakov, A. (2003). *Mitosis through the microscope: advances in seeing inside live dividing cells*. Science *300*, 91-96.

Rieder, C.L., Schultz, A., Cole, R., and Sluder, G. (1994). *Anaphase onset in vertebrate somatic cells is controlled by a checkpoint that monitors sister kinetochore attachment to the spindle*. J Cell Biol *127*, 1301-1310.

Rubin, C.I., French, D.L., and Atweh, G.F. (2003). *Stathmin expression and megakaryocyte differentiation: a potential role in polyploidy*. Exp Hematol *31*, 389-397.

Salpingidou, G., Smertenko, A., Hausmanowa-Petrucewicz, I., Hussey, P.J., and Hutchison, C.J. (2007). *A novel role for the nuclear membrane protein emerin in association of the centrosome to the outer nuclear membrane*. J Cell Biol *178*, 897-904.

Satzinger, H. (2008). *Theodor and Marcella Boveri: chromosomes and cytoplasm in heredity and development*. Nat Rev Genet *9*, 231-238.

Saurin, A.T., Durgan, J., Cameron, A.J., Faisal, A., Marber, M.S., and Parker, P.J. (2008). *The regulated assembly of a PKC[epsiv] complex controls the completion of cytokinesis*. Nat Cell Biol *10*, 891-901.

Schaffner, S.C., and Jose, J.V. (2006). *Biophysical model of self-organized spindle formation patterns without centrosomes and kinetochores*. Proc Natl Acad Sci *103*, 11166-11171.

Schnapp, B.J., Vale, R.D., Sheetz, M.P., and Reese, T.S. (1986). *Microtubules and the mechanism of directed organelle movement*. Ann N Y Acad Sci *466*, 909-918.

Shaner, N.C., Campbell, R.E., Steinbach, P.A., Giepmans, B.N.G., Palmer, A.E., and Tsien, R.Y. (2004). *Improved monomeric red, orange and yellow fluorescent proteins derived from Discosoma sp. red fluorescent protein*. Nat Biotech *22*, 1567-1572.

Shivji, M.K., Davies, O.R., Savill, J.M., Bates, D.L., Pellegrini, L., and Venkitaraman, A.R. (2006). *A region of human BRCA2 containing multiple BRC repeats promotes RAD51-mediated strand exchange*. Nucleic Acids Res *34*, 4000-4011.

Skop, A.R., Liu, H., Yates, J., III, Meyer, B.J., and Heald, R. (2004). *Dissection of the Mammalian Midbody Proteome Reveals Conserved Cytokinesis Mechanisms*. Science *305*, 61-66.

Song, L., Varma, C.A., Verhoeven, J.W., and Tanke, H.J. (1996). *Influence of the triplet excited state on the photobleaching kinetics of fluorescein in microscopy*. Biophysical Journal *70*, 2959-2968.

Sorlie, T., Tibshirani, R., Parker, J., Hastie, T., Marron, J.S., Nobel, A., Deng, S., Johnsen, H., Pesich, R., Geisler, S., *et al.* (2003). *Repeated observation of breast tumor subtypes in independent gene expression data sets*. Proc Natl Acad Sci *100*, 8418-8423.

Spain, B.H., Larson, C.J., Shihabuddin, L.S., Gage, F.H., and Verma, I.M. (1999). *Truncated BRCA2 is cytoplasmic: implications for cancer-linked mutations*. Proc Natl Acad Sci *96*, 13920 - 13925.

Stefansson, O., Jonasson, J., Johannsson, O., Olafsdottir, K., Steinarsdottir, M., Valgeirsdottir, S., and Eyfjord, J. (2009). *Genomic profiling of breast tumours in relation to BRCA abnormalities and phenotypes*. Breast Cancer Res *11*, R47.

Stefansson, O.A., Jonasson, J.G., Bjarnason, H., Johannesson, O.T., Olafsdottir, K., Bodvarsdottir, S., Valgeirsdottir, S., and Eyfjord, J.E. (*Manuscript submitted*). *Modeling BRCA2 associated breast cancer progression through genomic profiling.*

Storchova, Z., and Kuffer, C. (2008). *The consequences of tetraploidy and aneuploidy*. J Cell Sci *121*, 3859-3866.

Storchova, Z., and Pellman, D. (2004). *From polyploidy to aneuploidy, genome instability and cancer*. Nat Rev Mol Cell Biol *5*, 45-54.

Straight, A.F., Cheung, A., Limouze, J., Chen, I., Westwood, N.J., Sellers, J.R., and Mitchison, T.J. (2003). *Dissecting Temporal and Spatial Control of Cytokinesis with a Myosin II Inhibitor*. Science *299*, 1743-1747.

Stratton, M.R., and Rahman, N. (2008). *The emerging landscape of breast cancer susceptibility*. Nat Genet *40*, 17-22.

Sy, S.M.H., Huen, M.S.Y., and Chen, J. (2009). *PALB2 is an integral component of the BRCA complex required for homologous recombination repair*. Proc Natl Acad Sci *106*, 7155-7160.

Tarapore, P., and Fukasawa, K. (2002). *Loss of p53 and centrosome hyperamplification*. Oncogene *21*, 6234-6240.

Tavtigian, S.V., Simard, J., Rommens, J., Couch, F., Shattuck-Eidens, D., Neuhausen, S., Merajver, S., Thorlacius, S., Offit, K., Stoppa-Lyonnet, D., *et al.* (1996). *The complete BRCA2 gene and mutations in chromosome 13q-linked kindreds*. Nat Genet *12*, 333 - 337.

Thery, M., and Bornens, M. (2006). *Cell shape and cell division*. Curr Opin Cell Biol *18*, 648-657.

Thomson, T.M., and Guerra-Rebollo, M. (2010). *Ubiquitin and SUMO signalling in DNA repair*. Biochem SocTrans *38*, 116-131.

Thorlacius, S., Olafsdottir, G., Tryggvadottir, L., Neuhausen, S., Jonasson, J.G., Tavtigian, S.V., Tulinius, H., Ogmundsdottir, H.M., and Eyfjord, J.E. (1996). *A single BRCA2 mutation in male and female breast cancer families from Iceland with varied cancer phenotypes*. Nat Genet *13*, 117 - 119.

Thorlacius, S., Sigurdsson, S., Bjarnadottir, H., Olafsdottir, G., Jonasson, J.G., Tryggvadottir, L., Tulinius, H., and Eyfjord, J.E. (1997). *Study of a single BRCA2 mutation with high carrier frequency in a small population*. Am J Hum Genet *60*, 1079 - 1084.

Tirkkonen, M., Johannsson, O., Agnarsson, B., Olsson, H., Ingvarsson, S., Karhu, R., Tanner, M., Isola, J., Barkardottir, R., Borg, A., *et al.* (1997). *Distinct somatic genetic changes associated with tumor progression in carriers of BRCA1 and BRCA2 germ-line mutations*. Cancer Res *57*, 1222 - 1227.

Tryggvadottir, L., Sigvaldason, H., Olafsdottir, G.H., Jonasson, J.G., Jonsson, T., Tulinius, H., and Eyfjord, J.E. (2006). *Population-Based Study of Changing Breast Cancer Risk in Icelandic BRCA2 Mutation Carriers, 1920-2000*. J Natl Cancer Inst *98*, 116-122.

Tsai, M.-Y., Wiese, C., Cao, K., Martin, O., Donovan, P., Ruderman, J., Prigent, C., and Zheng, Y. (2003). *A Ran signalling pathway mediated by the mitotic kinase Aurora A in spindle assembly*. Nat Cell Biol *5*, 242-248.

Tulinius, H., Olafsdottir, G.H., Sigvaldason, H., Arason, A., Barkardottir, R.B., Egilsson, V., Ogmundsdottir, H.M., Tryggvadottir, L., Gudlaugsdottir, S., and Eyfjord, J.E. (2002). *The effect of a single BRCA2 mutation on cancer in Iceland*. J Med Genet *39*, 457-462.

Tutt, A., Gabriel, A., Bertwistle, D., Connor, F., Paterson, H., Peacock, J., Ross, G., and Ashworth, A. (1999). *Absence of Brca2 causes genome instability by chromosome breakage and loss associated with centrosome amplification*. Current Biology *9*, 1107-1110, S1101.

Tvarusko, W., Bentele, M., Misteli, T., Rudolf, R., Kaether, C., Spector, D.L., Gerdes, H.H., and Eils, R. (1999). *Time-resolved analysis and visualization of dynamic processes in living cells*. Proc Natl Acad Sci *96*, 7950 - 7955.

van Beers, E.H., van Welsem, T., Wessels, L.F.A., Li, Y., Oldenburg, R.A., Devilee, P., Cornelisse, C.J., Verhoef, S., Hogervorst, F.B.L., van't Veer, L.J., *et al.* (2005). *Comparative Genomic Hybridization Profiles in Human BRCA1 and BRCA2 Breast Tumors Highlight Differential Sets of Genomic Aberrations*. Cancer Res *65*, 822-827.

van Engeland, M., Ramaekers, F.C., Schutte, B., and Reutelingsperger, C.P. (1996). *A novel assay to measure loss of plasma membrane asymmetry during apoptosis of adherent cells in culture*. Cytometry *24*, 131-139.

Vandesompele, J., De Preter, K., Pattyn, F., Poppe, B., Van Roy, N., De Paepe, A., and Speleman, F. (2002). *Accurate normalization of real-time quantitative RT-PCR data by geometric averaging of multiple internal control genes*. Genome Biol *3*, RESEARCH0034.

Venkitaraman, A.R. (2002). *Cancer susceptibility and the functions of BRCA1 and BRCA2*. Cell *108*, 171-182.

Vernos, I., and Karsenti, E. (1995). *Chromosomes take the lead in spindle assembly*. Trends in Cell Biology *5*, 297-301.

Vorobjev, I.A., and Chentsov Yu, S. (1982). *Centrioles in the cell cycle. I. Epithelial cells*. J Cell Biol *93*, 938-949.

Vrolijk, J., Brouwer, A.K., Dirks, R.W., and Tanke, H.J. (*Manuscript in preparation*). *STACKS: a software program for particle tracking in living cells.*

Waddell, N., Arnold, J., Cocciardi, S., da Silva, L., Marsh, A., Riley, J., Johnstone, C.N., Orloff, M., Assie, G., Eng, C., *et al.* (2010). *Subtypes of familial breast tumours revealed by expression and copy number profiling*. Breast Cancer Res Treat *123*, 661-77.

Walczak, C.E., Vernos, I., Mitchison, T.J., Karsenti, E., and Heald, R. (1998). *A model for the proposed roles of different microtubule-based motor proteins in establishing spindle bipolarity*. Current Biology *8*, 903-913.

Warren, M., Lord, C., Masabanda, J., Griffin, D., and Ashworth, A. (2003). *Phenotypic effects of heterozygosity for a BRCA2 mutation*. Hum Mol Genet *12*, 2645 - 2656.

Weaver, B.A.A., Silk, A.D., Montagna, C., Verdier-Pinard, P., and Cleveland, D.W. (2007). *Aneuploidy Acts Both Oncogenically and as a Tumor Suppressor*. Cancer Cell *11*, 25-36.

Weglarz, T.C., Degen, J.L., and Sandgren, E.P. (2000). *Hepatocyte transplantation into diseased mouse liver. Kinetics of parenchymal repopulation and identification of the proliferative capacity of tetraploid and octaploid hepatocytes*. Am J Pathol *157*, 1963-1974.

Williams, B.R., and Amon, A. (2009). *Aneuploidy: cancer's fatal flaw?* Cancer Res *69*, 5289-5291.

Wolpert, L. (1995). *Evolution of the cell theory*. Philos Trans R Soc Lond B Biol Sci *349*, 227-233.

Wooster, R., Bignell, G., Lancaster, J., Swift, S., Seal, S., Mangion, J., Collins, N., Gregory, S., Gumbs, C., and Micklem, G. (1995). *Identification of the breast cancer susceptibility gene BRCA2*. Nature *378*, 789-792.

Xia, B., Sheng, Q., Nakanishi, K., Ohashi, A., Wu, J., Christ, N., Liu, X., Jasin, M., Couch, F.J., and Livingston, D.M. (2006). *Control of BRCA2 Cellular and Clinical Functions by a Nuclear Partner, PALB2*. MolCell *22*, 719-729.

Xia, F., Taghian, D.G., DeFrank, J.S., Zeng, Z.-C., Willers, H., Iliakis, G., and Powell, S.N. (2001). *Deficiency of human BRCA2 leads to impaired homologous recombination but maintains normal nonhomologous end joining*. Proc Natl Acad Sci *98*, 8644-8649.

Yamashita, Y.M., Mahowald, A.P., Perlin, J.R., and Fuller, M.T. (2007). *Asymmetric inheritance of mother versus daughter centrosome in stem cell division*. Science *315*, 518-521.

Yang, M.Q., Koehly, L.M., and Elnitski, L.L. (2007). *Comprehensive annotation of bidirectional promoters identifies co-regulation among breast and ovarian cancer genes*. PLoS Comput Biol *3*, e72.

Yano, K., Morotomi, K., Saito, H., Kato, M., Matsuo, F., and Miki, Y. (2000). *Nuclear localization signals of the BRCA2 protein*. Biochem Biophys Res Commun *270*, 171-175.

Yoder, B.J., Wilkinson, E.J., and Massoll, N.A. (2007). *Molecular and morphologic distinctions between infiltrating ductal and lobular carcinoma of the breast*. Breast J *13*, 172-179.

Yu, V.P., Koehler, M., Steinlein, C., Schmid, M., Hanakahi, L.A., van Gool, A.J., West, S.C., and Venkitaraman, A.R. (2000). *Gross chromosomal rearrangements and genetic exchange between nonhomologous chromosomes following BRCA2 inactivation*. Genes Dev *14*, 1400-1406.

Yuan, J., and Chen, J. (2010). *MRE11-RAD50-NBS1 Complex Dictates DNA Repair Independent of H2AX*. J Biol Chem *285*, 1097-1104.

Yuce, O., Piekny, A., and Glotzer, M. (2005). *An ECT2-centralspindlin complex regulates the localization and function of RhoA*. J Cell Biol *170*, 571-582.

Zou, C., Li, J., Bai, Y., Gunning, W.T., Wazer, D.E., Band, V., and Gao, Q. (2005). *Centrobin: a novel daughter centriole-associated protein that is required for centriole duplication*. J Cell Biol *171*, 437-445.

Paper I.

Cellular Oncology 31 (2009) 191–201
DOI 10.3233/CLO-2009-0465
IOS Press

BRCA2 heterozygosity delays cytokinesis in primary human fibroblasts

Asta Björk Jonsdottir [a,b,c], Maaike P.G. Vreeswijk [d], Ron Wolterbeek [f], Peter Devilee [d,e], Hans J. Tanke [c], Jorunn E. Eyfjörd [a,b,*] and Karoly Szuhai [c]

[a] *Faculty of Medicine, University of Iceland, Reykjavik, Iceland*
[b] *The University of Iceland and Icelandic Cancer Society Molecular and Cell Biology Research Laboratory, University of Iceland, Reykjavik, Iceland*
[c] *Department of Molecular Cell Biology, Leiden University Medical Center, Leiden, The Netherlands*
[d] *Department of Human Genetics, Leiden University Medical Center, Leiden, The Netherlands*
[e] *Department of Pathology, Leiden University Medical Center, Leiden, The Netherlands*
[f] *Department of Medical Statistics, Leiden University Medical Center, Leiden, The Netherlands*

Abstract. *Background*: Inherited mutations in the tumour suppressor gene *BRCA2* greatly increase the risk of developing breast, ovarian and other types of cancers. So far, most studies have focused on the role of BRCA-pathways in the maintenance of genomic stability.

In this study we investigated the potential role of the BRCA2 protein in cytokinesis in unmodified primary human fibroblast carrying a heterozygous mutation in the *BRCA2* gene.

Methods: Cell divisions were monitored with time lapse live-cell imaging. *BRCA2* mRNA expression levels in $BRCA2^{+/-}$ and $BRCA2^{+/+}$ cells were quantified with quantitative real-time polymerase chain reaction (qRT-PCR). To investigate the localization of the BRCA2 protein during cytokinesis, immunofluorescence staining using antibody directed against BRCA2 was carried out. Immunofluorescence staining was performed directly after live-cell imaging and cells with delayed cytokinesis, of which the co-ordinates were saved, were automatically repositioned and visualized.

Results: We demonstrate that unmodified primary human fibroblasts derived from heterozygous *BRCA2* mutation carriers show significantly prolonged cytokinesis.

A Subset of the $BRCA2^{+/-}$ cells had delayed cytokinesis (40 min or longer) making the mean cell division time 6 min longer compared with $BRCA2^{+/+}$ cells, 33 min versus 27 min, respectively. Lower *BRCA2* mRNA expression levels were observed in the *BRCA2* heterozygous samples compared with the *BRCA2* wild type samples.

The BRCA2 protein localizes and accumulates to the midbody during cytokinesis, and no difference was detected in distribution and localization of the protein between $BRCA2^{+/-}$ and $BRCA2^{+/+}$ samples or cells with delayed cytokinesis and normal division time.

Conclusions: The delayed cytokinesis phenotype of the *BRCA2* heterozygous cells and localization of the BRCA2 protein to the midbody confirms that BRCA2 plays a role in cytokinesis. Our observations indicate that in a subset of cells the presence of only one wild type *BRCA2* allele is insufficient for efficient cytokinesis.

Keywords: BRCA2, cytokinesis, live-cell imaging, primary human fibroblasts, heterozygous phenotype

1. Introduction

Inherited mutations in the breast cancer susceptibility genes *BRCA1* and *BRCA2* greatly increase the risk of developing breast cancer, and other cancers such as ovarian and prostate cancers [14,23,31]. About 15% of breast cancer cases cluster in families and among these cases, germline mutations in *BRCA1* and *BRCA2* have been shown to account for 15–40% [25,29].

Several functions have been ascribed for the BRCA proteins, but most studies reported so far have focused on the role of BRCA-pathways in the maintenance of genomic stability. A well studied function of the

* Corresponding author: Jorunn Erla Eyfjörd, Faculty of Medicine, University of Iceland, The University of Iceland and Icelandic Cancer Society Molecular and Cell Biology Research Laboratory, Vatnsmyrarvegi 16, 101 Reykjavik, Iceland. Tel.: +354 5255825; Fax: +354 5254884; E-mail: jorunne@hi.is.

BRCA2 protein is its role in homologous recombination, where RAD51, a DNA recombinase, interacts with the BRC repeats and the C-terminus of BRCA2. BRCA2 directs RAD51 to the sites of DNA double strand breaks and this interaction has been shown to be essential for error-free homologous recombination repair [3,4]. Reduced amount of functional BRCA2 protein in heterozygous *BRCA2* mutation carriers causes insufficient repair of DNA double strand breaks, a condition that could contribute to the impairment of genomic stability. *BRCA2* heterozygosity has shown to increase sensitivity to specific DNA damaging agents, reduce RAD51 focus formation after irradiation, increase cell death and reduce growth rate [1,30].

Complete BRCA2 inactivation in tumours gives rise to chromosomal aberrations including both numerical and structural alterations, such as translocations, chromatid breaks and tri- and quadri-radial chromosomes [7,17,32].

Defects in cytokinesis can lead to mis-segregation of chromosomes and aneuploidy, which are indeed also observed in BRCA2 deficient cells [19,26].

Several studies have linked BRCA2 with progression through mitosis. BRCA2 has been found to co-localize to the centrosome in S-phase and early M-phase cells and to have a centrosomal localization signal at the C-terminus, which indicates that it might be involved in regulation of migration and duplication of the centrosome during the cell cycle [8,15,26]. The activity of the polo-like protein kinase 1 (Plk-1) is required for cytokinesis and proper metaphase/anaphase transition. Hyperphosphorylation of BRCA2, by Plk-1, in M phase and dephosphorylation of the protein when cells exit M phase implicates a potential role of BRCA2 in modulation M phase progression [6,11,18].

A new function for BRCA2 has been discovered. By examining murine embryonic fibroblasts (MEFs) it was shown that BRCA2 deficiency delays and prevents cytokinesis. *BRCA2* heterozygous ($BRCA2^{Tr/+}$) and homozygous ($BRCA2^{Tr/Tr}$) MEFs showed longer cytokinesis than wild type cells ($BRCA2^{+/+}$) when studied *ex vivo*. HeLa cells treated with BRCA2 siRNA showed almost twice as long cell division time as HeLa cells treated with control siRNA [2]. However, it is still unknown how exactly BRCA2 participates in cytokinesis and, importantly, the role of BRCA2 in cytokinesis as observed in murine fibroblasts has never been studied in human fibroblasts.

The aim of this study was to investigate if BRCA2 plays a role in cytokinesis in human fibroblasts and to study the involvement of BRCA2 in these cells in the late stages of cell division. Unmodified primary human fibroblasts, from individuals that carry the Icelandic *999del5 BRCA2* founder mutation, the Dutch *1537del4 BRCA2* mutation, and individuals that do not carry a *BRCA2* mutation, were studied [16,24]. Both *BRCA2* mutations cause premature stop codons downstream of the mutation site. In an earlier study no protein could be detected from the mutant *BRCA2 999del5* allele [13]. Cell divisions were monitored and cell division time estimated from recordings obtained with time lapse live-cell imaging. *BRCA2* mRNA expression levels were quantified with qRT-PCR and localization of the BRCA2 protein during cytokinesis was investigated.

2. Materials and methods

2.1. Unmodified primary human fibroblasts

Primary human fibroblasts derived from *BRCA2* mutation carriers and *BRCA2* wild type individuals were cultured from skin biopsies. Samples were collected in Iceland and The Netherlands. All samples were handled in a coded fashion, according to National ethical guidelines "Code for Proper Secondary Use of Human Tissue", Dutch Federation of Medical Scientific Societies. Permissions from the National Bioethics Committee in Iceland and the Icelandic Data Protection Authority were obtained for the study.

Fibroblasts were cultured in Dulbecco's Modified Eagle's Medium (DMEM), supplemented with 10% fetal bovine serum, penicillin (100 U/ml), streptomycin (0.1 mg/ml) and 2 mM L-glutamine (Invitrogen Corporation, Breda, The Netherlands). Cells were maintained at 37°C and 5% CO_2 and all experiments were carried out with cells in passage 8–15.

2.2. Study setup

A pilot study was set up by using 3 coded unmodified primary human fibroblast samples from Iceland, which were either derived from individuals carrying the Icelandic *999del5* founder mutation in the *BRCA2* gene or derived from *BRCA2* wild type individuals (FIS 1, FIS 2 and FIS 3) (Table 1). Cells were analyzed by live-cell imaging and their cell division time estimated. FIS 1 and FIS 3 had longer cell division time than FIS 2. It was confirmed that FIS 1 and FIS 3 carry the *BRCA2 999del5* deletion and FIS 2 has $BRCA2^{+/+}$ genotype. The study was continued using

Table 1
Unmodified primary human fibroblast cells

Sample	Genotype	Mutation	Origin
FIS 1	BRCA2$^{+/-}$	999del5*	Iceland
FIS 2	BRCA2$^{+/+}$	Wild type	Iceland
FIS 3	BRCA2$^{+/-}$	999del5*	Iceland
FNE 1	BRCA2$^{+/-}$	1537del4**	The Netherlands
FNE 2	BRCA2$^{+/+}$	Wild type	The Netherlands

The Human Genetic Variation Society (HGVS) nomenclature: *c.771_775del p.Asn257Lysfsx17; **c.1309_1312del p.Lys437Ilefsx22.

FIS 1 and FIS 2 and subsequently, samples from The Netherlands were added (FNE 1 and FNE 2) (Table 1) to extend the study, and to investigate the influence of different *BRCA2* mutations. Sample FNE 1 has previously been published as family D [16]. At least two separate live-cell imaging experiments (sets) were carried out for each sample and reproducibility of the estimated cell division time was calculated with 2-way ANOVA test. At least 30 cell divisions were analyzed for each sample for every set of experiments. A non-significant difference was observed between repeated experiments ($p = 0.655$) and, therefore, data sets for each sample were pooled together.

2.3. Live-cell imaging

Unmodified primary human fibroblasts were seeded on MatTek glass bottom culture dish (MatTek, Ashland, USA) and imaged when approximately 70% confluent. Cell divisions were recorded with a Leica AS MDW microscope system (Multi-Dimensional Workstation for Live Cell Imaging), consisting of an inverted phase contrast Leica DM IRE2 microscope equipped with a climate chamber and CO_2 chamber (Leica Microsystems B.V. Rijswijk, The Netherlands). Both the temperature (T) and CO_2 concentration ([CO_2]) of the medium in the culture dish were strictly controlled at all steps of the recordings ($T = 37.0°C \pm 0.5°C$, [CO_2] $5.00\% \pm 0.05\%$), as it is known that minor changes in these parameters may induce stress type conditions thereby effecting cell cycle characteristics.

Time lapse images were collected from 20 different fields from each dish with an HCX PL FL L 40×/0.60 CORR XR (3.3–1.9 mm) objective using bright field light every 5 min for up to 24 h. The Leica AS MDW software was used to generate movies from the time lapse images collected.

In order to analyze distribution and localization of the BRCA2 protein in cells with delayed cytokinesis, cells were imaged for short time (2 hours) prior to immunofluorescence staining, enabling identification of cells with prolonged cytokinesis by using relocalization.

A well known limitation of the microscopy technique applied in our study is that prolonged illumination of cells in culture may interfere with cell cycle checkpoints, particularly when cells are fluorescently stained with vital dyes or expressing fluorescent tagged proteins [21]. The use of fluorescent tagged cell cycle related proteins, such as cyclin B1-GFP, could have provided more options but in the process examined, i.e. cytokinesis, the cells have already passed all checkpoints that control the cell cycle process and the transfection per se could influence the cell characteristics and, therefore, would not be informative. However, when using unstained cells, fluorescence excitation and formation of radicals is negligible. Furthermore, cells hardly absorb light in the wavelength range between 400 and 700 nm (except erythrocytes with hemoglobin and melanocytes containing melanin), which implies that no heat is locally produced as a consequence of the absorption process using bright-field microscopy only. We, therefore, used transmitted light only to avoid any photo damage.

2.4. Quantitative real-time polymerase chain reaction (qRT-PCR)

The *BRCA2* mRNA expression levels were investigated with qRT-PCR. 0.84 μg total RNA of each sample, isolated following standard procedure using TRIzol® Reagent (Invitrogen, Breda, The Netherlands), was treated with deoxyribonuclease 1 according to the manufacturer's instructions (Sigma-Aldrich Chemie B.V., Zwijndrecht, The Netherlands). First-strand cDNA was synthesized using 50 μM oligo(dT)$_{20}$ and Super-script III transcriptase according to the manufacturer's instructions (Invitrogen, Breda, The Netherlands). Each PCR was carried out in triplicate in a 25 μl amplification mixture containing template cDNA, iQ SYBR Green Supermix (12.5 μl) (Bio-Rad Laboratories, Veenendaal, The Netherlands) and 0.4 μM BRCA2 forward and reverse primers or 0.3 μM housekeeping gene forward and reverse primers. Reactions were run on a Bio-Rad iCycler Thermal Cycler (Bio-Rad Laboratories, Hercules, CA, USA). The cycling conditions comprised 10 min polymerase activation at 95°C and 40 cycles at 95°C for 30 s and 60°C for 60 s, followed by a melting curve analysis from 58°C–95°C.

geNorm [28] was used to calculate the gene-stability for all the control genes, succinate dehydrogenase complex, subunit A (SDHA), glyceraldehyde-3-phosphate dehydreogenase (GAPDH) and hypoxanthine phosphoribosyl-transferase 1 (HPRT1). The most stably expressing control gene (SDHA) was used as a reference to calculate the normalized expression level of *BRCA2*, using the standard delta C_t method [28]. The relative values for the controls were set to one.

The sequences of the primers used for qRT-PCR were as follows: BRCA2 forward, CCAAGTGGTCCACCCCAAC, reverse, CACAATTAGGAGAAGACATCAGAAGC; SDHA forward, TGGGAACAAGAGGGCATCTG, reverse, CCACCACTGCATCAATTCATG; GAPDH forward, TTCCAGGAGCGAGATCCCT, reverse, CACCCATGACGAACATGGG and HPRT1 forward, TGACACTGGCAAAACAATGCA, reverse, GGTCCTTTTCACCAGCAAGCT.

2.5. Flow cytometry

DNA content for DNA ploidy and cell cycle analysis was measured using flow cytometry. 1.0×10^6 cells were collected and suspended in 1×Phosphate Buffered Saline (PBS). After centrifugation cells were re-suspended in 0.5 ml 1×PBS. Cell suspension was transferred into tubes containing 4.5 ml ice cold 70% ethanol. Cells were kept cold in fixative for at least 2 h. Ethanol-suspended cells were centrifuged and ethanol decanted thoroughly. Pellet was suspended in 5 ml 1×PBS and waited for 1 min before centrifugation. Pellet was then suspended in 1 ml 0.02 mg/ml Propidium Iodine (PI)/0.1% Triton X-100/1×PBS staining solution containing 2 mg RNase A. Samples were kept at 37°C for 15 min and PI emission detected at Texas red wavelength using BD LSR II Flow Cytometer and the BD FACSDiva Software (BD Biosciences, Breda, The Netherlands). The ModFit LT™ flow cytometry software was used for the data analysis (Verity Software House, Topsham, ME, USA).

2.6. Annexin V detection of apoptotic cells using live-cell imaging

To investigate the fraction of apoptotic cells staining with PI and Annexin V conjugated to the Alexa Fluor® 488 fluorophore (Alexa Fluor® 488 annexin V) was carried out using the Vybrant® Apoptosis Assay Kit #2 (Invitrogen, Breda, The Netherlands). The method for utilizing Annexin V binding on adherent cells was adjusted from published methods [27]. Cells were plated and cultured in monolayer on MatTek glass bottom culture dish. 48 hours later (when approximately 70% confluent) cells were washed twice in 1×PBS. 100 µl containing culture medium, 10 µl of Alexa Fluor® 488 annexin V and 0.2 µg/ml PI were added drop vice to the dish and incubated with 5% CO_2 at RT for 10 min, followed up immediately with live-cell imaging at 37°C and 5% CO_2. Images were collected from 20 randomly selected positions from the microscope plate with an HPX PL APO 63× 1.3GLYC 37°C objective using Leica AF6000 LX live-cell imaging system (Leica Microsystems B.V. Rijswijk, The Netherlands).

2.7. Immunofluorescence

Unmodified primary human fibroblasts were cultured on glass slides or glass bottom culture dishes for 2 days. After removing culture medium cells were washed with 1×Tris Buffered Saline (TBS), fixed for 3 min in 3.7% paraformaldehyde/1×TBS at RT and washed with 1×TBS/0.1% Triton X-100. A separate BRCA2 antibody and specimen blocking step was performed by using a blocking buffer (1×TBS/0.1% Triton X-100/2% BSA) for 2 h at RT and for 30 min at RT, respectively. Incubation with polyclonal rabbit anti-BRCA2 (kindly provided by Prof. Venkitaraman, Cambridge, England) and Aurora-B (BD Biosciences, Breda, The Netherlands) was performed at 37°C for 45 min. Specimens were washed with blocking buffer before incubation with secondary antibodies at 37°C for 30 min. BRCA2 was revealed with Cy™3-conjucated affinity-purified goat anti-rabbit antibody (Brunschwig Chemie, Amsterdam, The Netherlands) and Aurora-B with Alexa 488-conjucated goat anti-mouse antibody (Invitrogen, Breda, The Netherlands). Antibody incubation was followed by three changed washing steps with 1×TBS/0.1% Triton X-100 before mounted in Vectashield with 4′,6-diamino-2-phenylindole-dihydrochloride (DAPI)/citifluor (500 ng/ml) (Brunschwig Chemie, Amsterdam, The Netherlands). Image acquisition was performed using a DM-RA epifluorescence microscope (Leica Microsystems B.V. Rijswijk, The Netherlands) equipped with a Quantix camera (Roper Scientific, Fairfield, IA, USA). Gray scale images were collected with 100× objective by using appropriate filters to visualize Alexa 488, Cy3 and DAPI. For further image processing an in house developed software (ColourProc) was used [22].

Table 2
ANOVA statistical analysis of the cell division time of BRCA2$^{+/+}$ and BRCA2$^{+/-}$ unmodified primary human fibroblasts

	BRCA2$^{+/-}$ vs. BRCA2$^{+/+}$				BRCA2$^{+/-}$ vs. BRCA2$^{+/-}$	BRCA2$^{+/+}$ vs. BRCA2$^{+/+}$
	FIS 1 vs. FIS 2	FIS 1 vs. FNE 2	FNE 1 vs. FIS 2	FNE 1 vs. FNE 2	FIS 1 vs. FNE 1	FIS 2 vs. FNE 2
p values	<0.01	<0.01	<0.01	<0.01	0.21	0.49

2.8. Interphase-fluorescent in situ hybridization (FISH)

To investigate the cell ploidy and the frequency of bi-nuclear cells interphase-FISH was performed by using nick translation labeled D15Z1 probe to detect centromere of chromosome 15 [9] and imaged as described earlier [22].

2.9. Statistical analysis

To compare cell division times, estimated from images obtained with time lapse live-cell imaging, including the outliers because of their biological origin but not measurement errors, ANOVA's with post hoc t-test were applied, using lsd (Table 2). To evaluate the reproducibility between the sets of experiments and difference between samples, a 2-way ANOVA was performed.

Paired sample test was applied on data obtained from flow cytometry analysis to compare the fraction of cells in the G_2/M phase of the cell cycle in the BRCA2$^{+/+}$ and BRCA2$^{+/-}$ samples.

BRCA2 mRNA expression levels between *BRCA2* wild type and heterozygous mutant samples were compared by calculating delta C_t values for every sample [28] and performing a t-test on the logarithm of the normalized expression values, BRCA2$^{+/+}$ versus BRCA2$^{+/-}$.

3. Results

3.1. Heterozygous mutation in the BRCA2 gene causes delay in cytokinesis in unmodified primary human fibroblasts

3.1.1. Cell division time of BRCA2 heterozygous mutant and BRCA2 wild type cells

Cell divisions in unmodified primary human fibroblasts were monitored by time lapse live-cell imaging to study the phenotype of cells that carry a mutation in the *BRCA2* gene. Bright field microscopy was used to minimize photo damage. Under strict control of temperature and CO_2 unmodified primary human fibroblasts derived from carriers of a *BRCA2* mutation (FIS 1, *BRCA2 999del5*, and FNE 1, *BRCA2 1537del4*) and non-mutation carriers (FIS 2 and FNE 2) were analyzed (Table 1).

The cytokinesis duration, the time from metaphase (when the chromosomes are visible and are aligned in an equatorial plane) until complete cell separation (when the daughter cells and their cytoplasm have separated) was estimated (Fig. 1).

In concordance with the mutation status and in line with previously published data on murine embryonic fibroblasts [2] cells carrying a mutation in the *BRCA2* gene had on average a longer cell division time than *BRCA2* wild type cells. The mean cell division time for the BRCA2$^{+/-}$ cells FIS1 and FNE1 was 32 and 33 min, respectively, which was significant longer than for the BRCA2$^{+/+}$ cells FIS2 and FNE2 that had mean cell division time of 27 and 26 min, respectively (Fig. 2(A)). The increase in cell division time for the BRCA2$^{+/-}$ cells was observed to be highly significant when compared with the BRCA2$^{+/+}$ unmodified primary human fibroblasts (FIS 1 vs. FIS 2, $p < 0.01$; FIS 1 vs. FNE 2, $p < 0.01$; FNE 1 vs. FIS 2, $p < 0.01$ and FNE 1 vs. FNE 2, $p < 0.01$) (Table 2). There was no significant difference between the cell division time for the two *BRCA2*$^{+/+}$ samples (FIS 2 vs. FNE 2, $p = 0.49$) nor for the two BRCA2$^{+/-}$ samples (FIS 1 vs. FNE 1, $p = 0.21$) (Table 2) manifesting that the different heterozygous mutants show the same phenotype.

After pooling the cell division time for the two *BRCA2* wild type and the two *BRCA2* heterozygous mutant samples a significant increase of 6 min in the mean cell division time was observed for the BRCA2$^{+/-}$ cells, 33 min compared to 27 min for the BRCA2$^{+/+}$ cells ($p < 0.01$) (Fig. 3).

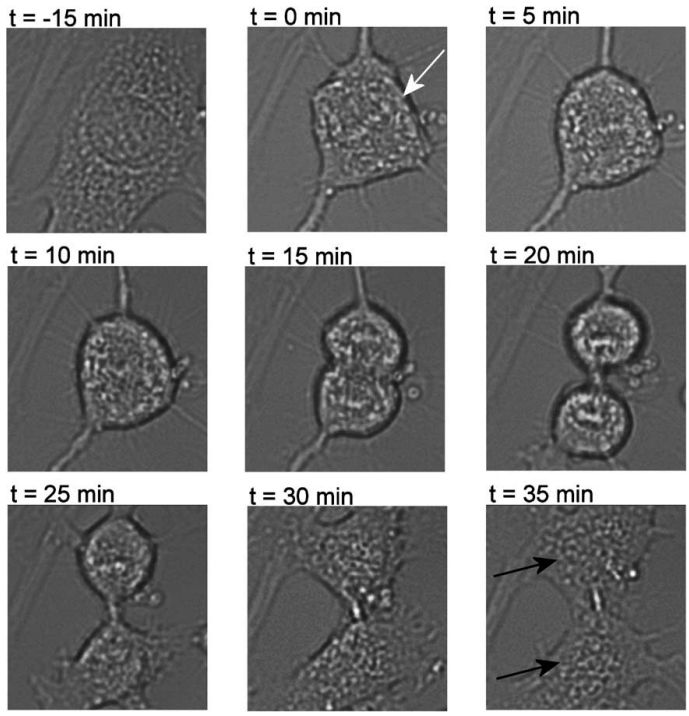

Fig. 1. Cytokinesis of unmodified primary human fibroblast. Representative time lapse images showing cell division of a BRCA2$^{+/-}$ unmodified primary human fibroblast. The cell division starts when chromosomes become visible and line up in an equatorial plane of the dividing cell ($t = 0$ min indicated by white arrow) and continues until the cytoplasm of the daughter cells has separated (black arrows indicate the end point). Cytokinesis is in this case completed in 35 min. Images were captured by time lapse live-cell imaging with a 40× objective and bright field light every 5 min.

Heterogeneity in cell division time was detected both in the *BRCA2* wild type and in the *BRCA2* heterozygous mutant samples. About 55% of the *BRCA2* wild type cells completed cell division within 25 min, for 40% the process took about 30–35 min and less than 5% had a delayed cytokinesis of 40–45 min. Of the *BRCA2* heterozygous mutant cells only 20% finished division within 25 min but for the majority (50–60%) cytokinesis took 30–35 min. Interestingly, about 20% of the *BRCA2* heterozygous cells took 40 min or longer to complete cell division, with maximum division time of 65 min (Fig. 2(A), FIS 1 and FNE 1). No cell failed to divide.

Furthermore, comparison on estimated replication time (from end of division of progenitor cell until the beginning of division of its daughter cell) in cells with delayed and normal cell division time revealed that the median replication time was approximately 20 h both for *BRCA2* wild type and heterozygous mutant samples.

3.1.2. BRCA2 mRNA expression levels

To investigate if the delay in cytokinesis in the *BRCA2* heterozygous mutant cells corresponded to lower *BRCA2* expression, a quantitative real-time polymerase chain reaction (qRT-PCR) was performed. The *BRCA2* mRNA expression levels of the two BRCA2$^{+/-}$ samples FIS 1 and FNE 1 were 0.167 and 0.254, respectively, compared with 0.987 and 1.00 for the BRCA2$^{+/+}$ samples, FIS 2 and FNE 2, respectively (Fig. 2(B)). The 5 times difference in *BRCA2* expression levels between the *BRCA2* heterozygous mutant samples and the *BRCA2* wild type samples was shown to be significant ($p = 0.03$) (Fig. 2(B)).

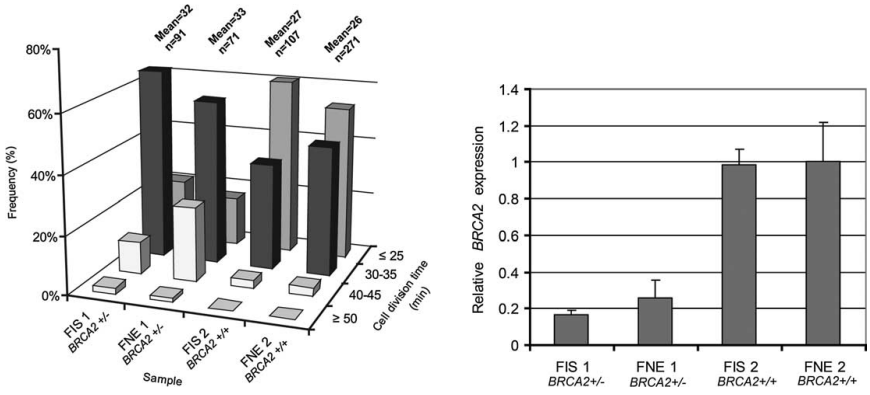

Fig. 2. Frequency distribution of the cell division time and *BRCA2* mRNA expression levlels of BRCA2$^{+/-}$ and BRCA2$^{+/+}$ unmodified primary human fibroblasts. (A) Cell division time was estimated from images obtained by time lapse live-cell imaging as shown in Fig. 1. The two BRCA2$^{+/-}$ samples, FIS 1 and FNE 1, show the same phenotype, delayed cytokinesis, but different from the two BRCA2$^{+/+}$ samples, FIS 2 and FNE 2. 50–60% of the BRCA2$^{+/+}$ cells completed cell division within 25 min and for 35–45% the process took about 30–35 min and less than 5% had a delayed cytokinesis of 40–45 min. Up to 20% of the *BRCA2* heterozygous mutant cells finished the process within 25 min but for the majority cytokinesis took 30–35 min. For about 20% of the BRCA2$^{+/-}$ cells cytokinesis proceeded for 40 min or longer with maximum cell division time of 65 min. No cell failed to divide. (B) *BRCA2* mRNA expression levels were quantified with qRT-PCR. The two BRCA2$^{+/-}$ samples, FIS 1 and FNE 1, show on average 5 times lower *BRCA2* expression than the two BRCA2$^{+/+}$ samples, FIS 2 and FNE 2, 0.167 and 0.254 versus 0.987 and 1.00, respectively. The difference between the BRCA2$^{+/-}$ and the BRCA2$^{+/+}$ samples was shown to be significant ($p = 0.03$).

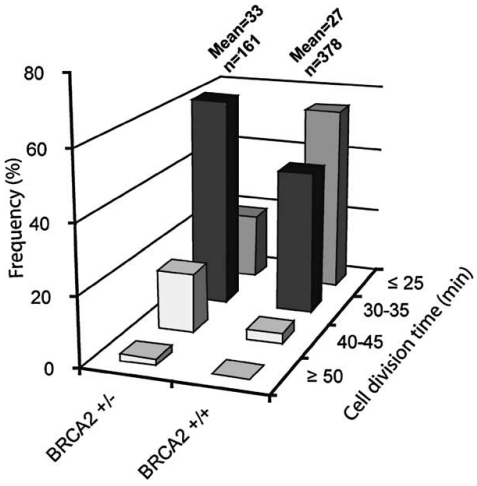

Fig. 3. Frequency distribution of the cell division time of BRCA2$^{+/-}$ versus BRCA2$^{+/+}$ unmodified primary human fibroblasts. The *BRCA2* heterozygous mutant cells have a significant longer cell division time than the *BRCA2* wild type cells, 6 min on average, indicating that the delay is associated with the mutation status in the *BRCA2* gene.

3.1.3. Fluorescent in situ hybridization (FISH) to investigate endo-reduplication

To investigate if the delayed cell division time was due to endo-reduplication, the frequency of binuclear cells and the cell ploidy was examined with interphase-FISH using probe against the centromere of chromosome 15. Four signals were detected in 6 of 478 (1.26%) and three signals in 2 of 478 analyzed BRCA2$^{+/-}$ cells (0.4%). This frequency was similar to normal cells (data not shown).

3.1.4. Flow cytometry and Alexa Fluor® 488 annexin V staining for ploidy and apoptosis estimation

Since mitotic defects can lead to increase in aneuploidy [20], we performed DNA flow cytometry. Aneuploid cell populations were not found. The BRCA2$^{+/-}$ cells did, however, have an increased fraction of cells in G_2/M phase of the cell cycle (2.22%) or 3.8× higher than in the BRCA2$^{+/+}$ samples. Statistical analysis showed the difference to be non-significant ($p = 0.49$).

To take into account the possibility that aneuploid cells undergo apoptosis the fraction of early apoptotic cells was measured by staining cells with Alexa Fluor® 488 annexin V and propidium iodide (PI) followed up

by live-cell imaging. No increase in cell death was observed in the *BRCA2* heterozygous cells compared with *BRCA2* wild type cells.

3.2. *BRCA2 localizes to the midbody of unmodified primary human fibroblasts in cytokinesis*

3.2.1. *Localization of BRCA2 in BRCA2$^{+/-}$ and BRCA2$^{+/+}$ cells during cytokinesis*

Numerous proteins, like Aurora B kinase in a complex with inner centromere protein, survivin and CSC-1, have been demonstrated to concentrate on the central spindle during cytokinesis [5]. To investigate the role of the BRCA2 protein during cytokinesis, its distribution and localization was examined in cells in cytokinesis by performing a double-immunofluorescence staining with antibodies directed against BRCA2 and Aurora B. The staining was both carried out in *BRCA2* wild type and *BRCA2* heterozygous mutant unmodified primary human fibroblasts.

The immunofluorescence staining revealed that BRCA2 localizes to the midbody in cells in cytokinesis (Fig. 4) as previously described [2]. Accumulation of the protein to the midbody increased as the process proceeded (Fig. 4) and concentrated adjacent to Aurora B in the abscission phase (Fig. 4, inset). A similar variation of the distribution of the BRCA2 protein along the midbody was observed both in BRCA2$^{+/+}$ and BRCA2$^{+/-}$ cells.

3.2.2. *Localization of BRCA2 in cells with delayed cytokinesis*

To investigate the localization of the BRCA2 protein in the sub-populations of cells with division time of 40 min or longer (delayed cytokinesis) observed in the BRCA2$^{+/-}$ samples (FIS 1 and FNE 1) (Fig. 2(A)), cell division was monitored with live-cell imaging for short time (2 hours) and followed up with immunofluorescence detection with BRCA2 and Aurora B antibodies. A computerized scanning stage and mapping of the x/y coordinates was used to relocate the cells of interest after the staining. In this way the BRCA2 staining pattern could be linked to particular cells allowing investigation of the BRCA2 protein distribution in cells with delayed cytokinesis specifically and compare it to cells with normal division time. These experiments showed no detectable difference of BRCA2 distribution between cells with normal or delayed cytokinesis.

4. Discussion

The role of the BRCA2 protein during cytokinesis was investigated in heterozygous *BRCA2* mutated human fibroblasts using live-cell imaging. This is an accurate and efficient technique to study individual cells, the cell cycle process in addition to the location, movement and interaction of cells and cell particles, cell behavior and phenotype *ex-vivo*.

Cell division time of unmodified primary human fibroblasts was estimated from images collected with time lapse live-cell imaging. Samples were obtained from individuals that carry different *BRCA2* mutations (Table 1). By comparing the cell division times of BRCA2$^{+/-}$ deletion mutants with BRCA2$^{+/+}$ cells, we observed, in concordance with the mutation status, that the BRCA2$^{+/-}$ cells had a significant delay. The mean cell division time of the BRCA2$^{+/-}$cells was shown to be 6 min longer than for the BRCA2$^{+/+}$ cells that completed the process in 27 min on average (Fig. 3). The cell division time was heterogeneous within samples. Cells with delayed cytokinesis (40 min

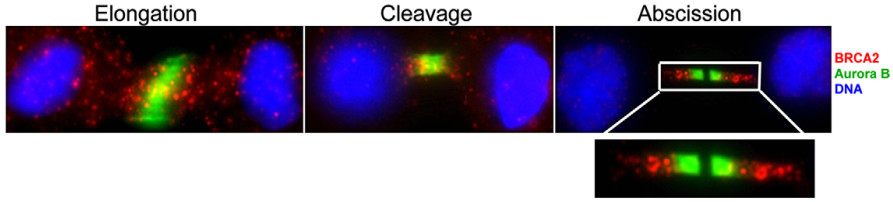

Fig. 4. Representative images of unmodified primary human fibroblasts after immunofluorescence staining to detect BRCA2 and Aurora B. Localization of the BRCA2 protein was investigated in cells in cytokinesis using polyclonal rabbit anti-BRCA2 (red) and monoclonal mouse anti-Aurora B (green) antibodies and DAPI (blue). In early steps of cytokinesis (elongation) little amount of BRCA2 is present between the forming daughter cells and mainly dispersed through out the nucleus. As the process proceeds, from elongation to cleavage phase, the accumulation of BRCA2 to the midbody increases and concentrates adjacent to the Aurora B kinase in the abscission phase as indicated by inset.

or longer) comprise a subset of the *BRCA2* heterozygous cell population, about 20%, as shown in Fig 2(A). Our data are in accordance with published data on murine cells. MEFs homozygous for a targeted *BRCA2* mutation ($BRCA2^{Tr/Tr}$) have severely extended cell division time compared with wild type and heterozygous cells. Cytokinesis was prevented in more than 30% cases in the $BRCA2^{Tr/Tr}$ murine fibroblasts and HeLa cells treated with BRCA2 siRNA [2].

The qRT-PCR results denote a correlation between lower expression levels of *BRCA2* mRNA with a delay in cytokinesis in the $BRCA2^{+/-}$ cells, where both of the $BRCA2^{+/-}$ samples studied showed similar and a relatively low expression levels The *BRCA2* wild type samples showed on average 5× higher *BRCA2* expression than the heterozygous mutant samples (Fig. 2(B)), suggesting that reduction of *BRCA2* is a rate limiting factor in this process.

The replication time of the cells did not vary between cells with different cell division time. These observations indicate that the delayed cytokinesis is not caused by replication related mechanisms [3,12].

Cytokinesis defects in *BRCA2* heterozygous cells might increase the number of aneuploid cells which then could predispose to carcinogenesis. Flow cytometry showed that $BRCA2^{+/-}$ cells accumulate in G_2/M phase of the cell cycle 3.8× more frequently than $BRCA2^{+/+}$ cells, which is in line with the 4× increase in number of cells that showed delayed cytokinesis compared with $BRCA2^{+/+}$ samples. As aneuploidy is defined as an additional G_0/G_1 peak with a small G_2/M peak and because both G_2/M diploids and G_0/G_1 tetraploids are 4N, the groups are un-distinguishable by flow cytometry [10,20].

Those results indicate that BRCA2 participates in the cytokinesis process.

The distribution and localization of BRCA2 was examined to investigate further the role of BRCA2 during cytokinesis. Immunofluorescence staining using antibodies to detect BRCA2 and the Aurora B kinase, which is known to localize and function at the midbody [5] revealed that BRCA2 localizes to the midbody in cells in cytokinesis and the accumulation increases as the process proceeds. This indicates that BRCA2 might affect or facilitate the organization of the central spindle and/or progression through cytokinesis. To investigate the molecular mechanism causing the delay in cytokinesis, observed in the $BRCA2^{+/-}$ samples, time lapse images were collected for short period (2 hours) with live-cell imaging and followed-up by immunofluorescence staining. We observed no difference in BRCA2 distribution between cells with prolonged division time ($\geqslant$40 min) and normal cell division time. Therefore, we conclude that the delayed cytokinesis phenotype is not directly linked to abnormal localization of the BRCA2 protein to the midbody.

BRCA2 is known to preserve chromosome structure and abnormal cytokinesis in *BRCA2* deficient cells may be an additional cause for chromosomal instability, a hallmark of genomic instability that contributes to tumorigenesis [7].

5. Conclusions

Our data reveal that primary human fibroblasts derived from $BRCA2^{+/-}$ individuals show significantly longer cell division time compared with $BRCA2^{+/+}$ cells, indicating that BRCA2 plays a role in cytokinesis.

Acknowledgements

We thank Prof. Helga M. Ögmundsdottir, Department of Medicine, University of Iceland, Reykjavik, Iceland and Dr. H.H. Kampinga, Cellbiology, UMC Groningen, Groningen, The Netherlands, for contributing samples, Prof. A. Venkitaraman, University of Cambridge, England, for donating BRCA2 antibody, Marja v.d. Burg for performing interphase-FISH, Jan Slats for assisting with flow cytometry analysis and Hans Baelde for qRT-PCR assistance. This work was funded by the Icelandic Center for Research Biomedicine Programme and the Margret Bjorgulfsdottir Memorial Fund. M.P.G.V. was funded by the Dutch Cancer Society (2001-2471).

References

[1] K. Arnold, M.K. Kim, K. Frerk, L. Edler, L. Savelyeva, P. Schmezer and R. Wiedemeyer, Lower level of BRCA2 protein in heterozygous mutation carriers is correlated with an increase in DNA double strand breaks and an impaired DSB repair, *Cancer Lett.* **243** (2006), 90–100.

[2] M.J. Daniels, Y. Wang, M. Lee and A.R. Venkitaraman, Abnormal cytokinesis in cells deficient in the breast cancer susceptibility protein BRCA2, *Science* **306** (2004), 876–879.

[3] A.A. Davies, J.Y. Masson, M.J. McIlwraith, A.Z. Stasiak, A. Stasiak, A.R. Venkitaraman and S.C.West, Role of BRCA2 in control of the RAD51 recombination and DNA repair protein, *Mol. Cell.* **7** (2001), 273–282.

[4] F. Esashi, V.E. Galkin, X.Yu, E.H. Egelman and S.C. West, Stabilization of RAD51 nucleoprotein filaments by the C-terminal region of BRCA2, *Nat. Struct. Mol. Biol.* **14** (2007), 468–474.

[5] M. Glotzer, The molecular requirements for cytokinesis, *Science* **307** (2005), 1735–1739.

[6] D.M. Glover, Polo kinase and progression through M phase in Drosophila: a perspective from the spindle poles, *Oncogene* **24** (2005), 230–237.

[7] S. Gretarsdottir, S. Thorlacius, R. Valgardsdottir, S. Gudlaugsdottir, S. Sigurdsson, M. Steinarsdottir, J.G. Jonasson, K. Anamthawat-Jonsson and J.E. Eyfjord, BRCA2 and p53 mutations in primary breast cancer in relation to genetic instability, *Cancer Res.* **58** (1998), 859–862.

[8] X. Han, H. Saito, Y. Miki and A. Nakanishi, A CRM1-mediated nuclear export signal governs cytoplasmic localization of BRCA2 and is essential for centrosomal localization of BRCA2, *Oncogene* **27** (2007), 2969–2977.

[9] M.J. Higgins, H.S. Wang, I. Shtromas, T. Haliotis, J.C. Roder, J.J. Holden and B.N. White, Organization of a repetitive human 1.8 kb KpnI sequence localized in the heterochromatin of chromosome 15, *Chromosoma* **93** (1985), 77–86.

[10] M. Levitus, H. Joenje and J.P. de Winter, The Fanconi anemia pathway of genomic maintenance, *Cell. Oncol.* **28** (2006), 3–29.

[11] H.R. Lin, N.S. Ting, J. Qin and W.H. Lee, M phase-specific phosphorylation of BRCA2 by Polo-like kinase 1 correlates with the dissociation of the BRCA2-P/CAF complex, *J. Biol. Chem.* **278** (2003), 35979–35987.

[12] M. Lomonosov, S. Anand, M. Sangrithi, R. Davies and A.R. Venkitaraman, Stabilization of stalled DNA replication forks by the BRCA2 breast cancer susceptibility protein, *Genes Dev.* **17** (2003), 3017–3022.

[13] E.K. Mikaelsdottir, S. Valgeirsdottir, J.E. Eyfjord and T. Rafnar, The Icelandic founder mutation BRCA2 999del5: analysis of expression, *Breast Cancer Res.* **6** (2004), R284–R290.

[14] Y. Miki, J. Swensen, D. Shattuck-Eidens, P.A. Futreal, K. Harshman, S. Tavtigian, Q. Liu, C. Cochran, L.M. Bennett and W. Ding, A strong candidate for the breast and ovarian cancer susceptibility gene BRCA1, *Science* **266** (1994), 66–71.

[15] A. Nakanishi, X. Han, H. Saito, K. Taguchi, Y. Ohta, S. Imajoh-Ohmi and Y. Miki, Interference with BRCA2, which localizes to the centrosome during S and early M phase, leads to abnormal nuclear division, *Biochem. Biophys. Res. Commun.* **355** (2007), 34–40.

[16] B. Nieuwenhuis, A.J. Assen-Bolt, M.A. Waarde-Verhagen, R.H. Sijmons, A.H. Van der Hout, T. Bauch, C. Streffer and H.H. Kampinga, BRCA1 and BRCA2 heterozygosity and repair of X-ray-induced DNA damage, *Int. J. Radiat. Biol.* **78** (2002), 285–295.

[17] K.J. Patel, V.P. Yu, H. Lee, A. Corcoran, F.C. Thistlethwaite, M.J. Evans, W.H. Colledge, L.S. Friedman, B.A. Ponder and A.R. Venkitaraman, Involvement of BRCA2 in DNA repair, *Mol. Cell.* **1** (1998), 347–357.

[18] Y.S. Seong, K. Kamijo, J.S. Lee, E. Fernandez, R. Kuriyama, T. Miki and K.S. Lee, A spindle checkpoint arrest and a cytokinesis failure by the dominant-negative polo-box domain of Plk1 in U-2 OS cells, *J. Biol. Chem.* **277** (2002), 32282–32293.

[19] Q. Shi and R.W. King, Chromosome nondisjunction yields tetraploid rather than aneuploid cells in human cell lines, *Nature* **437** (2005), 1038–1042.

[20] I.S. Smirnova, N.D. Aksenov, E.V. Kashuba, P. Payakurel, V.V. Grabovetsky, A.D. Zaberezhny, M.S. Vonsky, L. Buchinska, P. Biberfeld, J. Hinkula and M.G. Isaguliants, Hepatitis C virus core protein transforms murine fibroblasts by promoting genomic instability, *Cell. Oncol.* **28** (2006), 177–190.

[21] L. Song, C.A. Varma, J.W. Verhoeven and H.J. Tanke, Influence of the triplet excited state on the photobleaching kinetics of fluorescein in microscopy, *Biophys. J.* **70** (1996), 2959–2968.

[22] H.J. Tanke, J. Wiegant, R.P. van Gijlswijk, V. Bezrookove, H. Pattenier, R.J. Heetebrij, E.G. Talman, A.K. Raap and J. Vrolijk, New strategy for multi-colour fluorescence *in situ* hybridisation: COBRA: COmbined Binary RAtio labelling, *Eur. J. Hum. Genet.* **7** (1999), 2–11.

[23] S.V. Tavtigian, J. Simard, J. Rommens, F. Couch, D. Shattuck-Eidens, S. Neuhausen, S. Merajver, S. Thorlacius, K. Offit, D. Stoppa-Lyonnet, C. Belanger, R. Bell, S. Berry, R. Bogden, Q. Chen, T. Davis, M. Dumont, C. Frye, T. Hattier, S. Jammulapati, T. Janecki, P. Jiang, R. Kehrer, J.F. Leblanc, J.T. Mitchell, J. McArthur-Morrison, K. Nguyen, Y. Peng, C. Samson, M. Schroeder, S.C. Snyder, L. Steele, M. Stringfellow, C. Stroup, B. Swedlund, J. Swense, D. Teng, A. Thomas, T. Tran, M. Tranchant, J. Weaver-Feldhaus, A.K. Wong, H. Shizuya, J.E. Eyfjord, L. Cannon-Albright, M. Tranchant, F. Labrie, M.H. Skolnick, B. Weber, A. Kamb and D.E. Goldgar, The complete BRCA2 gene and mutations in chromosome 13q-linked kindreds, *Nat. Genet.* **12** (1996), 333–337.

[24] S. Thorlacius, G. Olafsdottir, L. Tryggvadottir, S. Neuhausen, J.G. Jonasson, S.V. Tavtigian, H. Tulinius, H.M. Ogmundsdottir and J.E. Eyfjord, A single BRCA2 mutation in male and female breast cancer families from Iceland with varied cancer phenotypes, *Nat. Genet.* **13** (1996), 117–119.

[25] H. Tulinius, G.H. Olafsdottir, H. Sigvaldason, A. Arason, R.B. Barkardottir, V. Egilsson, H.M. Ogmundsdottir, L. Tryggvadottir, S. Gudlaugsdottir and J.E. Eyfjord, The effect of a single BRCA2 mutation on cancer in Iceland, *J. Med. Genet.* **39** (2002), 457–462.

[26] A. Tutt, A. Gabriel, D. Bertwistle, F. Connor, H. Paterson, J. Peacock, G. Ross and A. Ashworth, Absence of BRCA2 causes genome instability by chromosome breakage and loss associated with centrosome amplification, *Curr. Biol.* **9** (1999), 1107–1110.

[27] M. van Engeland, F.C. Ramaekers, B. Schutte and C.P. Reutelingsperger, A novel assay to measure loss of plasma membrane asymmetry during apoptosis of adherent cells in culture, *Cytometry* **24** (1996), 131–139.

[28] J. Vandesompele, K. De Preter, F. Pattyn, B. Poppe, N. Van Roy, A. De Paepe and F. Speleman, Accurate normalization of real-time quantitative RT-PCR data by geometric averaging of multiple internal control genes, *Genome Biol.* **3** (2002), RESEARCH0034.

[29] A.R. Venkitaraman, Cancer susceptibility and the functions of BRCA1 and BRCA2, *Cell* **108** (2002), 171–182.

[30] M. Warren, C.J. Lord, J. Masabanda, D. Griffin and A. Ashworth, Phenotypic effects of heterozygosity for a BRCA2 mutation, *Hum. Mol. Genet.* **12** (2003), 2645–2656.

[31] R. Wooster, G. Bignell, J. Lancaster, S. Swift, S. Seal, J. Mangion, N. Collins, S. Gregory, C. Gumbs and G. Micklem, Identification of the breast cancer susceptibility gene BRCA2, *Nature* **378** (1995), 789–792.

[32] V.P. Yu, M. Koehler, C. Steinlein, M. Schmid, L.A. Hanakahi, A.J. van Gool, S.C. West and A.R. Venkitaraman, Gross chromosomal rearrangements and genetic exchange between nonhomologous chromosomes following BRCA2 inactivation, *Genes Dev.* **14** (2000), 1400–1406.

Paper II.

Jonsdottir *et al. BMC Cell Biology* 2010, **11**:34
http://www.biomedcentral.com/1471-2121/11/34

BMC Cell Biology

RESEARCH ARTICLE Open Access

Centriole movements in mammalian epithelial cells during cytokinesis

Asta Björk Jonsdottir*[1,2], Roeland W Dirks[2], Johannes Vrolijk[2], Helga M Ögmundsdottir[1], Hans J Tanke[2], Jorunn E Eyfjörd[1] and Karoly Szuhai[2]

Abstract

Background: In cytokinesis, when the cleavage furrow has been formed, the two centrioles in each daughter cell separate. It has been suggested that the centrioles facilitate and regulate cytokinesis to some extent. It has been postulated that termination of cytokinesis (abscission) depends on the migration of a centriole to the intercellular bridge and then back to the cell center. To investigate the involvement of centrioles in cytokinesis, we monitored the movements of centrioles in three mammalian epithelial cell lines, HeLa, MCF 10A, and the p53-deficient mouse mammary tumor cell line KP-7.7, by time-lapse imaging. Centrin1-EGFP and α-Tubulin-mCherry were co-expressed in the cells to visualize respectively the centrioles and microtubules.

Results: Here we report that separated centrioles that migrate from the cell pole are very mobile during cytokinesis and their movements can be characterized as 1) along the nuclear envelope, 2) irregular, and 3) along microtubules forming the spindle axis. Centriole movement towards the intercellular bridge was only seen occasionally and was highly cell-line dependent.

Conclusions: These findings show that centrioles are highly mobile during cytokinesis and suggest that the repositioning of a centriole to the intercellular bridge is not essential for controlling abscission. We suggest that centriole movements are microtubule dependent and that abscission is more dependent on other mechanisms than positioning of centrioles.

Background

A centrosome consists of a pair of centrioles surrounded by pericentriolar material, and it duplicates once during the cell cycle. The two centrioles have different structures and function. The older "mother" centriole is associated with centriolar appendages, specific proteins such as cenexin and centrobin, it attaches microtubules and supports ciliogenesis. The younger "daughter" centriole lacks all these structures [1-4]. The centrosome duplication begins in G_1 by separation of the centrioles. At early S phase procentrioles start to nucleate near the base of the pre-existing centrioles, that then elongate and mature [5,6]. As a cell exits G_2 each centrosome nucleates microtubules and the mitotic spindle is formed [7]. Although cells with depleted centrosomes can divide, the presence of centrosomes ensures efficient formation of the mitotic spindle and facilitates cell division [8-10]. Cells with supernumerous centrosomes can form multipolar spindles leading to serious aberrations in chromosomal segregation [11,12]. Cytokinesis starts during anaphase, when the microtubules gradually concentrate at the spindle midzone and a perpendicular ring of actomyosin contracts to form a cleavage furrow. Subsequently, the cleavage furrow ingresses and an intercellular bridge is formed containing the midbody [13,14]. The midbody consists of overlapping microtubules and additional proteins, many of which are required for cytokinesis. These proteins are mainly secretory and membrane-trafficking proteins, actin and microtubule associated proteins and protein kinases [15,16]. Contractile ring assembly is directed by the RhoA guanosine triphosphatase (GTPase) and the non-muscle myosin II is among proteins required for furrow formation [17-19]. Cytokinesis is terminated by midbody cleavage (abscission) [20,21] and each daughter cell then receives only one centrosome [22]. The process of abscission is carefully regulated [16,23,24], but the con-

* Correspondence: astajo@hi.is
[1] Cancer Research Laboratory, Faculty of Medicine, University of Iceland, Vatnsmyrarvegi 16, 101 Reykjavik, Iceland
Full list of author information is available at the end of the article

trol mechanisms have not been fully elucidated. Many studies support the idea that the centrosomes facilitate the final division into two daughter cells. It has been postulated that they promote and regulate to some extent the abscission phase of cytokinesis by acting as a scaffold or by providing essential signaling molecules [9,22]. Also, a role for the centrioles has been suggested in determining abscission. Reports of possible centriole movements prior to abscission go back to 1973 when the centrioles were studied by using electron microscopy. It was then noticed that in late cytokinesis centrioles were present at a region near the midbody [25], and these observations were supported by later publications [26,27]. Studies have shown that when the cleavage furrow has been formed one of the two centrioles moved to the intercellular bridge, and then back to the cell center. This type of movement was observed in 90% of analyzed HeLa cells [28]. Centriolin, a maternal component of centrioles, localizes also to the intercellular bridge and it has been shown that silencing centriolin causes cells to have severe difficulties in completing cytokinesis and that the dividing cells remain interconnected [3,29]. Centriolar repositioning to the midbody is therefore thought to be important for the termination of cytokinesis.

In a previous study we observed that cytokinesis was delayed in *BRCA2* heterozygous primary cells [30], which prompted us to investigate the process of cytokinesis in more detail. We asked whether the migration of a centriole to the intracellular bridge is part of a general mechanism and required for completion of cytokinesis. To this end we analyzed the movements of fluorescently labeled centrioles during cytokinesis by time-lapse imaging in three different mammalian epithelial cell lines. Our observations indicate that the suggested key function of centrioles at the intercellular bridge in controlling the abscission phase of cytokinesis [28] may not be universally valid and could be cell-line dependent.

Results

Characterization and quantitative analysis of centriole mobility during cytokinesis

To investigate whether centrioles play a key role in regulating abscission and thereby in completing cytokinesis we analyzed their positioning and movements in human as well as in mouse epithelial cells by time-lapse fluorescence imaging using centrin1-EGFP as a marker.

Centrin1-EGFP and α-Tubulin-mCherry were co-expressed in both human mammary epithelial MCF 10A and HeLa cells by transient transfection to label respectively the centrioles and microtubules. Centriole mobility was analyzed in living cells by collecting 3D image stacks every 10 min for 4 to 6 hrs. Both fluorescence excitation and differential interference contrast (DIC) were used. DIC images were taken to follow the progression through cell division and used to identify the nuclear envelope and visualize the movement of the cells. As a control for potential transient transfection artifacts, HeLa cells stably expressing centrin1-EGFP [31] were analyzed.

Centrin1-EGFP and α-Tubulin-mCherry were also co-expressed in the p53-deficient mouse mammary tumor cells KP-7.7. Human centrin1 shows only 90% sequence homology to its mouse variant. Correct localization of centrin1 was confirmed by immunostaining for γ-Tubulin in mouse cells expressing the centrin1-EGFP (data not shown).

By analyzing the movements of centrioles in both human and mouse epithelial cells we noticed that centrioles were highly mobile in all cell lines and moved in different directions with varying speeds. To preclude subjective assessment of centriole mobility, we performed a quantitative analysis of the centriole movements using the tracking software Stacks (Figure 1A and Additional file 1 movie 1). The tracking showed that the mouse epithelial cell line KP-7.7 had the most mobile centrioles from anaphase onset until 60 min after abscission. Their centrioles moved on average $3.2 \cdot 10^3$ μm^2, with the average speed of 0.35 μm/min, which is 1.5-2.7 times faster than measured for centrioles of the human epithelial cell lines tested (Table 1). Cells were taken as random effects when comparing the mean square displacement (MSDp) of centrioles between the different cell lines because of great variations between cells within every sample (Figure 1B). The variance of centriole mobility was calculated to be 10 times greater between cells within a sample than within a cell, $30.3 \cdot 10^8$ versus $3.06 \cdot 10^8$ respectively.

Three main types of movements were detected: 1) migration along the nuclear envelope, 2) irregular, where centrioles moved in the cytoplasm or cell center with no specific direction and 3) traveling along microtubules forming the spindle axis.

Before abscission one of the separated centrioles or the whole centrosome was frequently found to be associated with and to migrate along the newly formed nuclear envelope in G_1 daughter cells. However, centriole migration was found to vary between daughter cells and between cell lines. A centriole moving along the nuclear envelope was detected in 58% of imaged KP-7.7 cells, 62% of MCF 10A cells, 75% of HeLa cells and 44% of imaged centrin1-EGFP HeLa cells (Figure 2A). Centrioles usually migrated along the nuclear envelope in one direction only, towards the intercellular bridge. Occasionally they detached from the nuclear envelope before reaching the intercellular bridge. Centrioles with a bi-directional movement migrated to the intercellular bridge and then back to the nuclear envelope by the same path. Tubulin foci were detected around the centrosomes at the nuclear envelope where the centrioles showed independent and irregular movements (Additional file 2 Figure S1). This

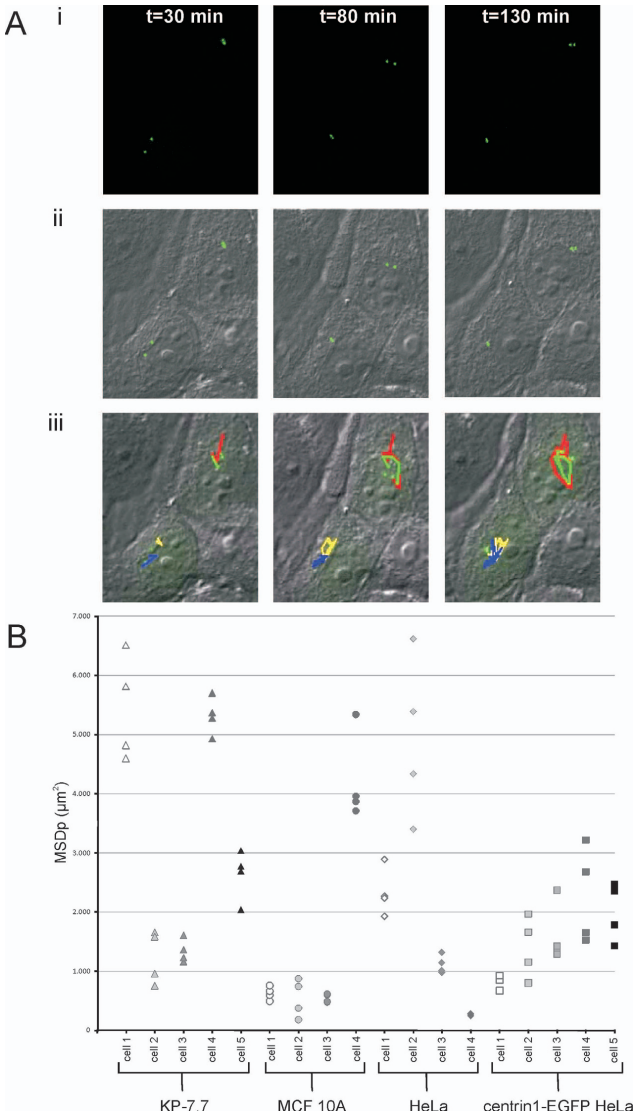

Figure 1 Tracking centrioles during cytokinesis. **A)** Representative images of centriole tracks in live MCF 10A cells are shown at three different time points as obtained with the tracking software Stacks (see Additional file 1 movie 1). i) The images show centriole (green) positioning at three different time points, 30 min, 80 min and 130 min after the onset of telophase. ii) The images are an overlay of centrin1-EGFP (green) and DIC. iii) The images are an overlay of centrin1-EGFP (green), DIC and the tracks of the centrioles for 130 min, from the onset of telophase. Every centriole track is represented by a unique pseudo-color and the tracks are determined by linking the centrioles between time-points. Analysis of the tracks revealed that these centrioles moved as fast as 0.35 μm/min on average (see Table 1). **B)** Distribution of the mean square displacement (MSDp) of movements of all 4 centrioles in individual cells (therefore 4 values for every cell) of all cell lines. Different gray tones are used to separate individual cells within a cell line. Triangles represent KP-7.7, circles MCF 10A, diamonds HeLa and squares centrin1-EGFP HeLa. The tracks presented in A) is MCF 10A cell 4. Mobility varied greatly between cells within every cell line. KP-7.7 had the most mobile centrioles (Table 1). MSDp of centrioles was compared using linear mixed model, taking cells as random effects.

Table 1: Centriole mobility during cytokinesis of various mammalian epithelial cell lines

Cell line	Average MSDp (μm^2)	Average speed (μm/min)
KP 7.7	$3.2 \cdot 10^3$	0.35
MCF 10A	$1.5 \cdot 10^3$	0.13
HeLa	$2.2 \cdot 10^3$	0.24
centrin1-EGFP HeLa	$1.6 \cdot 10^3$	0.17

was more frequently seen around immobile centrosomes that stayed close to the cell pole during cytokinesis. When centrioles did not move along the nuclear envelope in the direction of the cleavage site, they migrated through the cell center along microtubules containing α-Tubulin (Figure 2B).

Migration of centrioles to the intercellular bridge is not essential for abscission in human and mouse epithelial cells

In agreement with previously published data [28] we observed separation of mother and daughter centrioles in 90% of dividing cells after the formation of the cleavage furrow. In 3 out of 11 (27%) MCF 10A cells that completed abscission a centriole was observed to migrate to the intercellular bridge (Figure 3, Additional file 3-movie 2). In HeLa cells this was shown to occur 2 times more frequently than in MCF 10A cells (Table 2). No difference in centriole migration was observed between HeLa cells transiently or stably expressing centrin1-EGFP (50% versus 55%). In 7 out of 12 (58%) KP-7.7 cells either a whole centrosome or only the mother or the daughter centriole left the cell pole. This behavior was observed in one or both daughter cells. In mouse cells with mobile centrioles, centrioles showed an irregular movement along the nuclear envelope (Figure 4). Repositioning of a centriole to the intercellular bridge was not observed in any of the KP-7.7 cells (Table 2). Together, these observations suggest that abscission can take place without separation and repositioning of the centrioles.

As centriole mobility might be influenced by confluency of the cell culture, the centriole mobility was investigated at different cell densities. Mobile centrioles were more frequently found to reposition to the intercellular bridge when cells were grown at low or intermediate density (up to 70%) as compared with cells grown at high density showing much cell-cell contact, in 35% and 50%

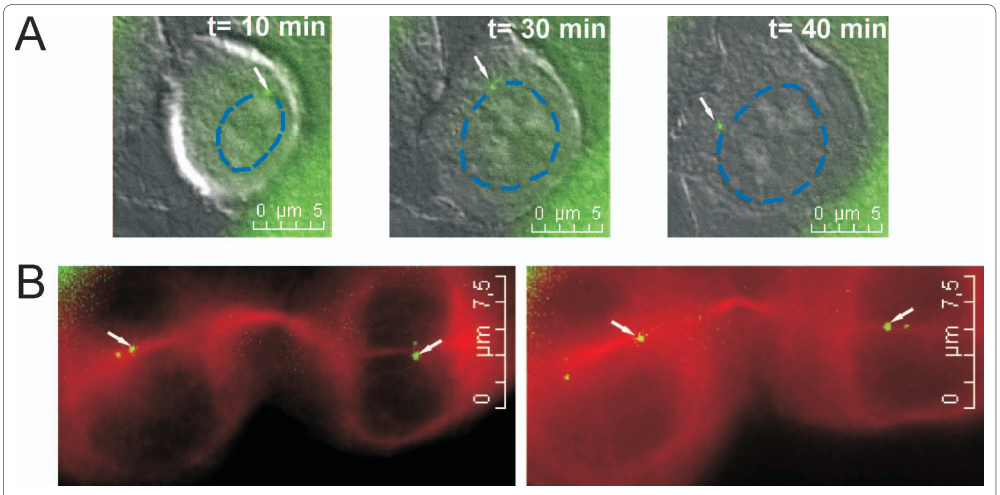

Figure 2 Centrioles move either along the nuclear envelope or along microtubules containing α-Tubulin. **A)** Centriole moving along the nuclear envelope in a centrin1-EGFP HeLa cell. The images shown are an overlay of centrin1-EGFP (green) and DIC. An arrow indicates mobile centrioles migrating along the nuclear envelope. The nuclear envelope is emphasized with a blue dotted line. **B)** A dividing HeLa cell showing centrioles that leave the cell pole and migrate through the cell center towards the intercellular bridge along microtubules. White arrows point at centrioles migrating along α-Tubulin towards the intercellular bridge.

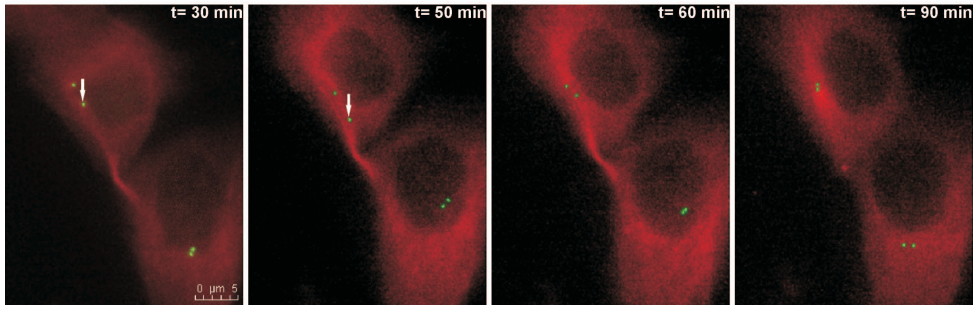

Figure 3 Centrioles migrate occasionally towards the intercellular bridge during cytokinesis in human epithelial cells. Representative images of centriole migration to the intercellular bridge prior to abscission (first 3 time points) and after abscission (t = 90 min) are shown for the human MCF 10A epithelial cell line (see Additional file 3 movie 2). The cells were transiently co-transfected with centrin1-EGFP (green) and α-Tubulin-mCherry (red) expression constructs, to label centrioles and the microtubules, respectively. White arrows point at a centriole migrating to the intercellular bridge.

of analyzed cells versus 15%, respectively (Additional file 4 Table S1).

When centrioles migrated to the intercellular bridge, the time they remained at or near the bridge before abscission occurred varied between cell lines. In most cells (84%) the centrioles stayed ≤ 30 min at the intercellular bridge, which is in line with previously published data [28]. The main difference between the cell lines was the length of the time interval between the relocation of the centriole from the intercellular bridge until the abscission. MCF 10A cells completed abscission within 30 min, 10 min on average, after the centriole left the intercellular bridge. For HeLa cells, this time period varied from 0 min up to 130 min and was on average 35 min (48 min for transiently transfected HeLa cells and 27 min for stably expressing centrin1-EGFP HeLa cells). Following abscission, the centrioles or even the whole centrosome became more mobile and frequently detached from the nuclear envelope.

We observed no correlation between the migration of a centriole to the intercellular bridge and any special characteristics of microtubule disassembly at the intercellular bridge. We noticed, however, that microtubule particles are released from the midbody and float in the extracellular space (Additional file 5 Figure S2).

Discussion

In this study we observed that centrioles are highly mobile during cell division and that their movements are different among the mammalian epithelial cell lines studied. During cytokinesis they move primarily along the nuclear envelope and along microtubules containing α-Tubulin. Importantly, repositioning of a centriole to the intercellular bridge was not found to be prerequisite for completion of abscission.

Table 2: Frequency of centriole(s) at the intercellular bridge of various mammalian epithelial cell lines

Cell line	Mobile centriole(s) at the intercellular bridge		Mobile centriole(s) not observed at the intercellular bridge	Immobile centrioles
	from one daughter cell	from both daughter cells		
KP 7.7 (n = 12)	0 (0%)	0 (0%)	7 (58%)	5 (42%)
MCF 10A (n = 11)	2 (18%)	1 (9%)	7 (64%)	1 (9%)
HeLa (n = 16)	5 (31%)	3 (19%)	3 (19%)	5 (31%)
centrin1-EGFP HeLa (n = 22)	10 (46%)	2 (9%)	6 (27%)	4 (18%)

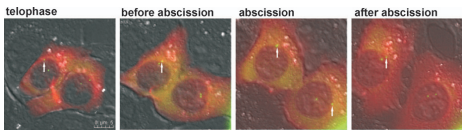

Figure 4 Centriole movement in mouse mammary epithelial cells during cytokinesis. During cytokinesis, centrioles show increased mobility and either one centriole or the complete centrosome is frequently associated with the nuclear envelope. After abscission centrioles increase their mobility and frequently detach from the nuclear envelope. The images show an overlay of DIC, green and red recordings to show centriole-specific centrin1-EGFP localization together with the intercellular bridge marker α-Tubulin-mCherry. White arrows indicate centrioles by the nuclear envelope.

Consistent with previously published data showing that centrosome movement during cytokinesis is microtubule-dependent [26], we observed that in newly formed G_1 daughter cells centrioles attach to and migrate along the nuclear envelope. In *Caenorhabditis elegans*, centrosomes are tightly associated with the nuclear envelope and dynein, zyg-12 and sun-1 are essential for centrosome attachment to the outer nuclear membrane [32,33]. In line with this, emerin was found to associate with microtubules to link centrosomes to the nuclear envelope [34]. In *Saccharomyces cerevisiae* the spindle pole body (SPB) is anchored in the nuclear envelope by hook-like appendages that originate in the central plaque [35]. The SPB membrane proteins Mps2p and Ndc1 attach the SPB to the nuclear envelope [36,37]. Whether other proteins are involved in the controlled movement of centrioles along the nuclear envelope in mammalian cells remains to be determined.

Abscission is a regulated process. Nuclear and cytoplasmic signaling proteins concentrate on centrosomes and other elements of the mitotic apparatus during G_2/M transition. After the onset of anaphase, recruitment of myosin II drives the formation of the cleavage furrow in animal cells [17]. Assembly of the contractile ring and ingression of the cleavage furrow to form the intercellular bridge, are key events before abscission. Abnormal furrowing and deficiency of or defects in proteins mediating cytokinesis, as BRCA2, can lead to a delay in the process and more severely, to incomplete cytokinesis [38].

A current model, supported by earlier findings [26], describes that the mother centriole has to reposition from the cell pole to the intercellular bridge and that abscission can take place only when the centriole moves back to the cell center [28]. We observed that centrioles migrate to the intercellular bridge in only about one third of human mammary epithelial MCF 10A cells analyzed and in half of all HeLa cells. In the p53-deficient mouse mammary tumor cells KP-7.7 centrioles were never observed to migrate to the intercellular bridge. It has been stated that cytokinesis rarely fails in various cell lines, including PtK_1, CV-1, BHK and LLC-PK, in which a centriole does not migrate towards the intercellular bridge [39]. These and our own observations are inconsistent with those published by Piel *et.al* [28]. They studied centriole motility in stable centrin1-EGFP expressing HeLa cells and in two mouse fibroblast cell lines, L929 and 3T3. A centriole was seen to migrate to the intercellular bridge in 90% of the analyzed centrin1-EGFP HeLa cells but in none of the 3T3 cells. We observed centrioles migrating towards the intercellular bridge in 55% of the centrin1-EGFP HeLa cells. The observed differences between those two studies may be the cause of sub-populations within the cell line, which have evolved during sub-culturing and transfers between institutes. Only epithelial cell lines were included in our study, eliminating cell type specific differences. Furthermore, the conditions under which the cells were imaged were kept constant as well as cell density. Notably, in relatively cell dense areas we observed little centriole mobility and at lower cell density we observed centrioles at least twice as frequently by the intercellular bridge.

It is known that cell-cell contact, cell density and cell adhesion can influence centrosome behavior, mitotic progression and ultimately the phenotype of cells. Recent studies demonstrate that the adhesion pattern of cells is conserved. Daughter cells spread precisely as their mother cell and the mitotic spindle is aligned along the traction field which is preserved from progenitor cell to daughter cells. The daughter cells transmit the tension to each other via the intercellular bridge [40]. This suggests that cell adhesion and traction forces are among the key regulators of abscission [28,41,42]. Dubreuil *et.al.* observed that particles were formed at the midbody and released into the extracellular space. They suggested that this might play a role in changing the tension in the intercellular bridge and thereby facilitate abscission [43]. We observed an increase in centriole mobility when daughter cells were beginning to attach to the culture dish (see Figure 2A, 20-30 min). At that time we also noticed that microtubule particles were released from the midbody, which were not necessarily adopted by either of the daughter cells (see Additional file Figure S2).

Conclusions

In this study we provide evidence that migration of the centriole towards the intercellular bridge is not a key event in regulating abscission. Centrioles are temporarily very mobile during mitosis and show three different types of movements: 1) along the nuclear envelope, 2) irregular, and 3) along microtubules containing α-Tubulin. Based on the observed variation in centriole mobility in different epithelial cell lines we conclude that the movements

and positioning of centrioles in late telophase cells, until abscission occurs, is highly cell line dependent.

Materials and methods

Cell lines

HeLa cells were cultured in Dulbecco's Modified Eagle's Medium (DMEM) supplemented with 10% fetal bovine serum (FBS), 100 units/ml penicillin and 0.1 mg/ml streptomycin (all from Invitrogen Corporation, Breda, The Netherlands). HeLa cells stably expressing centrin1-EGFP (kindly provided by Dr. Fanni Gergely, Cancer Research UK Cambridge Research Institute, Cambridge, England, with permission from Dr. Matthieu Piel [31]) were cultured using the same culture medium supplemented with 0.4 mg/ml Geneticin (Invitrogen Corporation). MCF 10A (American Type Culture Collection) cells were cultured in DMEM/F12 supplemented with 5% horse serum, 100 units/ml penicillin, 0.1 mg/ml streptomycin, 20 ng/ml epidermal growth factor (EGF) (from Invitrogen Corporation), 10 μg/ml insulin, and 0.5 μg/ml hydrocortisone (both from Sigma-Aldrich Chemie B.V., Zwijndrecht, The Netherlands) and 0.1 μg/ml cholera toxin (Gentaur, Kampenhout, Belgium). The KP-7.7 cell line (kindly provided by Dr. Jos Jonkers, The Netherlands Cancer Institute, Amsterdam, The Netherlands) was derived from a p53-deficient mouse mammary tumor as described [44] and cultured in DMEM/F12 (Invitrogen Corporation) supplemented with 10% FBS, 100 units/ml penicillin, 0.1 mg/ml streptomycin, 5 ng/ml EGF, 50 μg/ml insulin and 5 ng/ml cholera toxin. All cells were cultured in a 5% CO_2 humidified incubator at 37°C.

Transfection

Cells were transiently transfected at approximately 30% confluency with centrin1-EGFP and α-Tubulin-mCherry expression constructs by using Lipofectamine™ 2000 according to manufacturer's instructions (Invitrogen Corporation). Centrin1-EGFP [31] was kindly provided by Dr. Michel Bornens, Institute Curie, Paris, France and YFP-α Tubulin [45] by Dr. Jan Ellenberg, EMBL, Heidelberg, Germany. YFP was exchanged for mCherry by performing a polymerase chain reaction (PCR) on a mCherry expression construct [46] (kind gift of Dr. R. Tsien, Howard Hughes Medical Institute, University of California, San Diego, USA), with the following forward and reverse primers; 5' ATATAGCTAGCGCTACCGGTCGCCACCATGGTGAGCAAGGGCGAGGAG 3', 5' TATATCTCGAGATCTGAGTCCGGACTTGTACTTGTACAGCTCGTCCATGCC 3', respectively. After gel extraction, purification of the PCR products and digestion with *Xho*I and *Nhe*I restriction enzymes (New England BioLabs, Westburg B.V., Leusden, The Netherlands) at 37°C for 2 hrs subsequent purification steps were performed according to protocol. YFP-α-Tubulin construct was digested with the same restriction enzymes and after gel extraction and purification the mCherry sequence was ligated to the α-Tubulin expression construct.

Time-lapse live-cell imaging

Transiently transfected cells cultured in glass-bottom culture dishes (MatTek) were imaged at approximately 70% confluency 48 hrs after transfection. Cytokinesis and centriole movements were recorded with a Leica AF6000 LX microscope system equipped with an inverted DMI 6000B microscope, a DFC350 FX monochrome digital camera (1.4 Megapixel, 12 bit) and a climate chamber (Leica Microsystems). 3D image stacks were collected, each stack containing about 10 optical sections with 1 μm thickness, every 10 min for up to 6 hrs using a HCX PL APO 63×/1.30 GLYC [ne = 1.460 CORR 37°C] objective embedded in glycerin solution (Leica Microsystems). Cells were exposed to both differential interference contrast (DIC, also known as Nomarski microscopy) transmitted light as well as fluorescence light. A TexasRed filter was used to visualize mCherry and a B/G/R filter with separate FITC excitation to visualize green fluorescence emission. The LAS AF software (Leica Microsystems) was used to process the collected time-lapse images and to generate movies. Temperature, CO_2 concentration and humidity were strictly controlled and kept constant to avoid induction of stress responses, which could influence the processes under study [47]. In addition, the size of image stacks, exposure times and the number of exposures were kept to minimum in all experiments as those factors are known to induce free radical formation and photo damage [48,49].

Tracking of centriole movements

An in-house developed tracking software, Stacks, was used to quantitatively analyze centriole kinetics. This program allows visualization of time-lapse 2D and 3D image data, offers movie facilities, and provides great flexibility to enhance, process and analyze image stacks. To track the centrioles, image segmentation was performed using global thresholding and additionally the threshold was adjusted for each slice in a time series or in case of one slice at a specific time-point. Following segmentation, the position, size and total density of each centriole particle was measured for all time-points. Then tracks were determined by linking the centrioles between successive time-points, which had the highest calculated probability based on these features. Every identified centriole was assigned with a unique pseudo-color, so that we could identify which centriole was classified as being the same when scrolling between time-points. By manual, interaction tracks were split and reconnected to correct for errors made by the automatic procedure. Finally kinetic parameters such as mean squared displacement

(MSDp) were calculated to characterize the mobility of individual centrioles.

Statistical analysis

The null hypothesis stating that all cells tested would reveal an equal mean value of the mean square displacement was tested by using linear mixed model calculations. Cells were taken as random effects as there were great variations of centriole mobility between cells within every cell line.

Additional material

Additional file 1 Centriole tracks in MCF 10A cells during cytokinesis. Centrioles were tracked using the tracking software Stacks (see Figure 1A). Every centriole track is represented by a different color.

Additional file 2 Centrosome is mobile in an α-Tubulin net. Centrosome show low mobility in α-Tubulin foci close by the nuclear envelope (inset). Blue-dotted lines represent the nuclear envelope. Images shown are an overlay of centrin1-EGFP (green) and α-Tubulin-mCherry (red).

Additional file 3 Centriole mobility in MCF 10A cell during cytokinesis. Representative movie of centriole mobility in epithelial MCF 10A cells during cytokinesis (see Figure 3). Images were collected every 10 minutes using fluorescent excitation and DIC. The centrosome compartments centrioles are marked green and in red are microtubules. Microtubules accumulate and form the intercellular bridge during cytokinesis. A centriole migrates to the intercellular bridge before abscission occurs.

Additional file 4 Frequency of centriole repositioning to the intercellular bridge in relation to cell density.

Additional file 5 Midbody in extracellular space after abscission. Representative images of release of microtubule particles from the intercellular bridge and fate of midbody after abscission. Intercellular bridge containing the midbody (white arrows) links the two daughter cells. During abscission the bridge is cut. The midbody floats in the extracellular space after abscission.

Authors' contributions

ABJ participated in the design of the study, setup and performed the experiments, processed the data, participated in interpretation of the results and drafted the manuscript. RWD, HMÓ, HJT, JEE and KS participated in the design of the study, assisted with interpretation of the data and drafting the manuscript. RWD, HMÓ and KS critically revised the manuscript. JV programmed the Stacks computer software, assisted with processing the data and with calculations. HJT, JEE and KS supervised the project. All authors read and approved the final manuscript.

Acknowledgements

Prof. Michel Bornens, Institute Curie, Paris, France, for centrin1-EGFP expression construct and Dr. Matthieu Piel, Institute Curie, Paris, France for stable centrin1-EGFP HeLa cell line and their helpful discussion and comments during the preparation of this manuscript. We thank Dr. Jan Ellenberg, EMBL, Heidelberg, Germany and Prof. Roger Tsien, Howard Hughes Medical Institute, University of California, San Diego, USA, for providing expression constructs. Dr. Jos Jonkers and Dr. Bastiaan Evers, The Netherlands Cancer Institute, Amsterdam, The Netherlands and Dr. Fanni Gergely, Cancer Research UK Cambridge Research Institute, Cambridge, England, for collaboration and Dr. Jos Jonkers for reviewing the manuscript. Willem Sloos, Leiden University Medical Centre, Leiden, The Netherlands for technical assistance. Prof. Gunnar Stefansson and Johanna Sigmundsdottir, Statistics Centre, University of Iceland, Reykjavik, Iceland, for assistance with statistical analysis. This work is funded by the University of Iceland Research Fund (ABJ), Soroptimist International of Europe (ABJ) and Gongum Saman (ABJ).

Author Details

[1]Cancer Research Laboratory, Faculty of Medicine, University of Iceland, Vatnsmyrarvegi 16, 101 Reykjavik, Iceland and [2]Department of Molecular Cell Biology, Leiden University Medical Center, Einthovenweg 20, 2300 RC Leiden, the Netherlands

Received: 22 December 2009 Accepted: 21 May 2010
Published: 21 May 2010

References

1. Vorobjev IA, Chentsov Yu S: **Centrioles in the cell cycle. I. Epithelial cells.** *J Cell Biol* 1982, **93:**938-949.
2. Lange BM, Gull K: **A molecular marker for centriole maturation in the mammalian cell cycle.** *J Cell Biol* 1995, **130:**919-927.
3. Gromley A, Jurczyk A, Sillibourne J, Halilovic E, Mogensen M, Groisman I, Blomberg M, Doxsey S: **A novel human protein of the maternal centriole is required for the final stages of cytokinesis and entry into S phase.** *J Cell Biol* 2003, **161:**535-545.
4. Anderson CT, Stearns T: **Centriole age underlies asynchronous primary cilium growth in mammalian cells.** *Curr Biol* 2009, **19:**1498-1502.
5. Azimzadeh J, Bornens M: **Structure and duplication of the centrosome.** *J Cell Sci* 2007, **120:**2139-2142.
6. Alvey PL: **An investigation of the centriole cycle using 3T3 and CHO cells.** *J Cell Sci* 1985, **78:**147-162.
7. Piehl M, Tulu US, Wadsworth P, Cassimeris L: **Centrosome maturation: Measurement of microtubule nucleation throughout the cell cycle by using GFP-tagged EB1.** *Proc Natl Acad Sci* 2004, **101:**1584-1588.
8. Khodjakov A, Cole RW, Oakley BR, Rieder CL: **Centrosome-independent mitotic spindle formation in vertebrates.** *Curr Biol* 2000, **10:**59-67.
9. Khodjakov A, Rieder CL: **Centrosomes enhance the fidelity of cytokinesis in vertebrates and are required for cell cycle progression.** *J Cell Biol* 2001, **153:**237-242.
10. Schaffner SC, Jose JV: **Biophysical model of self-organized spindle formation patterns without centrosomes and kinetochores.** *Proc Natl Acad Sci* 2006, **103:**11166-11171.
11. Borel F, Lohez OD, Lacroix FB, Margolis RL: **Multiple centrosomes arise from tetraploidy checkpoint failure and mitotic centrosome clusters in p53 and RB pocket protein-compromised cells.** *Proc Natl Acad Sci* 2002, **99:**9819-9824.
12. Storchova Z, Kuffer C: **The consequences of tetraploidy and aneuploidy.** *J Cell Sci* 2008, **121:**3859-3866.
13. Krystal G, Rattner JB, Hamkalo BA: **Partial purification and characterization of the intercellular bridge from cultured mouse cells.** *Proc Natl Acad Sci* 1978, **75:**4977-4981.
14. Glotzer M: **The mechanism and control of cytokinesis.** *Curr Opin Cell Biol* 1997, **9:**815-823.
15. Skop AR, Liu H, Yates J III, Meyer BJ, Heald R: **Dissection of the mammalian midbody proteome reveals conserved cytokinesis mechanisms.** *Science* 2004, **305:**61-66.
16. Glotzer M: **The molecular requirements for cytokinesis.** *Science* 2005, **307:**1735-1739.
17. Straight AF, Cheung A, Limouze J, Chen I, Westwood NJ, Sellers JR, Mitchison TJ: **Dissecting temporal and spatial control of cytokinesis with a myosin II inhibitor.** *Science* 2003, **299:**1743-1747.
18. Piekny A, Werner M, Glotzer M: **Cytokinesis: welcome to the Rho zone.** *Trends Cell Biol* 2005, **15:**651-658.
19. Mishima M, Kaitna S, Glotzer M: **Central spindle assembly and cytokinesis require a kinesin-like protein/RhoGAP complex with microtubule bundling activity.** *Dev Cell* 2002, **2:**41-54.
20. Saurin AT, Durgan J, Cameron AJ, Faisal A, Marber MS, Parker PJ: **The regulated assembly of a PKCepsilon complex controls the completion of cytokinesis.** *Nat Cell Biol* 2008, **10:**891-901.
21. Steigemann P, Gerlich DW: **Cytokinetic abscission: cellular dynamics at the midbody.** *Trends Cell Biol* 2009, **19:**606-616.
22. Doxsey S, Zimmerman W, Mikule K: **Centrosome control of the cell cycle.** *Trends in Cell Biology* 2005, **15:**303-311.
23. Steigemann P, Wurzenberger C, Schmitz MHA, Held M, Guizetti J, Maar S, Gerlich DW: **Aurora B-mediated abscission checkpoint protects against tetraploidization.** *Cell* 2009, **136:**473-484.
24. Carmena M, Earnshaw WC: **The cellular geography of Aurora kinases.** *Nat Rev Mol Cell Biol* 2003, **4:**842-854.

25. Rattner JB, Phillips SG: **Independence of centriole formation and DNA synthesis.** *J Cell Biol* 1973, **57:**359-372.
26. Mack G, Rattner JB: **Centrosome repositioning immediately following karyokinsis and prior to cytokinesis.** *Cell Motil Cytoskel* 1993, **26:**239-247.
27. Young YO, Jerome BR: **Post-karyokinesis centrosome movement leaves a trail of unanswered questions.** *Cell Motil Cytoskel* 2002, **51:**123-132.
28. Piel M, Nordberg J, Euteneuer U, Bornens M: **Centrosome-dependent exit of cytokinesis in animal cells.** *Science* 2001, **291:**1550-1553.
29. Gromley A, Yeaman C, Rosa J, Redick S, Chen CT, Mirabelle S, Guha M, Sillibourne J, Doxsey SJ: **Centriolin anchoring of exocyst and SNARE complexes at the midbody Is required for secretory-vesicle-mediated abscission.** *Cell* 2005, **123:**75-87.
30. Jonsdottir AB, Vreeswijk MPG, Wolterbeek R, Devilee P, Tanke HJ, Eyfjörd JE, Szuhai K: **BRCA2 heterozygosity delays cytokinesis in primary human fibroblasts.** *Cell Oncol* 2009, **31:**191-201.
31. Piel M, Meyer P, Khodjakov A, Rieder CL, Bornens M: **The respective contributions of the mother and daughter centrioles to centrosome activity and behavior in vertebrate cells.** *J Cell Biol* 2000, **149:**317-330.
32. Malone CJ, Misner L, Le Bot N, Tsai MC, Campbell JM, Ahringer J, White JG: **The C. elegans hook protein, ZYG-12, mediates the essential attachment between the centrosome and nucleus.** *Cell* 2003, **115:**825-836.
33. Meyerzon M, Gao Z, Liu J, Wu JC, Malone CJ, Starr DA: **Centrosome attachment to the C. elegans male pronucleus is dependent on the surface area of the nuclear envelope.** *Dev Biol* 2009, **327:**433-446.
34. Salpingidou G, Smertenko A, Hausmanowa-Petrucewicz I, Hussey PJ, Hutchison CJ: **A novel role for the nuclear membrane protein emerin in association of the centrosome to the outer nuclear membrane.** *J Cell Biol* 2007, **178:**897-904.
35. O'Toole ET, Winey M, McIntosh JR: **High-voltage electron tomography of spindle pole bodies and early mitotic spindles in the yeast Saccharomyces cerevisiae.** *Mol Biol Cell* 1999, **10:**2017-2031.
36. Munoz-Centeno MdlC, McBratney S, Monterrosa A, Byers B, Mann C, Winey M: **Saccharomyces cerevisiae MPS2 encodes a membrane protein localized at the spindle pole body and the nuclear envelope.** *Mol Biol Cell* 1999, **10:**2393-2406.
37. Chial HJ, Rout MP, Giddings TH, Winey M: **Saccharomyces cerevisiae Ndc1p Is a Shared Component of Nuclear Pore Complexes and Spindle Pole Bodies.** *J Cell Biol* 1998, **143:**1789-1800.
38. Daniels MJ, Wang Y, Lee M, Venkitaraman AR: **Abnormal cytokinesis in cells deficient in the breast cancer susceptibility protein BRCA2.** *Science* 2004, **306:**876-879.
39. Rieder CL, Faruki S, Khodjakov A: **The centrosome in vertebrates: more than a microtubule-organizing center.** *Trends in Cell Biology* 2001, **11:**413-419.
40. Thery M, Bornens M: **Cell shape and cell division.** *Curr Opin Cell Biol* 2006, **18:**648-657.
41. Thery M, Racine V, Pepin A, Piel M, Chen Y, Sibarita JB, Bornens M: **The extracellular matrix guides the orientation of the cell division axis.** *Nat Cell Biol* 2005, **7:**947-953.
42. Thery M, Jimenez-Dalmaroni A, Racine V, Bornens M, Julicher F: **Experimental and theoretical study of mitotic spindle orientation.** *Nature* 2007, **447:**493-496.
43. Dubreuil V, Marzesco AM, Corbeil D, Huttner WB, Wilsch-Brauninger M: **Midbody and primary cilium of neural progenitors release extracellular membrane particles enriched in the stem cell marker prominin-1.** *J Cell Biol* 2007, **176:**483-495.
44. Evers B, Drost R, Schut E, de Bruin M, Burg E van der, Derksen PWB, Holstege H, Liu X, van Drunen E, Beverloo HB, *et al.*: **Selective inhibition of BRCA2-deficient mammary tumor cell growth by AZD2281 and cisplatin.** *Clin Can Res* 2008, **14:**3916-3925.
45. Gerlich D, Beaudouin J, Kalbfuss B, Daigle N, Eils R, Ellenberg J: **Global chromosome positions are transmitted through mitosis in mammalian cells.** *Cell* 2003, **112:**751-764.
46. Shaner NC, Campbell RE, Steinbach PA, Giepmans BNG, Palmer AE, Tsien RY: **Improved monomeric red, orange and yellow fluorescent proteins derived from Discosoma sp. red fluorescent protein.** *Nat Biotech* 2004, **22:**1567-1572.
47. Frigault MM, Lacoste J, Swift JL, Brown CM: **Live-cell microscopy - tips and tools.** *J Cell Sci* 2009, **122:**753-767.
48. Song L, Varma CA, Verhoeven JW, Tanke HJ: **Influence of the triplet excited state on the photobleaching kinetics of fluorescein in microscopy.** *Biophys Journal* 1996, **70:**2959-2968.
49. Knight MM, Roberts SR, Lee DA, Bader DL: **Live cell imaging using confocal microscopy induces intracellular calcium transients and cell death.** *Am J Physiol Cell Physiol* 2003, **284:**C1083-1089.

doi: 10.1186/1471-2121-11-34
Cite this article as: Jonsdottir *et al.*, Centriole movements in mammalian epithelial cells during cytokinesis *BMC Cell Biology* 2010, **11**:34

Paper III.

Tetraploidy in *BRCA2* breast tumours

Asta Bjork Jonsdottir[1], Olafur Andri Stefansson[1], Johannes Bjornsson[2,3], Jon G. Jonasson[2,3,4], Helga M. Ogmundsdottir[1,2], Jorunn E. Eyfjord[1,2*].

[1] Cancer Research Laboratory, Faculty of Medicine, University of Iceland, Reykjavik, Iceland.

[2] Faculty of Medicine, University of Iceland, Reykjavik, Iceland.

[3] Department of Pathology, Landspitali University Hospital, Reykjavik, Iceland.

[4] Icelandic Cancer Registry, Icelandic Cancer Society, Reykjavik, Iceland.

[*]Corresponding author

Cancer Research Laboratory

Faculty of Medicine

University of Iceland

Vatnsmyrarvegi 16

101 Reykjavik

Iceland

Compteting interests

The authors declare that they have no competing interests.

Word count: 2217

Abstract

Tetraploidy and aneuploidy can be caused by cell division errors and are frequently observed in many human carcinomas. We have recently reported delayed cytokinesis in primary human fibroblasts from *BRCA2* mutation carriers, implying a function for the BRCA2 tumour suppressor in completion of cell division. Here, we address ploidy aberrations in breast tumours derived from *BRCA2* germline mutation carriers. Ploidy aberrations were evaluated from flow cytometry histograms on selected breast tumour samples (n=236), previously screened for local *BRCA* mutations. The ploidy between *BRCA2*-mutated (n=71) and matched sporadic (n=165) cancers was compared. Differences in ploidy distribution were examined with respect to molecular tumour subtypes, previously defined by immunohistochemistry on tissue microarray sections. Tetraploidy was significantly 3 times more common in *BRCA2* breast cancers than sporadic. However, no differences were found in the overall ploidy distribution between *BRCA2*-mutation carriers and non-carriers. In *BRCA2* cancers, tetraploidy was associated with luminal characteristics. The increased frequency of tetraploidy in *BRCA2* associated cancers may be linked to cell division errors, particularly cytokinesis. Additionally, tetraploidy emerges predominantly in *BRCA2* breast cancers displaying luminal rather than triple-negative phenotypes.

Key words: Breast Cancer, BRCA2, tetraploidy, aneuploidy, diploidy, luminal, triple-negative phenotype, cytokinesis.

Introduction

Inherited mutations in the breast cancer susceptibility genes *BRCA1* and *BRCA2* increase the risk of breast cancer as well as ovarian, prostate and other types of cancers [1]. For carriers of the Icelandic founder mutation *BRCA2 999del5,* the risk translates into over 70% by the age of 70 [2]. The increased susceptibility has been attributed to functions of the BRCA proteins in repair of DNA double strand breaks, via homologous recombination. Defects in the repair mechanisms can alter recombination pathways, giving rise to chromosomal re-arrangements, which have been implicated as the main cause for chromosomal instability found in the tumours of *BRCA2* mutation carriers [3, 4]. More recently, it has been suggested that the BRCA2 protein functions in cytokinesis [5, 6]. Defects in daughter cell separation can cause mis-segregation of chromosomes, giving rise to polyploidy [7] and could therefore contribute to the increased cancer susceptibility in *BRCA2*-mutation carriers.

Genomic alterations are common in breast tumours. Variations in gene expression patterns can be accompanied by corresponding phenotypic diversity of breast tumours. Breast tumours can arise from at least two distinct cell types: basal-like and luminal epithelial cells, and can be categorized into five subtypes based on expression of three biomarkers, oestrogen receptor (ER), progesterone receptor (PR) and human epidermal growth factor receptor 2 (HER2). Better definition can be achieved by adding epidermal growth factor receptor (EGFR) and cytokeratin 5/6 (CY5/6) expression analysis [8, 9]. The five subtypes of breast tumours are luminal A and luminal B (positive for either ER or PR), HER2 overexpressing (ER and PR negative), normal-like and basal-like, including triple-negative phenotype (TNP) for ER, PR and HER2. The basal-like subtype can further be subdivided into five-marker negative phenotype (5NP) or Core Basal [10]. *BRCA2* tumours are predominantly luminal A or luminal

B [11, 12]. They show frequent and complex genomic alterations [13, 14] and have relatively large deletions and few high-level amplifications [14].

A potential function for the BRCA2 protein in cytokinesis has been shown in modified mouse embryonic fibroblasts and HeLa cells [5]. We have recently reported that BRCA2 plays a role in the process in primary human fibroblast cells [6]. It is well known that unsuccessful cell division can cause incomplete chromosomal segregation, give rise to altered ploidy and supernumerary centrosomes [7, 15]. Tetraploidy can emerge through various mechanisms, such as cell fusion, mitotic slippage, and failure to undergo cytokinesis. A failure to undergo cytokinesis may occur because of a failure or disturbance of cleavage furrow formation, giving rise to a new G_1 bi-nucleated cell with two centrosomes [16, 17]. It has been proposed that tetraploid cells represent an important intermediate on the route to aneuploidy [7]. Active checkpoints prevent tetra- and aneuploidization. They act to ensure accurate cell division and inhibit cycling of cells that have not exited mitosis efficiently [18, 19].

There is an indication that *BRCA2*-mutation status is associated with bi-nucleation and amplification of centrosomes [20]. Mouse cells deficient for *Brca2* produce polyploid cells [21]. The majority of the Icelandic *BRCA2 999del5* breast cancer cases have been shown to be non-diploid [3]. A study presenting an association between *BRCA2* mutation and high grade tumour progression additionally to increased proliferation rate, also found that non-diploidy was of higher frequency in *BRCA2*-mutated tumours than sporadic [22].

The aim of this study was to investigate the proportion of tetraploidy and aneuploidy in *BRCA2*-mutated breast tumours, as a potential consequence of cytokinesis defects. We compared the DNA content in *BRCA2*-mutated and sporadic breast tumours, measured with flow cytometry. Ploidy aberrations were then linked to molecular classification of the tumours.

Material and Methods

Patient samples

Malignant breast tumour samples were selected from a patient cohort that had previously been screened for local *BRCA* germline mutations and had been diagnosed from 1990-2006. Fulfilling these criteria were 101 *BRCA2*-mutation carriers. Two hundred and two sporadic cases that matched for year and age at diagnosis were selected as controls. Flow cytometry data for ploidy evaluation were available for 71 tumours from selected *BRCA2*-mutation carriers and 165 from sporadic controls.

All *BRCA2*-mutated samples carry an Icelandic founder mutation, *BRCA2 999del5* [23]. Exon 9 of the *BRCA2* gene was PCR-amplified from peripheral blood DNA and run on 7.5% polyacrylamide gels for detection of the *999del5* mutation [23, 24].

This work was carried out according to permissions from the Icelandic Data Protection Commission (2006050307) and National Bioethics Committee (VSNb2006050001/03-16). Informed consent was obtained from all patients.

Ploidy data

Flow cytometry analysis has been performed routinely on invasive breast tumour samples at the Department of Pathology, Landspitali University Hospital, Reykjavik, Iceland, since 1990. Flow cytometry histograms, indicating DNA content, were classified as diploid when they showed a single G_0/G_1 peak. Samples with at least two clear distinct peaks were classified as aneuploid. When the ratio was 1.80-2.10, and therefore the DNA content in the

cells in the second peak was about twice as much as in the normal peak, the sample was classified as tetraploid. Tumours containing both aneuploid and tetraploid cells were classified as mixed aneu- and tetraploid. DNA ploidy index and S-phase assessment were performed and classified as described [25]. Only one DNA content measurement from each tumour was included.

The S-phase value of <7% was defined as low S-phase, and ≥ 7% was defined as high S-phase.

Immunohistochemistry and Tissue microarray

For molecular characterization of the breast tumour samples immunohistochemistry was performed on tissue microarray sections. Expression analysis was carried out for ER, PR, HER-2, EGFR, CK5/6, CK8, CK18 and BRCA1, as described earlier [14, 26].

Statistical analysis

Statistical analysis was carried out using SPSS 17.0 and R 2.10.1. Associations between the *BRCA2* mutation status of the breast tumours and ploidy, as well as between the phenotype of tumours and ploidy in *BRCA2*-mutated and sporadic samples were calculated using χ^2-tests.

Results

Ploidy aberrations of BRCA2 and sporadic breast tumours

Ploidy was examined in a selected set of 236 breast tumours derived both from *BRCA2*-mutation carriers and sporadic breast cancer cases. The frequency of diploidy, aneuploidy, tetraploidy and mixed aneu- and tetraploidy was compared between *BRCA2* and sporadic tumours.

Table 1 summarizes the ploidy distribution of sporadic and *BRCA2*-mutated tumours showing no differences in the overall distribution between the two groups (χ^2 test statistic 6.18, *P*-value 0.103). Nearly half of both sporadic and *BRCA2* tumours were diploid (47.9% and 42.3% respectively).

Although the overall distribution was the same, tetraploidy was significantly more common in *BRCA2* breast tumours than sporadic. The difference was almost 3 fold, 14.1% (10 of 71) as compared with 4.8% (8 of 165) (χ^2 test statistic 4.77, *P*-value 0.029) (Figure 1).

The percentage of cells in S-phase of the cell cycle is an indicator of the proliferation rate of a tumour. The S-phase in *BRCA2* tumours was higher than in sporadic tumours (χ^2 test statistic 3.71, *P*-value 0.054). High S-phase was associated with polyploidy both in *BRCA2*-*(*χ^2 test statistic 47.03, *P*-value <0.001) and sporadic tumours (χ^2 test statistic 47.03, *P*-value <0.001) (Additional file Table 1).

Molecular classification of BRCA2 and sporadic breast tumours in relation to ploidy

Breast cancers are classified into subtypes based on their molecular profiles. Expression data for ER, PR and HER2, analysed by immunohistochemistry (IHC) on tissue

microarrays, was available from another study [26] for a subset of the study group (52 *BRCA2* and 43 sporadic cancers). This allowed us to examine ploidy aberrations in relation to molecular phenotypes established through a validated classification scheme [10].

All of the *BRCA2* cancers sub-categorised as either luminal (37 of 52, 71.1%) or TNP (15 of 52, 28.9%) as none displayed HER2 overexpression. From Table 2 and Figure 2 it is clear that within the group of *BRCA2* cancers the differences between luminal and TNP subtypes are reflected in the type of ploidy abnormalities, and the association between ploidy aberrations and molecular subtype was highly significant (χ^2 test statistic 18.48, *P*-value < 0.001). All of the 7 tetraploid *BRCA2* cancers and 5 out of the 6 mixed aneu- and tetraploid belonged to the luminal phenotype (χ^2 test statistic 8.65, *P*-value 0.003) (Figure 2).

In contrast, all except one of the TNP *BRCA2* tumours displaying ploidy aberrations were aneuploid only (11 of 12, 91.7%) (Table 2).

The group of sporadic cancers also showed a statistically significant association between subtype and ploidy (χ^2 test statistic 20.47, *P*-value 0.015) (Table 2), as those of the luminal phenotype were mostly diploid or aneuploid, with only one out of 29 being tetraploid (Table 2). Although the numbers are very low they do not suggest the association between luminal phenotype and tetraploidy that was seen in the *BRCA2* group.

Discussion

The results presented here describe an analysis of ploidy in cancers derived from *BRCA2* germline mutation carriers and sporadic cancers. The study was carried out to follow up on our previous report describing a function for BRCA2 in the completion of cell division of primary human cells [6]. We observed that tetraploidy was significantly more frequent in

BRCA2-mutated than sporadic breast carcinomas. Furthermore, our results showed that tetraploidy in *BRCA2* cancers was almost confined to tumours of a luminal subtype.

When studying tetraploidy specifically, a 3 fold difference between *BRCA2*-mutated and sporadic cancers was detected, but tetraploidy for *BRCA2* cancers has not been described previously. There was no overall association between *BRCA2* status and ploidy, and this is in line with previously published data [3, 22]. Molecular classification was available for a subset of the studied tumour samples [26]. Tetraploid *BRCA2*-mutated cancers displayed luminal- rather than triple-negative phenotype. This is in contrast with that observed in sporadic cancers of luminal phenotype, not HER-2 related, which were mostly diploid or aneuploid and rarely showed tetraploid features.

Recently, it has been proposed that the wild-type *BRCA2* allele is not consistently lost in breast tumours from *BRCA2* mutation carriers [26, 27]. Ongoing studies indicate that deletion of the wild-type *BRCA2* allele may be more frequent in *BRCA2* cancers displaying luminal rather than triple-negative phenotype [28]. Given a role for BRCA2 in cytokinesis, this might explain why tetraploidy emerges in luminal- rather than triple-negative *BRCA2* cancers.

Tetraploidy is known to arise through incomplete cytokinesis. By using time-lapse live cell imaging to estimate cell division time we found that *BRCA2*-heterozygous primary human fibroblasts showed delayed cytokinesis [6, 28], supporting a role for BRCA2 in this process [5]. The *BRCA2* heterozygous primary fibroblasts had a slightly increased number of cells in G_2/M phase [6]. Spontaneous tetraploidy has been observed in cultured primary human skin fibroblasts derived from *BRCA2*-mutation carriers (Ogmundsdottir, H.M. unpublished data).

Previously established functions of the BRCA2 protein include an essential role in error-free repair of DNA double strand breaks via homologous recombination [29]. It is also needed at stalled replication forks [30], and it may regulate mitotic entry to some extent [31]. Cytokinesis can fail because of defects in or deficiency of proteins mediating cytokinesis. Also, chromosome bridges formed during anaphase can cause furrow regression leading to generation of bi-nucleated cells [32-34]. End-to-end fusions of chromosomes are more common in breast tumours from *BRCA2* carriers than in sporadic breast tumours [29, 35, 36]. These chromosomes frequently contain two or more centromeres, which makes segregation of sister-chromatids during mitosis difficult. The high degree of chromosomal re-arrangements and other genetic instability in *BRCA2*-deficient cell lines and tumours has been explained by inefficient repair of DNA double strand breaks, via error-prone non-homologous end joining, which can result in G_1 arrest. *BRCA2* mutations could therefore facilitate polyploidization through cytokinesis failure as well as creation of chromosome bridges.

Polyploidy is not necessarily a disadvantage [37]. Only when growth arrest, cell death or increased genomic instability is triggered can it be catastrophic [38]. Thus, polyploidy can be tolerated so long as cells retain the cellular machinery to duplicate and segregate their genome and centrosomes accurately during subsequent divisions. Tetraploid cells do not always produce tetraploid progeny. Aneuploidy can evolve either through tetraploidy or directly from diploidy [39]. Tetraploid cells frequently contain two extra centrosomes. Only when polarity is maintained, by forming a bipolar spindle, can a normal cell division be executed. Amplification of centrosomes can cause multipolar spindles, resulting in unequal distribution of chromatids between the daughter cells, giving rise to aneuploid progenies [15, 40]. The aneuploid and the mixed aneu- and tetraploid cell populations may have been promoted through the tetraploid rout, or they may have evolved directly from diploid cells,

possibly as a consequence of multipolar spindle or spindle checkpoint failure, resulting in mis-segregation of chromosomes.

In conclusion, tetraploidy was more frequent in *BRCA2*-mutated tumours than sporadic. We have previously reported that *BRCA2* heterozygous cells have delayed cytokinesis. We suggest that the increased tetraploidy in the *BRCA2* tumours may be related to defects in cytokinesis. Tetraploidy was found to be associated with luminal phenotype in the *BRCA2* samples. Thus, it may be speculated that loss of the BRCA2 function is more prominent in *BRCA2* cancers displaying luminal characteristics rather than triple-negative.

Acknowledgements

Holmfridur Hilmarsdottir, Cancer Research Laboratory, Faculty of Medicine, University of Iceland, Reykjavik, Iceland, and Gudridur Helga Olafsdottir, Icelandic Cancer Registry, Icelandic Cancer Society, Reykjavik, Iceland, for selecting cases and controls. Laufey Tryggvadottir, Icelandic Cancer Registry, Icelandic Cancer Society, Reykjavik, Iceland, for assistance with setting up the study. Kristrun Olafsdottir, Department of Pathology, Landspitali University Hospital, Reykjavik, Iceland, for performing IHC and TMA.

This work is funded by the University of Iceland Research Fund (ABJ and OAS) and Soroptimist International of Europe (ABJ).

Authors' contributions

Asta Bjork Jonsdottir (ABJ), Helga M. Ogmundsdottir (HMO), Johannes Bjornsson (JB) and Jorunn E. Eyfjord (JEE) designed the study. JB and Jon G. Jonasson (JGJ) provided flow

cytometry histograms that were analyzed by ABJ with the assistance from JGJ and HMO. ABJ, HMO and JEE interpreted the data, with the contribution of Olafur Andri Stefansson (OAS), who provided the molecular classification results. ABJ and OAS performed the statistical analyses. ABJ wrote the manuscript with assistance from HMO, JEE and OAS. All authors read the manuscript and agreed on its content.

List of abbreviations:

CGH = comparative genome hybridisation

CY = cytokeratin

EGFR = epidermal growth factor receptor

ER = oestrogen receptor

HER = human epidermal growth factor receptor

ICH = immunohistochemistry

PR = progesterone receptor

TNP = triple negative phenotype

5NP = five-marker negative phenotype

Online Supporting Information

Supporting Information Table 1: High- and low- S-phase frequency and ploidy distribution of *BRCA2* mutated and sporadic breast tumours.

References

1. Miki Y, Swensen J, Shattuck-Eidens D*, et al.* A strong candidate for the breast and ovarian cancer susceptibility gene BRCA1. *Science* 1994; **266**: 66-71.

2. Tryggvadottir L, Sigvaldason H, Olafsdottir GH*, et al.* Population-Based Study of Changing Breast Cancer Risk in Icelandic BRCA2 Mutation Carriers, 1920-2000. *J Natl Cancer Inst* 2006; **98**: 116-122.

3. Gretarsdottir S, Thorlacius S, Valgardsdottir R*, et al.* BRCA2 and p53 mutations in primary breast cancer in relation to genetic instability. *Cancer Res* 1998; **58**: 859-862.

4. Venkitaraman AR. Cancer susceptibility and the functions of BRCA1 and BRCA2. *Cell* 2002; **108**: 171-182.

5. Daniels MJ, Wang YM, Lee MY*, et al.* Abnormal cytokinesis in cells deficient in the breast cancer susceptibility protein BRCA2. *Science* 2004; **306**: 876-879.

6. Jonsdottir AB, Vreeswijk MPG, Wolterbeek R*, et al.* BRCA2 heterozygosity delays cytokinesis in primary human fibroblasts. *Cellular Oncology* 2009; **31**: 191-201.

7. Storchova Z, Kuffer C. The consequences of tetraploidy and aneuploidy. *J Cell Sci* 2008; **121**: 3859-3866.

8. Perou C, Sorlie T, Eisen M*, et al.* Molecular portraits of human breast tumours. *Nature* 2000; **406**: 747 - 752.

9. Chin K, DeVries S, Fridlyand J*, et al.* Genomic and transcriptional aberrations linked to breast cancer pathophysiologies. *Cancer Cell* 2006; **10**: 529 - 541.

10. Cheang M, Voduc D, Bajdik C*, et al.* Basal-like breast cancer defined by five biomarkers has superior prognostic value than triple-negative phenotype. *Clin Cancer Res* 2008; **14**: 1368 - 1376.

11. Sorlie T, Tibshirani R, Parker J*, et al.* Repeated observation of breast tumor subtypes in independent gene expression data sets. *Proc Natl Acad Sci U S A* 2003; **100**: 8418-8423.

12. Waddell N, Arnold J, Cocciardi S*, et al.* Subtypes of familial breast tumours revealed by expression and copy number profiling. *Breast Cancer Res Treat* 2009.

13. Tirkkonen M, Johannsson O, Agnarsson B*, et al.* Distinct somatic genetic changes associated with tumor progression in carriers of BRCA1 and BRCA2 germ-line mutations. *Cancer Res* 1997; **57**: 1222 - 1227.

14. Stefansson OA, Jonasson JG, Johannsson OT*, et al.* Genomic profiling of breast tumours in relation to BRCA abnormalities and phenotypes. *Breast Cancer Res* 2009; **11**: R47.

15. Gisselsson D. Classification of chromosome segregation errors in cancer. *Chromosoma* 2008; **117**: 511-519.

16. Storchova Z, Pellman D. From polyploidy to aneuploidy, genome instability and cancer. *Nat Rev Mol Cell Biol* 2004; **5**: 45-54.

17. Andreassen PR, Lohez OD, Lacroix FB*, et al.* Tetraploid state induces p53-dependent arrest of nontransformed mammalian cells in G1. *Mol Biol Cell* 2001; **12**: 1315-1328.

18. Meraldi P, Sorger PK. A dual role for Bub1 in the spindle checkpoint and chromosome congression. *EMBO J* 2005; **24**: 1621-1633.

19. Lanni JS, Jacks T. Caracterization of the p53-dependent postmitotic checkpoint following spindle disruption. *Mol Cell Biol* 1998; **18**: 1055-1064.

20. Tutt A, Gabriel A, Bertwistle D*, et al.* Absence of Brca2 causes genome instability by chromosome breakage and loss associated with centrosome amplification. *Current Biology* 1999; **9**: 1107-1110, S1101.

21. Lee H, Trainer AH, Friedman LS*, et al.* Mitotic checkpoint inactivation fosters transformation in cells lacking the breast cancer susceptibility gene, Brca2. *Mol Cell* 1999; **4**: 1-10.

22. Agnarsson BA, Jonasson JG, Bjornsdottir IB*, et al.* Inherited BRCA2 mutation associated with high grade breast cancer. *Breast Cancer Res Treat* 1998; **47**: 121-127.

23. Thorlacius S, Olafsdottir G, Tryggvadottir L*, et al.* A single BRCA2 mutation in male and female breast cancer families from Iceland with varied cancer phenotypes. *Nat Genet* 1996; **13**: 117-119.

24. Gudmundsdottir K, Thorlacius S, Jonasson JG*, et al.* CYP17 promoter polymorphism and breast cancer risk in males and females in relation to BRCA2 status. *Br J Cancer* 2003; **88**: 933-936.

25. Jonasson JG, Hrafnkelsson J. Nuclear DNA analysis and prognosis in carcinoma of the thyroid gland. *Virchows Archiv* 1994; **425**: 349-355.

26. Stefansson OA, Jonasson JG, Bjarnason H*, et al.* Characterization of *BRCA2* breast cancers by copy number profiling reveals genetic networks linked to progression. *Manuscript in preparation*.

27. King T, Li W, Brogi E*, et al.* Heterogenic loss of the wild-type BRCA allele in human breast tumorigenesis. *Ann Surg Oncol* 2007; **14**: 2510 - 2518.

28. Stefansson OA, Jonasson JG, Bjarnason H*, et al.* Characterization of *BRCA2* breast cancers by copy number profiling reveals genetic networks linked to progression. *Submitted for publication*.

29. Patel KJ, Yu VPCC, Lee H*, et al.* Involvement of Brca2 in DNA Repair. *Mol Cell* 1998; **1**: 347-357.

30. Lomonosov M, Anand S, Sangrithi M*, et al.* Stabilization of stalled DNA replication forks by the BRCA2 breast cancer susceptibility protein. *Genes Dev* 2003; **17**: 3017-3022.

31. Ayoub N, Rajendra E, Su X*, et al.* The carboxyl terminus of Brca2 links the disassembly of Rad51 complexes to mitotic entry. *Curr Biol* 2009; **19**: 1075-1085.

32. Ganem NJ, Storchova Z, Pellman D. Tetraploidy, aneuploidy and cancer. *Curr Opin Genet Dev* 2007; **17**: 157-162.

33. Weaver BAA, Silk AD, Cleveland DW. Cell biology: Nondisjunction, aneuploidy and tetraploidy. *Nature* 2006; **442**: E9-E10.

34. Glotzer M. The molecular requirements for cytokinesis. *Science* 2005; **307**: 1735-1739.

35. Yu VP, Koehler M, Steinlein C*, et al.* Gross chromosomal rearrangements and genetic exchange between nonhomologous chromosomes following BRCA2 inactivation. *Genes Dev* 2000; **14**: 1400-1406.

36. Eyfjord JE, Bodvarsdottir SK. Genomic instability and cancer: networks involved in response to DNA damage. *Mutat Res* 2005; **592**: 18 - 28.

37. Weglarz TC, Degen JL, Sandgren EP. Hepatocyte transplantation into diseased mouse liver. Kinetics of parenchymal repopulation and identification of the proliferative capacity of tetraploid and octaploid hepatocytes. *Am J Pathol* 2000; **157**: 1963-1974.

38. Weaver BA, Silk AD, Montagna C*, et al.* Aneuploidy acts both oncogenically and as a tumor suppressor. *Cancer Cell* 2007; **11**: 25-36.

39. King RW. When 2+2=5: the origins and fates of aneuploid and tetraploid cells. *Biochim Biophys Acta* 2008; **1786**: 4-14.

40. Borel F, Lohez OD, Lacroix FB*, et al.* Multiple centrosomes arise from tetraploidy checkpoint failure and mitotic centrosome clusters in p53 and RB pocket protein-compromised cells. *Proc Natl Acad Sci U S A* 2002; **99**: 9819-9824.

Tables

Table 1: Comparison of ploidy between *BRCA2* and sporadic cancers.

	Diploid (%)	Aneuploid (%)	Tetraploid (%)	Mixed Aneu- and Tetraploid (%)	Total
Sporadic	79 (47.9)	63 (38.2)	8 (4.8)	15 (9.1)	165 (100%)
***BRCA2*-mutated**	30 (42.3)	24 (33.8)	10 (14.1)	7 (9.9)	71 (100%)
Total	109	87	18	22	236

χ^2 test statistic 6.18, *P*-value 0.103

Table 2: Ploidy of *BRCA2* and sporadic cancers in relation to molecular subtypes.

	Diploid (%)	Aneuploid (%)	Tetraploid (%)	Mixed Aneu- and Tetraploid (%)	Total
***BRCA2*-mutated**					
Luminal	20 (54.1)	5 (13.5)	7 (18.9)	5 (13.5)	37 (100%)
TNP	3 (20.0)	11 (73.3)	0 (0.0)	1 (6.7)	15 (100%)
Total	**23**	**16**	**7**	**6**	**52**
χ^2 test statistic 18.48, *P*-value < 0.001					
Sporadic					
Luminal	17 (58.6)	11 (37.9)	1 (3.4)	0 (0.0)	29 (100%)
TNP	1 (12.5)	4 (50.0)	1 (12.5)	2 (25.0)	8 (100%)
Luminal-HER	0 (0.0)	1 (25.0)	1 (25.0)	2 (50.0)	4 (100%)
Non-Luminal-HER2	1 (50.0)	1 (50.0)	0 (0.0)	0 (0.0)	2 (100%)
Total	**19**	**17**	**3**	**4**	**43**
χ^2 test statistic 20.47, *P*-value 0.015					

Figure legends

Figure 1: Ploidy distribution of sporadic (dark grey) and *BRCA2* (light grey) breast cancers. The proportion of diploidy, aneuploidy and mixed aneu- and tetraploidy was similar in sporadic and *BRCA2* cancers. Tetraploidy was 2.9 fold higher in *BRCA2* cancers compared with sporadic cancers (*P*-value 0.029), see details in Table 1.

Figure 2: Ploidy distribution of *BRCA2* breast cancers, in relation to molecular subtype. Dark grey bars represent luminal subtype and light grey triple-negative phenotype (TNP). A strong association was seen between luminal phenotype and tetraploidization (only tetraploidy or mixed aneu-and tetraploidy) (P-value 0.003), and TNP and aneuploidy (P-value <0.001) in *BRCA2* cancers. TNP was rarely diploid.

Figure 1

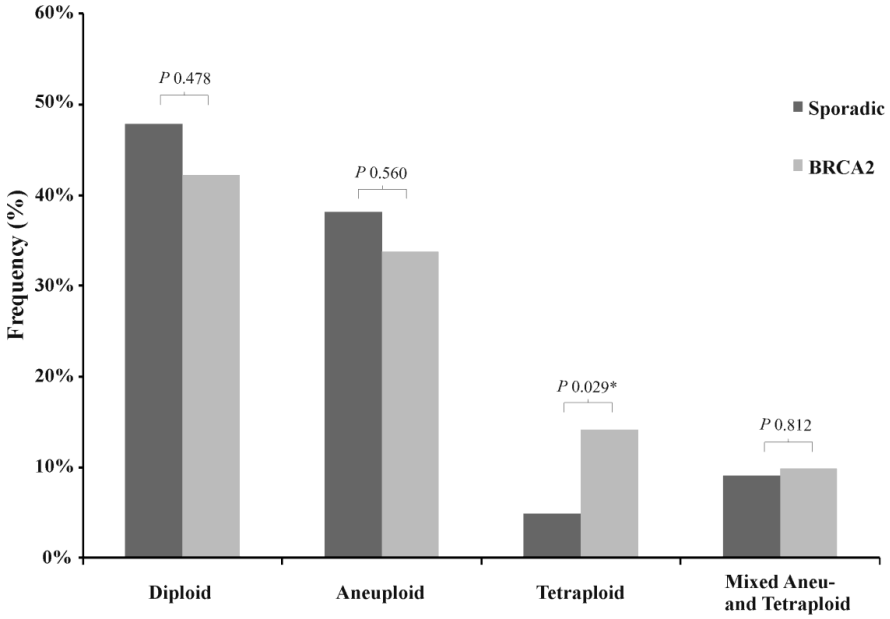
60%
50%
40%
30%
20%
10%
0%
Frequency (%)
P 0.478
P 0.560
P 0.029*
P 0.812
Sporadic
BRCA2
Diploid
Aneuploid
Tetraploid
Mixed Aneu- and Tetraploid

Figure 2

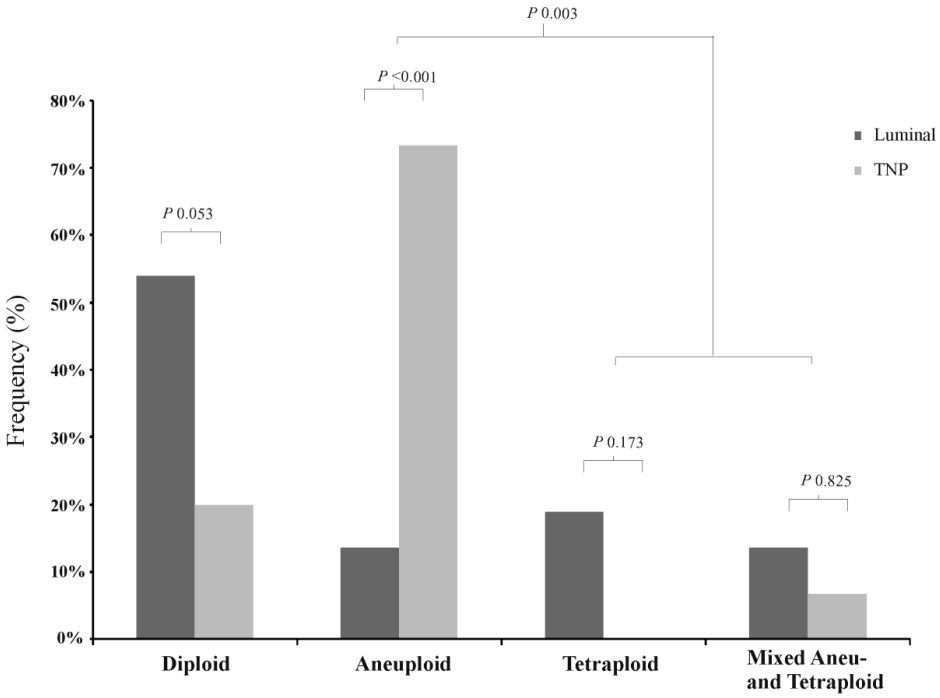
P 0.003
P <0.001
P 0.053
P 0.173
P 0.825
80%
70%
60%
50%
40%
30%
20%
10%
0%
Frequency (%)
Luminal
TNP
Diploid
Aneuploid
Tetraploid
Mixed Aneu- and Tetraploid